Analysis of the kinase NEK7 in the regulation of G1 progression and procentriole formation

Gupta, Akshari

Doctor of Philosophy

Department of Genetics
School of Life Science
SOKENDAI (The Graduate University for Advanced Studies)

Analysis of the kinase NEK7 in the regulation of G1 progression and procentriole formation

by

Gupta, Akshari

A thesis submitted for the degree of

Doctor of Philosophy

Department of Genetics
The Graduate University for Advanced Studies
(SOKENDAI)

2017

This thesis is submitted in partial fulfillment of the requirements for the degree of Doctor of Philosophy awarded by The Graduate University for Advanced Studies (SOKENDAI), Japan.

Doctoral supervisor:

Prof. Daiju Kitagawa	National Institute of Genetics, SOKENDAI

Doctoral examination committee:

Prof. Akatsuki Kimura	National Institute of Genetics, SOKENDAI
Prof. Hiroyuki Araki	National Institute of Genetics, SOKENDAI
Prof. Hitoshi Sawa	National Institute of Genetics, SOKENDAI
Assoc. Prof. Yuta Shimamoto	National Institute of Genetics, SOKENDAI
Prof. Tatsuo Fukagawa	Osaka University

A large part of the work presented in this thesis has been accepted for publication in the journal *Molecular Biology of the Cell*, and is available under the title "NEK7 is required for G1 progression and procentriole formation" (doi: 10.1091/mbc.E16-09-0643) [1].

“If you want to write, write!”

- Michael Crichton

Summary

After mitotic exit, mammalian cells must make several important decisions based upon extracellular and intracellular conditions during the G1 phase, which determine whether or not they will commit to enter a new cell cycle. Progression through G1 and transition into the S phase are under the control of several complex signalling networks, which involve the phosphorylation of many different proteins to initiate DNA replication. Not only DNA replication, but another process known as centriole duplication is initiated at the G1/S transition, which involves the formation of a daughter centriole at the base of a pre-existing mother centriole. Centrioles must be duplicated exactly once per cell cycle, as they play an important role in the organization of the mitotic spindle, and aberrations in centriole number can result in chromosome segregation defects.

The NIMA-related kinase NEK7 was found to be one of the many factors that are required for centriole duplication, as well as timely cell cycle entry. However, the exact functions of NEK7 had not been characterized in detail, and its specific roles in these events were poorly understood. Thus, as part of my doctoral research, I decided to conduct an in-depth investigation on the roles played by NEK7 in cell cycle progression and centriole duplication.

In this study, I largely focused on characterizing the consequences of NEK7 depletion on various human cancer cell lines, in order to gain insights towards its function. I observed that the depletion of NEK7 inhibited progression through the G1 phase in U2OS cells by the downregulation of various important cyclins and CDKs. Additionally, I found that the depletion of NEK7 induced the formation of primary cilia in human RPE1 cells, a phenotype that is frequently observed upon serum starvation, suggesting that NEK7 may play a role in mitogenic signalling pathways that are active during G1. The depletion of NEK7 also inhibited the earliest stages of procentriole formation, and led to the downregulation of various centriolar proteins such as STIL. Furthermore, I observed that in the absence of NEK7, there was an abnormal accumulation of Cdh1 at the vicinity of the centrioles, which is a cofactor of the anaphase promoting complex (APC/C). In NEK7-depleted cells, the ubiquitin ligase APC/C^{Cdh1} was found to actively target the centriolar

protein STIL for degradation, thus inhibiting procentriole assembly. Collectively, my results demonstrate that NEK7 is involved in the timely regulation of G1 progression, S phase entry, and procentriole formation.

Apart from the roles of NEK7 in the cell cycle, my study also provides a functional role for the APC/C cofactor Cdh1 at the centrioles. I found that Cdh1 associated with the centrioles throughout the cell cycle in a highly specific pattern. As cells enter mitosis, the amount of Cdh1 at the centrioles increased with the expansion of the pericentriolar material (PCM), which is necessary for the formation of the mitotic spindle, and this Cdh1 then abruptly disappeared from the centrioles upon the metaphase-anaphase transition. However, in certain conditions such as depletion of the centriolar satellite protein PCM1, which is involved in trafficking proteins away from the centrioles, Cdh1 exhibited a high accumulation at the centrioles, similar to NEK7-depleted cells. This suggests that Cdh1 localization near the centrioles is maintained alongside the cell cycle, and it may possibly play a role in the regulation of centriole duplication.

In conclusion, my research strongly suggests that NEK7 is an important kinase in the regulation of G1 phase progression and the G1/S transition, and also provides valuable insights towards the regulation of Cdh1 around the centrioles.

Acknowledgments

The acceptance of this thesis marks the end of my student life, yet I will always be a student at heart. Here, I would like to thank everyone who has taught me to be a better researcher and a better person.

First and foremost, I would like to express my heartfelt gratitude towards my supervisor Daiju Kitagawa. He has taught me how to be an independent thinker by giving me intellectual freedom in my research, and he has humored my whimsical ideas and criticisms alike many a time to expand my understanding of science. He would say to me often, “You can do anything in my lab!”, provided that I could convince him of my wild hypotheses. And indeed, it has felt like I have achieved many things during my stay in his lab, both professionally and personally. I will forever be indebted to him for all the support and encouragement he has given me, and it has been an honor to be his first PhD student.

All of the work described in this thesis could not have been possible without the help and guidance of my fellow lab members, who provided me with practical assistance and constructive criticism at every step of the way. In particular, I would like to thank Midori Ohta, for teaching me the ways of experimental design and also how to drink wine; Takumi Chinen, for bearing my (many) cribs about academic life; and Yuki Tsuchiya, for making me smile when I needed it.

I am grateful to all the faculty members who have supported my graduate research and provided me with different perspectives over the last few years. I am especially thankful to my thesis committee members: Profs. Akatsuki Kimura, Hiroyuki Araki, Hitoshi Sawa, Yuta Shimamoto, and Tatsuo Fukagawa, for their time and effort in assessing my work, and helping me improve my project with their valuable feedback.

I am glad to have had the opportunity to meet Prof. Yasushi Hiromi, whose shrewd questions and profound insights have made me keep my wits around me at all times. I am also thankful to Yan Zhu, for her positivity and enthusiasm, and to Chikako Miura, for her help and friendly banter.

A special mention goes out to all of the members belonging to the online community that is UED. I have made many new and diverse friends here, all of whom have introduced me to many new facets of the world, and helped me through times of difficulty. With them I have realized that it is okay to be silly at times and dance your troubles away.

To Andrew and our spot at the vending machines, we must have discussed every topic under the sun (and rain), yet never fell short of a conversation.

I could never manage to sufficiently thank my family for the love and encouragement they have given me throughout my life. My father, for backing my decisions and driving me to achieve the best of my abilities; my brother, for comforting me at times of need primarily through his pranks and multitude of faces; and my mother, not only for her love and support, but also for being a strong and successful female role model.

Last but not the least, I could not have done any of this without Harsh, with whom I have shared my adventures for almost a decade, and I hope to continue to do so for a very long time to come.

Table of Contents

List of Figures and Tables

1. Introduction

The major goal of my research is to understand the complex pathways involved in cell cycle progression and the regulation of the centrosome cycle, with a focus on the functions of the kinase NEK7 in these processes. NEK7 has been found to be one of the many factors that are required for proper centriole duplication, as well as timely cell cycle progression; however, its specific roles in these events have remained unclear and controversial.

In the "Background" section, I will present a quick summary of the available literature that is necessary to provide some context for my research. I will go over some of the pathways that are involved in cell cycle progression, with an emphasis on the parts played by various cyclin/CDK complexes, as well as the APC/C, which are key regulators of the progression through G1 and the G1/S transition. I will then provide a brief overview of the importance of centrioles in the eukaryotic cell cycle, and the molecules that are involved in the centriole duplication pathway. Lastly, I will summarize the known functions and the emerging significance of NEK7 in the cell cycle.

The "Results" section consists of the bulk of my doctoral work. I will highlight some of my most important findings about the roles played by NEK7 in the cell cycle, the centrosome cycle, and its regulation by the cell cycle. Most of the experiments performed in this study use a combination of cell and molecular biology techniques to address the impact of NEK7 depletion using short interfering RNAs (siRNA) under various conditions. When necessary, I will provide the relevant scientific background in order to better understand the reasoning behind specific experimental ideas.

In the "Discussion" section, I summarize the significance of my results that demonstrate the roles of NEK7 in G1 progression and centriole assembly, and I will present my hypotheses about the putative functions of NEK7 based upon my findings. Additionally, I will discuss the significance of centrosomal Cdh1 and how it could possibly regulate centriole duplication.

Lastly, in the “Current and Future Studies” section, I will briefly introduce some of my research interests that were not directly related to my work on NEK7 and the cell cycle. I have been interested in the structural aspects of centriole assembly, and, in this section, I will show some of my preliminary findings about the interactions between several centriolar proteins, as well as discuss what I believe are the important questions that still need to be addressed with respect to centriole structure.

2. Background

In this literature review, I will briefly go over the major events that occur during the human cell cycle, and the key regulators involved in these mechanisms. I will then discuss the importance of centrioles in eukaryotic cells and the roles they play in the human cell cycle in particular. Lastly, I will introduce the NIMA-related kinases (NEKs) and their significance in the cell cycle, and summarize the known functions of the kinase NEK7 as they are currently understood, in order to provide context for my doctoral study.

2.1 The cell cycle

The eukaryotic cell cycle is a crucial process to ensure the proper segregation of genetic material to the resultant offspring. The various stages of the cell cycle have been characterized across many different phyla of eukaryotes, and although most species exhibit tremendous diversity in cell morphology and function, the basic mechanisms behind cell division have remained constant over time. Understanding the fundamental processes that govern the regulation of cell division is an important area of biological research, as many human diseases and disorders have been linked to defects in the cell cycle.

The most common approach to describe the individual stages of the cell cycle is by addressing chromosome behaviour as the cell cycle progresses. G1 is typically described as a "growth phase", as the cell increases the biosynthesis of many molecules required for DNA replication and overall cell growth. The S phase is marked as the duration in which the genetic material of the cell is replicated. G2 is described as the second "growth phase", as the cell produces more biomolecules that are necessary for cell division. Finally, during mitosis or the M phase, chromosomes condense and align along the division plane of the cell, and spindle fibers pull and separate the chromosomes into the resulting daughter cells.

This approach, while not incorrect, constitutes a very rudimentary overview of the cell cycle. The cell is not, in fact, made up only of genetic material and spindle fibers; it consists

of many organelles and macromolecular complexes that are essential for the functioning of the cells, and also undergo highly dynamic changes with the progression of the cell cycle. Along with chromosomes, most of these organelles are similarly "replicated" and subsequently inherited to future generations [2][*]. Deregulation of any of these organelles or their associated signalling pathways can often result in alterations or defects to the cell cycle or cell division, and an overall understanding of how organelle dynamics are linked to the cell cycle is essential.

Many signal transduction pathways play a huge role in coordinating the changes accompanying various organelles across the cell to ensure smooth transitions between the different stages of the cell cycle. Several thousands of molecules are involved in these pathways and commonly transmit "signals" via enzymatic modification of downstream components, and when molecules from one pathway overlap those in another pathway, they form signalling networks. Within the cell cycle, these signalling networks are indispensable in determining the transitions between consecutive stages of the cell cycle, and are necessary to clear several cell cycle "checkpoints". In recent decades, a huge and impressive amount of progress has been made in deciphering the roles of the individual molecules involved in cell cycle-associated signalling networks. However, as with many other complex biological systems, the precise details behind how these molecules interact and are regulated remain incompletely understood.

In the following subsections, I will briefly discuss the importance of various cell cycle checkpoints, as well as the roles of several kinases that are involved in checkpoint-associated signalling.

[*] I found this to be a particularly concise review highlighting how various organelles undergo morphological and functional changes across the cell cycle. This review covers the spatiotemporal dynamics of the smooth and rough endoplasmic reticula (ER), the Golgi apparatus, mitochondria, endosomes, and peroxisomes in interphase and mitotic cells.

2.1.1 Cell cycle checkpoints

Cell cycle checkpoints serve as surveillance mechanisms to ensure the integrity and fidelity of major cellular components during various stages of the cell cycle. Unregulated progression of the cell cycle can lead to the accumulation of various cellular defects, before the cell even receives the opportunity to correct these problems. Thus, cell cycle checkpoints function as barriers to the next stage, whereupon the cell can carry out several internal checks before making the decision to commit to the next stage (Figure 1).

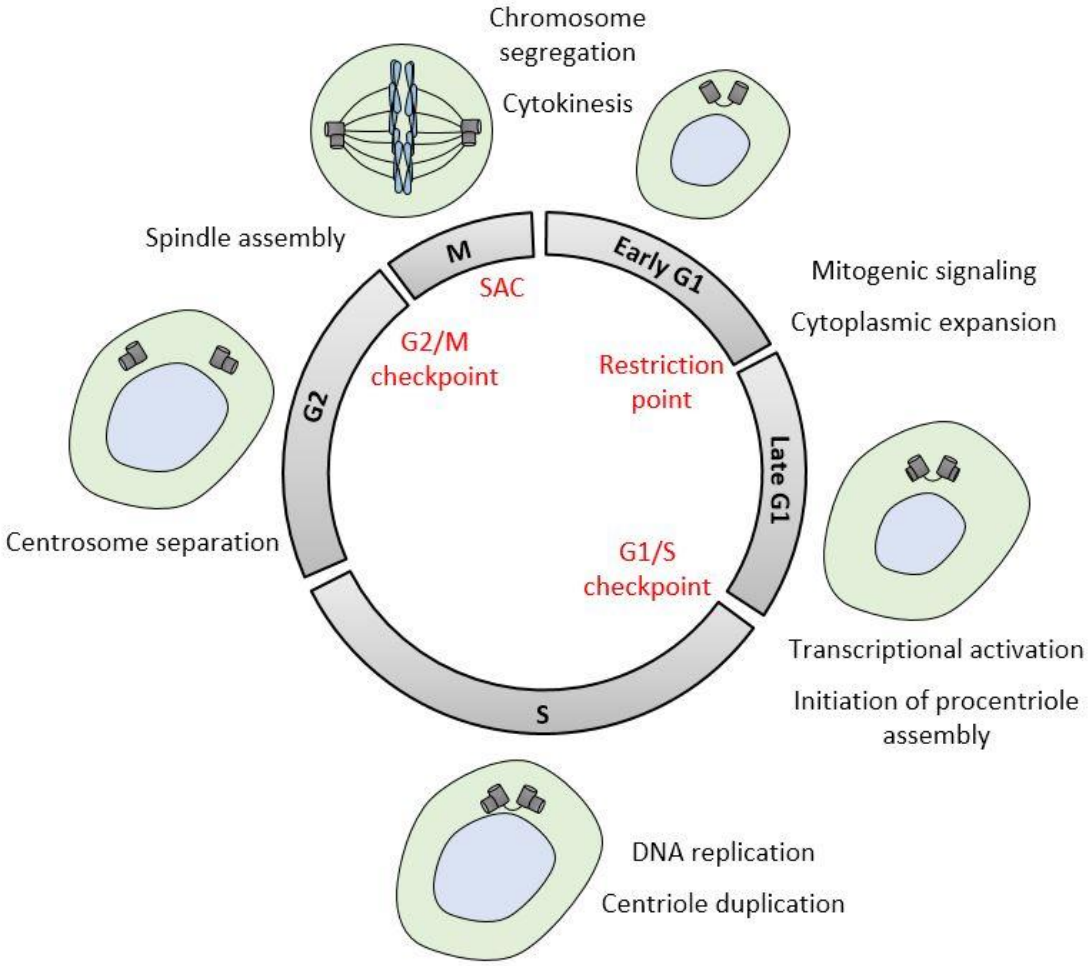

Figure 1. Major checkpoints in the cell cycle. The earliest checkpoint is the restriction point during G1, which determines whether there are sufficient growth factors present in the surroundings to ensure cell proliferation. The next checkpoint is at the G1/S transition, and clearing this checkpoint is necessary for the initiation of DNA replication at early S phase. The G2/M checkpoint prevents premature entry into mitosis. The spindle assembly checkpoint (SAC) ensures the proper and equal segregation of chromosomes into each daughter cell. Lastly, the DNA damage checkpoint (not shown) is active most of the time during interphase, and can activate DNA repair pathways in the event of DNA damage or replicative stress. The nucleus is indicated in blue, centrioles in grey, and cytoplasm in green.

2.1.2 Checkpoints during G1

After mitotic exit, mammalian cells are required to make several important decisions based upon extracellular and intracellular conditions during the G1 phase, and these decisions determine whether or not they will commit to enter a new cell cycle. There are two main checkpoints that exist during G1: the oft-discussed G1/S checkpoint that regulates entry into S phase and the initiation of DNA replication, and the lesser known restriction point, which determines whether a cell should proliferate or become quiescent.

Restriction point (R): The concept of the "restriction point" is not one that has been examined in detail in many studies about G1 progression. Indeed, there has only been one recent review that discusses the molecular basis of this checkpoint at length in light of recent work [3]. It has been proposed that the restriction point (R) functions as the switch between G0 (resting or quiescent state of the cell) and G1 (proliferating state) [4,5]. Passage through the restriction point is largely dependent on growth factors and mitogenic signalling [3], and the absence of these signals causes the cells to become quiescent. In certain cell types, primary cilia function as sensors of growth factors and nutrients present in the medium, and hence, the formation of primary cilia, or ciliogenesis, is a commonly observed phenotype in cells that have been grown in the absence of serum, [6]. In cycling mammalian cells, the restriction point has been mapped to roughly 3.5 hours post-mitosis [7], and the time from R to S phase entry constitutes the rest of the G1 phase.

G1/S checkpoint: Passage through the G1/S checkpoint results in the initiation of DNA replication and the commitment of the cells to enter a new cell cycle. The G1/S transition has been found to be irreversible; cells cannot return to a quiescent state after the green signal has been given for DNA replication [8,9]. Thus, various signalling pathways that regulate entry into S phase are under strict control via both positive and negative feedback loops [10], and deregulation of these pathways in resting or differentiated cells can promote oncogenesis.

2.1.3 The role of cyclin/CDK complexes in the cell cycle

Cyclin-dependent kinases (CDKs) are a family of protein kinases that have been well-studied for the roles they play in the eukaryotic cell cycle. CDKs are activated through their binding to specific cyclins, and are involved in regulating many cellular processes such as gene transcription, protein function, DNA synthesis, chromosome and organelle dynamics, rearrangements of the cytoskeleton, mitotic spindle assembly, and chromosome segregation, to name a few [11]. Cyclin/CDK activity is strongly dependent on the total levels of the respective cyclins present within a cell, which are tightly regulated via gene transcription as well as ubiquitin-dependent proteolysis.

A summary of the various cyclin/CDK complexes active at different stages in the cell cycle is presented in Table 1.

Table 1. Cyclin/CDK complexes in the cell cycle. Progression through the cell cycle and passage through various checkpoints is largely dependent on the activity of various cyclin/CDK complexes, which regulate the expression and functions of many essential proteins [12].

Stage	Checkpoint	Major events	CDKs
Early G1	Restriction point	Mitogenic signalling	Cyclin D/CDK4 Cyclin D/CDK6
Late G1	G1/S	Transcriptional activation Procentriole formation	Cyclin E/CDK2
S	DNA damage checkpoint	DNA replication Centriole duplication	Cyclin A/CDK2
G2	G2/M	Centrosome separation PCM assembly	Cyclin A/CDK1
Mitosis	Spindle assembly checkpoint	Spindle assembly Chromosome segregation	Cyclin B/CDK1

Cyclin/CDK complexes in G1: Progression through G1 and transition into the S phase are largely under the control of the G1 cyclin/CDK complexes, which interact with and phosphorylate many different proteins to initiate DNA replication. During early G1, extracellular growth factors can activate various signalling pathways, which lead to an increase in cyclin D transcription [13,14]. Cyclin D interacts with either CDK4 or CDK6, and these cyclin D/CDK complexes can phosphorylate the retinoblastoma tumor suppressor protein (Rb) to generate what is called hypophosphorylated Rb [15] *. Hypophosphorylated Rb can bind and inhibit the E2F family of transcription factors, which activate various genes associated with DNA replication, and are critical for transition into the S phase [16]. Hypophosphorylation of Rb by cyclin D/CDK4 or cyclin D/CDK6 also leads to the dissociation of histone deacetylases from Rb, which results in an increase in cyclin E expression [16]. Once expressed, cyclin E can bind to and activate CDK2, which phosphorylate many substrates and create several feedback loops. One of the substrates of cyclin E/CDK2 is hypophosphorylated Rb; Rb is converted to hyperphosphorylated Rb by cyclin E/CDK2 leading to its dissociation from the E2F transcription factors [3,15]. The activated E2F factors initiate the transcription of many genes required for S phase entry, including the genes for cyclin E and cyclin A, which creates a positive feedback loop resulting in surges in transcription towards the G1/S transition [10].

Following cyclin E/CDK2-mediated gene transcription and entry into S phase, an increase in the levels of cyclin A (which itself is an E2F target) creates a negative feedback loop as cyclin A replaces cyclin E in the complex with CDK2 [10]. One of the major roles of cyclin A/CDK2 is to initiate DNA replication and ensure that DNA is replicated only once per cell cycle. Although cyclin A plays several roles in the cell during S phase, it has been shown that cyclin A itself is dispensable for the G1/S transition, which primarily depends on the activity of the cyclin E/CDK2 complex [8,9] †.

* This is a very nice study that utilizes 2D immunoblots to characterize the extent of phosphorylation on Rb alongside the timing of phosphorylation.

† These two are fantastic papers that use alternative approaches to interpret live-cell imaging data, and provide clear evidence of how individual molecules contribute to signalling pathways that permit the initiation of DNA replication.

2.1.4 The role of p21 in the G1/S transition

p21 is a small molecular interactor of the cyclin-dependent kinases, and functions as a negative regulator of the cell cycle [17]. During G1, p21 binds to and promotes the kinase activities of cyclin D/CDK4 and cyclin D/CDK6, thus promoting progression through G1 [18]. On the other hand, p21 can directly bind and inhibit CDK2, and hence also prevents S phase entry [19]. p21 can also associate with E2F proteins and suppress their transcriptional activity [20]. Additionally, nuclear p21 inhibits DNA replication by binding PCNA and interfering with PCNA-dependent DNA polymerase activity [21].

2.1.5 The role of the APC/C in G1 and the G1/S transition

The anaphase-promoting complex/cyclosome (APC/C) is a large multi-subunit E3 ubiquitin ligase which plays two major roles in the cell cycle. During metaphase, the APC/C associates with its cofactor Cdc20 and remains inactive until the spindle assembly checkpoint (SAC) has been satisfied, and the subsequent activation of APC/C^{Cdc20} is essential for chromosome segregation and the transition into anaphase [22]. Towards mitotic exit, Cdc20 is replaced by Cdh1 in the complex with the APC/C, and APC/C^{Cdh1} directs the ubiquitin-mediated proteolysis of Cdc20 as well. Within G1, APC/C^{Cdh1} is an important regulator of the decisions made within the cell regarding its fate, such as whether to become quiescent, differentiate, or re-enter the cell cycle [23]. The APC/C is completely inactivated in late G1 and remains inactive until early mitosis [9].

In G1, APC/C^{Cdh1} does several things. It limits the transcription of cyclin D by promoting the degradation of the transcription factor Ets2, and thus prevents aberrant cell cycle entry [23,24]. APC/C^{Cdh1} targets Skp2 for degradation and thus prevents SCF^{Skp2}-mediated proteolysis of p21, resulting in an accumulation of p21 in the cell [23]. APC/C^{Cdh1} is also involved in a complex feedback loop with Rb and E2F; Cdh1 can compete with E2F for hypophosphorylated Rb, thus regulating the activity of E2F-mediated transcription [25]. Conversely, the E2F transcription factors stimulate the expression of Emi1, which functions as an inhibitor of APC/C^{Cdh1} activity [8,9,26].

In mammalian cells, the complete inactivation of APC/C^{Cdh1} is the ultimate step necessary for the commitment to the cell cycle [9]. It has been shown that cells can be triggered to reversibly exit the cell cycle in G1 before the APC/C^{Cdh1} has been inactivated, but not after [9]. Emi1 is believed to be the primary factor responsible for the complete activation of APC/C^{Cdh1}; depletion of Emi1 induced rereplication of DNA due to the unscheduled reactivation of APC/C^{Cdh1} [27], whereas overexpression of Emi1 accelerated S phase entry [28]. Finally, phosphorylation of the APC/C^{Cdh1} by cyclin/CDK complexes also creates a negative feedback loop that promotes its inactivation [23].

2.2 The centrosome cycle

Centrosomes are highly conserved organelles in most eukaryotes that play an important role in the organization of the mitotic spindle and proper chromosome segregation. Within many cycling cells, centrosomes function as the primary microtubule-organizing centers (MTOCs) during both interphase and mitosis; whereas in resting or differentiated cells, centrosomes serve as basal bodies and mediate the development of cilia or flagella, which project from the cell membrane to enable cell movement or sensing the environment around the cells. Abnormalities in centrosome organization and function often result in genomic instability and aberrant cell division, and are a cause of many cancers [29]. Mutations in many centrosomal proteins have also been implicated as a cause of autosomal recessive primary microcephaly (MCPH), a neurodevelopmental disorder characterized by a reduced brain growth and non-progressive mental retardation. Therefore, strict control of the organization and function of centrosomes is essential for the healthy development of the organism.

A single centrosome consists of one or two centrioles which are highly conserved cylindrical bodies, surrounded by an amorphous protein matrix known as pericentriolar material (PCM). The number of centrosomes within a cell is strictly regulated, as too few centrosomes can lead to the formation of monopolar spindles in mitosis, and too many centrosomes can lead to the formation of multipolar spindles. Defects in centrosome

function can result in a variety of cellular defects such as aneuploidy, polyploidy, bi- or multinucleated cells, or even apoptosis (Figure 2). Similar to DNA replication, centrosomes duplicate exactly once per cell cycle in cycling cells, and this process is tightly linked to cell cycle progression (Figure 3).

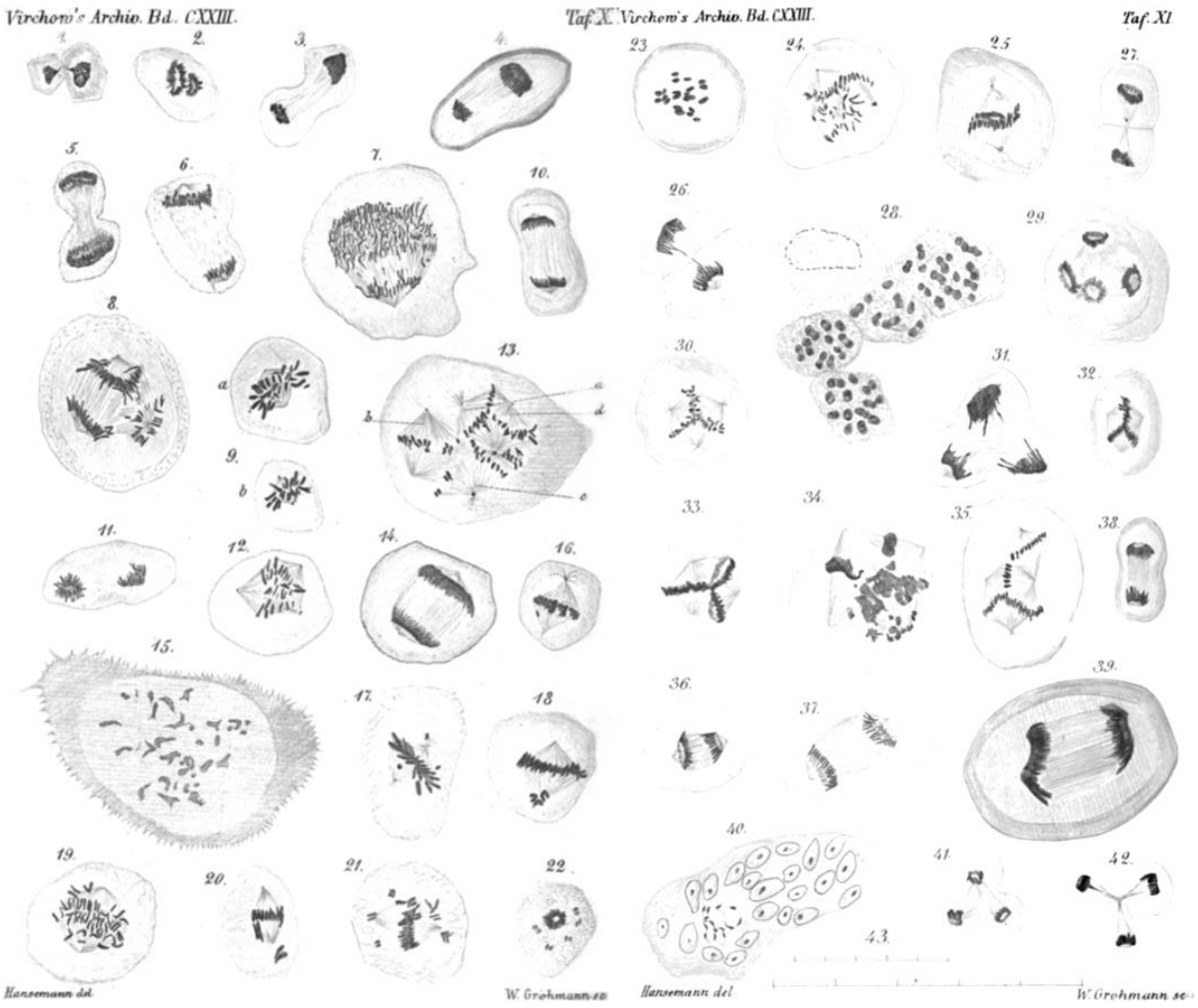

Figure 2. David Hansemann's drawings of faulty mitoses in cancerous tissues. Hansemann beautifully captured many of the different abnormalities that can result from improper spindle assembly or deregulation of the cell cycle in his illustrations. Some of the defects that can be seen are: monopolar spindles (number 22); multipolar spindles (numbers 8, 12, 13, 24, 29-35, 41, and 42); asymmetrical mitoses (number 4); and abnormally large nuclei or multinucleated cells (numbers 15, 28, and 40). Many of these deviations from regular mitoses can be attributed to an improper number of centrosomes within the cell, or unlinking of the centrosome cycle from the cell cycle. Images are reproduced from the 1891 manuscript "Ueber pathologisches Mitosen" (About pathological mitoses) [30].

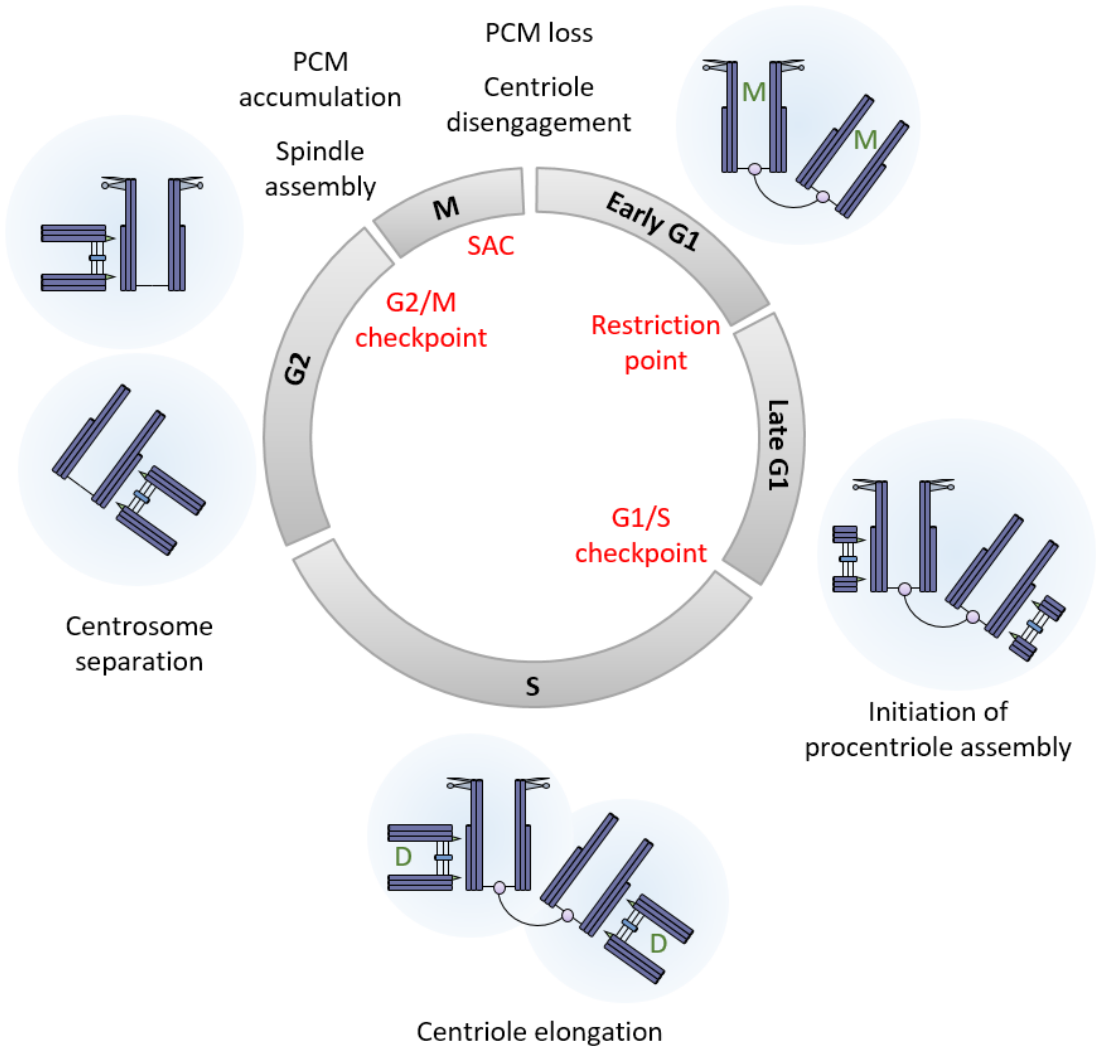

Figure 3. The centrosome cycle. Upon mitotic exit, new daughter cells inherit one centrosome containing two mother centrioles (M) that are connected together by a proteinaceous linker and surrounded by the PCM (light blue). Procentriole assembly is initiated at the proximal end of a mother centriole towards late G1. As the cell cycle progresses, these procentrioles continue to elongate and form daughter centrioles (D). Towards the end of G2, the proteinaceous linker connecting the two mother centrioles is dissolved by the activity of the kinase NEK2, and the two centrosomes migrate to the opposite ends of the cell. The PCM expands and recruits many components required for microtubule nucleation at the spindle poles, which is followed by assembly of the mitotic spindle and chromosome alignment. Upon clearance of the spindle assembly checkpoint (SAC) at metaphase, pulling forces from spindle microtubules as well as pulling forces on the centrosomes away from the center mediate chromosome segregation. Upon cytokinesis, each daughter cell retains one centrosome containing two centrioles; the daughter cell from the previous cell cycle functions as a mother centriole in the next round of centriole duplication.

2.2.1 Centriole structure

Centrioles are highly conserved cylindrical bodies, and consist of nine sets of triplet microtubules organized around a central cartwheel (Figure 4). In human cells, the cartwheel is essential primarily at the earliest stages of procentriole formation, and is lost towards the later stages of mitosis. Additionally, the mother centriole also contains distal and sub-distal appendages which play a role in microtubule assembly and enable docking of the mother centriole/basal body at the cell membranes during ciliogenesis [31].

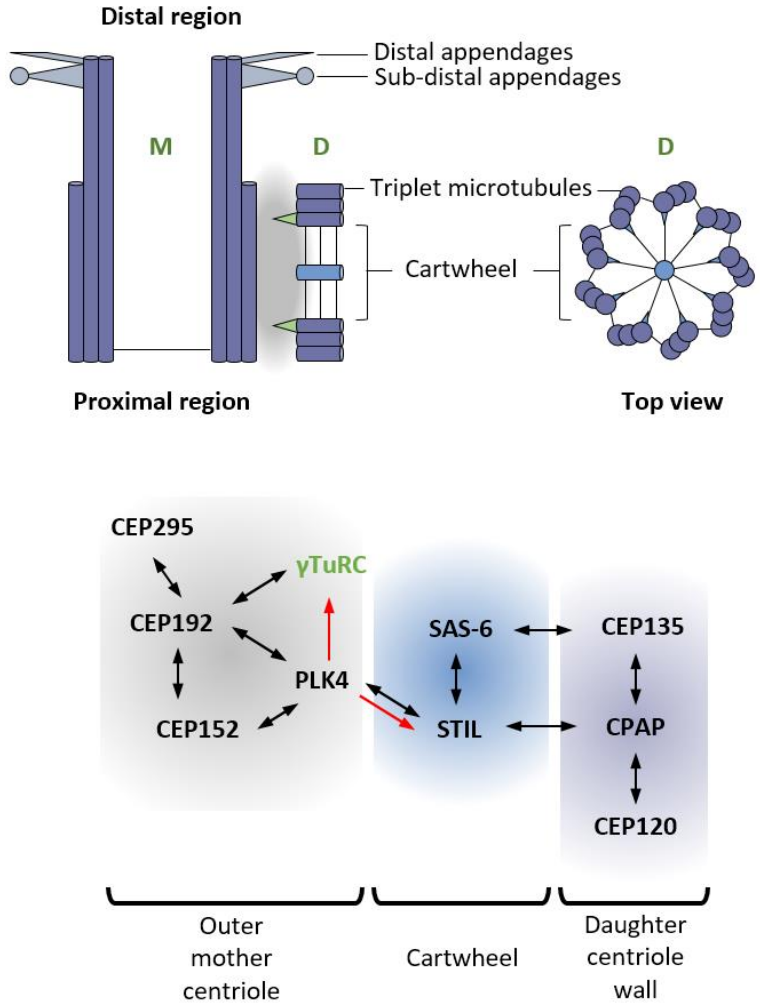

Figure 4. Centriole structure and composition. Schematic representations of longitudinal (top left) and cross-sections (top right) of the mother (M) and daughter (D) centrioles. Triplet microtubules (purple) are arranged around the nine-spoked cartwheel in the daughter centriole, whereas the mother centriole usually loses its cartwheel towards mitotic exit. The bottom panel shows the proteins involved in centriole formation in human cells, and their respective localizations. Black arrows between two proteins indicate interactions, whereas red arrows indicate modification by phosphorylation.

2.2.2 The centriole duplication pathway

Most of the components involved in the centriole duplication pathway are evolutionarily conserved (Figure 4). The most upstream factor critical for procentriole assembly is the recently characterized CEP295, which localizes around the walls of the mother centriole and is required for the recruitment of the scaffolding protein CEP192 [32–35]. CEP152 and the kinase PLK4 are then recruited onto the centrosomes by CEP192, and CEP152 competes with CEP192 for PLK4 binding to regulate its function [36,37]. The activation of the kinase PLK4 is critical for procentriole assembly, as it recruits and phosphorylates the procentriolar protein STIL [38,39]. Phosphorylated STIL can then form a complex with the protein SAS-6, which is capable of self-assembling into oligomers that display the 9-fold symmetry essential for centriole structure, known as the cartwheel [40,41]. CEP135, which is a microtubule-binding protein and interacts with both SAS-6 and CPAP [42,43], is required for the assembly of the SAS-6 cartwheel [44]. PLK4 also phosphorylates CPAP, a microtubule-binding protein [45,46], as well as the γTuRC (γ-tubulin ring complex) component GCP6 [47], both of which are presumably required for the formation of centriolar microtubules alongside cartwheel assembly. Finally CPAP and CEP120, which is also a microtubule-binding protein, cooperate to elongate and stabilize the centriolar triplet microtubules [46,48,49] along with the distal end-capping protein CP110 [50].

This conserved pathway has been studied and characterized to some extent within different model systems such as human cancer cell lines, *Drosophila* (fruit flies), *Caenorhabditis elegans* (nematodes), and *Chlamydomonas reinhardtii* (green algae) [51,52]. However, despite recent advances, many aspects of centriole duplication remain unknown, for example, the exact roles of individual protein domains and mapping them to the 3D architecture of centrioles, as well as the components responsible for the formation of centriolar triplet microtubules.

2.2.3 Regulation of centriole duplication at the G1/S transition

In cycling cells, centriole duplication occurs exactly once per cell cycle, and regulation of this process is tightly linked to the cell cycle as well. Both the transcriptional levels as well

as protein levels of the various components essential for the centriole duplication pathway are controlled in a cell cycle-dependent manner. The expression levels of the proteins PLK4, STIL, and SAS-6 in particular are strictly regulated, as low expression of these proteins inhibits centriole duplication, whereas their overexpression triggers overduplication of centrioles [53–55]. STIL, SAS-6, and CPAP are all known targets of the APC/C^{Cdh1} ubiquitin ligase, and all of them contain a Lys-Glu-Asn motif, or KEN-box, which can be recognized by Cdh1 for ubiquitination and subsequent degradation towards late mitosis [46,56–58]. Their expression levels increase again towards late G1, coinciding with the timing of initiation of centriole formation [46,54,55]. The STIL gene itself has been reported to be under transcription control of the E2F proteins, and transcription of STIL increases with E2F activation at late G1 [59]. Additionally, several centriolar proteins can be phosphorylated by cyclin/CDK complexes to regulate centriole duplication and mitotic spindle assembly [60,61].

2.2.4 Centrosomes and cilia

Other than their roles in mitotic spindle assembly, centrioles serve another very important function in many eukaryotic cells. Centrioles can act as basal bodies that allow the formation of either cilia or flagella, which are outward projections of the cell membrane and play important roles in intercellular signalling, cell polarity, the generation of fluid flow, or cellular movement [62]. The structural strength of cilia or flagella is conferred by the axoneme; the axoneme consists of nine sets of doublet microtubules, and depending on the ciliary type, a central pair of microtubules may also be occasionally present [63].

In certain cell types, primary cilia, which are non-motile in nature, are typically formed in G1 or G0 depending upon intracellular or extracellular signalling cues. Ciliogenesis involves the docking of the mother centriole at the cell membrane via its appendages, and elongation of the centriolar microtubules into the cell membrane to form ciliary doublet microtubules [62]. In cultured retinal pigmented epithelial (RPE1) cells, ciliogenesis can be initiated either when the cells undergo contact inhibition, or upon prolonged serum starvation which arrests the cells at the restriction point.

2.3 The NIMA-related kinases (NEKs) in the cell cycle

Several kinases and kinase families play crucial roles to regulate the progression of the cell cycle as well as control of various cell cycle checkpoints. These kinases include the previously described cyclin-dependent kinases (CDKs), Aurora kinases, as well as the Polo-like kinases (PLKs). However, there is another important, less-characterized family of kinases whose members have key roles in mitosis, and recently discovered roles in the rest of the cell cycle as well. The NIMA-related kinases or NEKs are named after the never-in-mitosis A (NIMA) protein of *Aspergillus nidulans*, in which it was found to play roles similar to the cyclin B/CDK1 complex as a master regulator of mitotic progression [64]. Following the discovery of NIMA, various NEKs have been identified in a wide range of organisms from protists to multicellular eukaryotes.

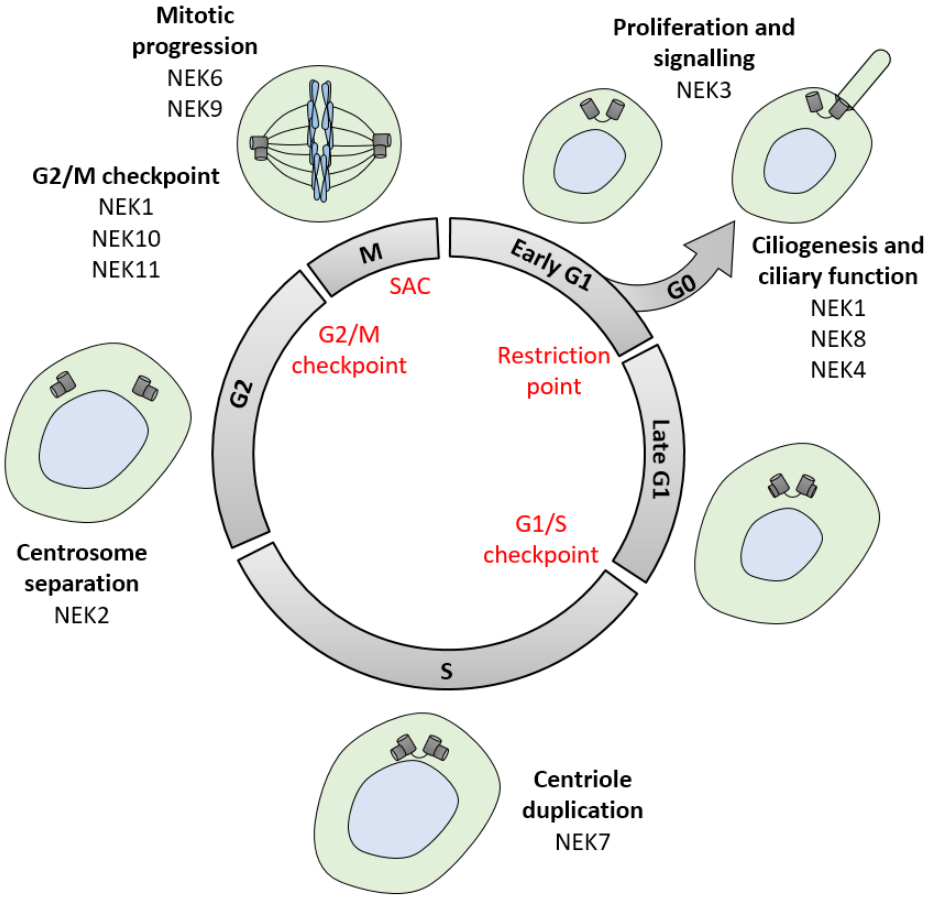

Figure 5. The NIMA-related kinases in the cell and centrosome cycles. Human NEKs contribute to various different processes during cell cycle progression and differentiation, some of which include cell proliferation and signalling, ciliogenesis and ciliary function, centriole duplication and centrosome separation, chromatin condensation, nuclear envelope breakdown, formation of a robust bipolar spindle, and cytokinesis [65,66].

The human genome encodes eleven NEK genes that have been found to function in different events during cell cycle progression and differentiation (Figure 5) [65]. Mutations in several of these genes have been linked to various tumors and diseases, particularly ciliopathies, an example of which is polycystic kidney disease which is caused due to impaired cilia-mediated signalling [66]. With advancing research on the NEKs in the last few decades, it has become increasingly apparent that these kinases perform important roles in cycling cells, particularly within microtubule-dependent processes such as mitosis and ciliogenesis.

2.3.1 The NIMA-related kinases in the centrosome cycle

Various NEKs have been implicated in the regulation of centrosome and ciliary function. Perhaps the best characterized member is NEK2, which can phosphorylate various centrosomal linker proteins to promote oligomer disassembly and their subsequent displacement from the centrosomes, which leads to centrosome separation and is required for the G2/M transition [67]. NEK1 and NEK8 are known to function within cilia, and several ciliopathies have been linked to mutations in these two kinases [65]. NEK6, NEK7, and NEK9 have been associated with several roles in generating the mitotic spindles, and these three proteins have been reported to act together [68–70]. NEK9 is activated by a two-step mechanism that involves CDK1 and PLK1, and plays a role in the recruitment of the adaptor protein NEDD1 for microtubule nucleation during mitotic spindle assembly [71,72]. NEK9 can also phosphorylate NEK6 and NEK7 leading to their activation, and at least in the case of NEK6, it has been shown to be activated by NEK9 during mitosis [69]. The roles of NEK6 and NEK7 in mitotic spindle assembly and cell cycle progression have thus far been less clear.

2.3.2 The emerging roles of the kinase NEK7

Some of the earliest studies on NEK7 have found it to be crucial for mitotic spindle organization and cytokinesis [68,73–75], and also reported that NEK7 is required for centriole duplication and cell cycle progression [73,74,76]. Atypical overexpression of

NEK7 has been implicated in various cancers [77–79], and could possibly induce proliferation of otherwise resting cells [80], suggesting NEK7 has oncogenic potential. Likewise, downregulation of NEK7 could lead to a delay in S-phase entry [76,78] and early mortality during murine embryogenesis [75]. Although these studies so far indicate that NEK7 may play a crucial role in the progression of the cell cycle, and particularly during G1, how exactly NEK7 may contribute to cell cycle regulation has been unclear.

Thus, in this study, I decided to conduct a detailed investigation of the functions of NEK7 and the various phenotypes caused by its depletion in human cells, with a particular emphasis on cell cycle progression and centriole duplication. Through my research, I will demonstrate that NEK7 is required for progression through the G1 phase of the cell cycle, in the absence of which cells are invariably arrested near the G1/S transition, and I will discuss the consequences of this arrest on proteins involved in the cell cycle and centrosome function.

3. Results

In this section, I will present my findings regarding the role of NEK7 in the cell and centrosome cycles that I obtained over the course of my doctoral research. I primarily worked with human cell lines and used a combination of cell and molecular biology techniques to address the impact of NEK7 depletion using short interfering RNAs (siRNA) under various conditions. The two siRNAs that I used against NEK7 were highly effective in depleting NEK7 (Figure 6) and exhibited almost identical phenotypes in many experiments shown in the next few sections, confirming that my observations were not consequences of the off-target effects of the siRNAs.

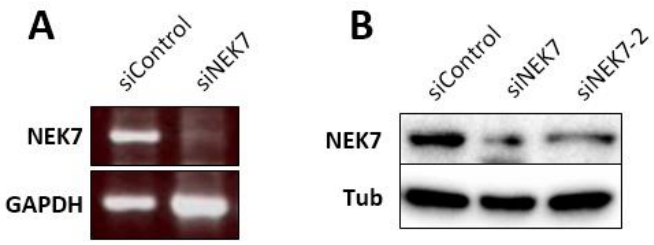

Figure 6. Efficiency of the different siRNAs used against NEK7. U2OS cells were transfected against control or NEK7 siRNAs for a total of 48 hours. (A) RT-PCR analyses were performed on total cell RNAs extracted in the indicated conditions. GAPDH was used as an internal control. (B) Total cell lysates were analyzed by immunoblotting against the indicated antibodies. The antibody against α-tubulin was used as a loading control.

3.1 Depletion of NEK7 induces a G1 arrest

Depletion of NEK7 has previously been shown to have an impact on cell cycle progression, causing a range of phenotypes such as a prometaphase arrest with spindle assembly defects [68,73,74], delays in the cell cycle, and inhibition of cell proliferation [76,78]. Some of the earliest experiments I performed suggested that the depletion of NEK7 has a severe impact on cell cycle progression, so I decided to characterize these phenotypes in more detail.

3.1.1 DNA content profiles of control and NEK7-depleted cells

First of all, I analyzed the DNA content profiles of U2OS cell cultures that had been treated with either control or NEK7 siRNAs. I found that treatment of asynchronous U2OS cells with siRNAs against NEK7 caused a slight increase in the G0/G1 cell population compared to cells treated with a control siRNA (Figure 7A). To confirm whether or not these cells indeed represent a cell cycle arrest, I performed experiments in which I arrested U2OS cells in the presence of control or NEK7 siRNAs at early mitosis using nocodazole, which is an inhibitor of microtubule polymerization, and released them into fresh medium (Figure 7B). This allowed me to examine whether these cells were capable of exiting mitosis and continuing with the next cell cycle. Interestingly, I found that although most NEK7-depleted cells exited mitosis, most of them were unable to exit G1 phase and initiate DNA replication (Figure 7C-D).

3.1.2 NEK7-depleted cells exhibit reduced levels of cell cycle proteins

In order to further characterize the cell cycle delays in cells depleted of NEK7, I analyzed the expression levels of various cyclins and CDKs in total cell lysates collected at different points after the nocodazole release (Figure 8).

Expression levels of the mitotic cyclin B1 were diminished in cells treated with NEK7 siRNA compared to control cells upon mitotic exit (Figure 8B). CDK1, which forms a complex with cyclin B1, undergoes inhibitory phosphorylations during interphase to prevent premature mitotic entry [81]. Accordingly, I could observe an upshifted band of CDK at the 12 hour time point in control cells (Figure 8C, red arrows). In contrast, CDK1 did not appear to undergo phosphorylation in NEK7-depleted samples, presumably reflecting the cell cycle delay in G1.

Cyclin D1, which forms complexes with CDK4 and CDK6 in early G1, functions in passage through the restriction point, and low levels of cyclin D1 have been shown to be associated with a G1 arrest in previous studies [3,82]. Interestingly, I found that expression of cyclin D1 was drastically reduced during G1 in NEK7-depleted cells, even though CDK6 levels did not appear to be significantly affected (Figure 8B, C), which

suggests that these cells may not be able to pass the restriction point.

In late G1, cyclin E1 forms a complex with CDK2 to mediate the G1/S transition by increasing E2F-mediated transcription [10]. In cells that had been depleted of NEK7, cyclin E1 levels remained unaltered compared to control cells (Figure 8B). On the other hand, cyclin A2, which gradually replaces cyclin E1 in the complex with CDK2 during S phase progression, exhibited very low expression levels in NEK7-depleted cells. Additionally, I was astonished to discover that CDK2 levels were severely downregulated in NEK7-depleted cells (Figure 8C). The low levels of cyclin A2 and CDK2 in NEK7-depleted cells suggests that these cells would be incapable of carrying out DNA replication, as the cyclin A/CDK2 complex is essential for the maintenance and completion of S phase [8,9]. The periodic fluctuations of cyclin A in the cell cycle have been well-characterized, and a G1 arrest in NEK7-depleted cells can account for these low levels. However, for CDK2, the factors involved in the transcription, expression, or degradation of CDK2 have not been analyzed in detail to my knowledge.

I also looked at the expression levels of the APC/C cofactor Cdc20 under these conditions. Cdc20, which is expressed from early S phase to late mitosis, was also significantly downregulated upon NEK7 depletion (Figure 8C).

Additionally, I looked at the expression levels of the procentriolar protein STIL, which is also a cell-cycle regulated protein and increases in expression around the G1/S transition [55,59]. In control cells, STIL protein levels sharply increased around the 8 hour time point, which roughly corresponds to the G1/S transition (Figure 9). However, STIL protein levels remained very low for the duration of the time course experiment upon NEK7 depletion.

Lastly, I also checked whether the reduction in the levels of G1 proteins could be explained by the low levels of cyclin D1 by treating U2OS cells with siRNAs against cyclin D1. However, the siNEK7 phenotypes in terms of low levels of STIL and CDK2 could not be recaptured upon cyclin D1 depletion (Figure 10), suggesting that low cyclin D1 levels are not the leading cause of this G1 arrest.

Taken together, all these results strongly suggested that NEK7 is required for cell cycle progression during early G1 phase.

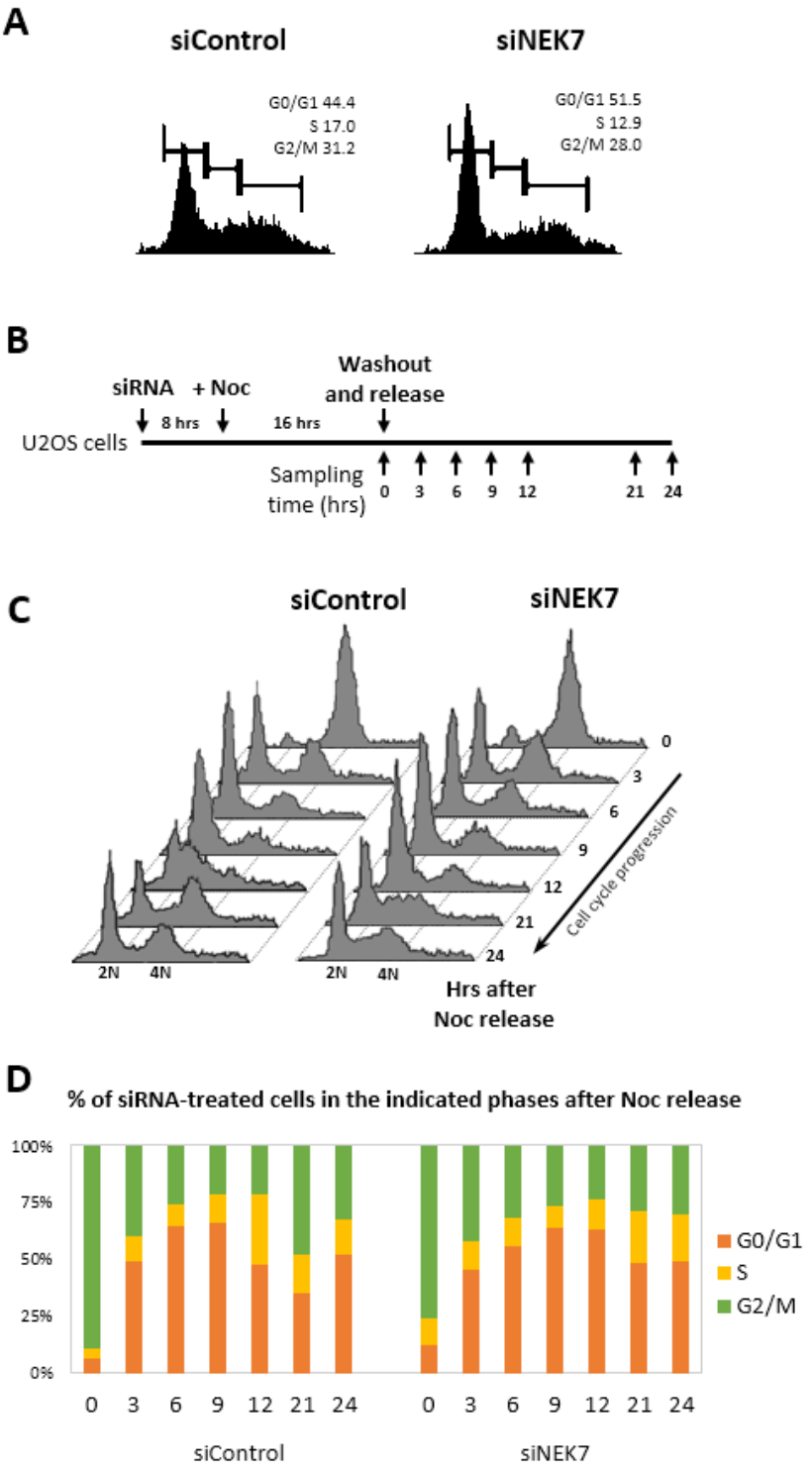

Figure 7. DNA content profiles of control and NEK7-depleted cells after a nocodazole arrest. (A) Asynchronous U2OS cells were transfected with control or NEK7 siRNAs for 48 hours, and the cells were analyzed for their DNA content profiles. (B) Schematic of the experimental conditions in (C-D). U2OS cells were transfected with control or NEK7 siRNAs for 8 hours, and then synchronized at early mitosis with 100 ng/ml nocodazole (Noc) for 16 hours. The cells were then released into fresh medium and collected at the indicated time points. (C) The DNA content profiles for individual time points are indicated. (D) A histogram for the DNA content profiles in (C) is shown.

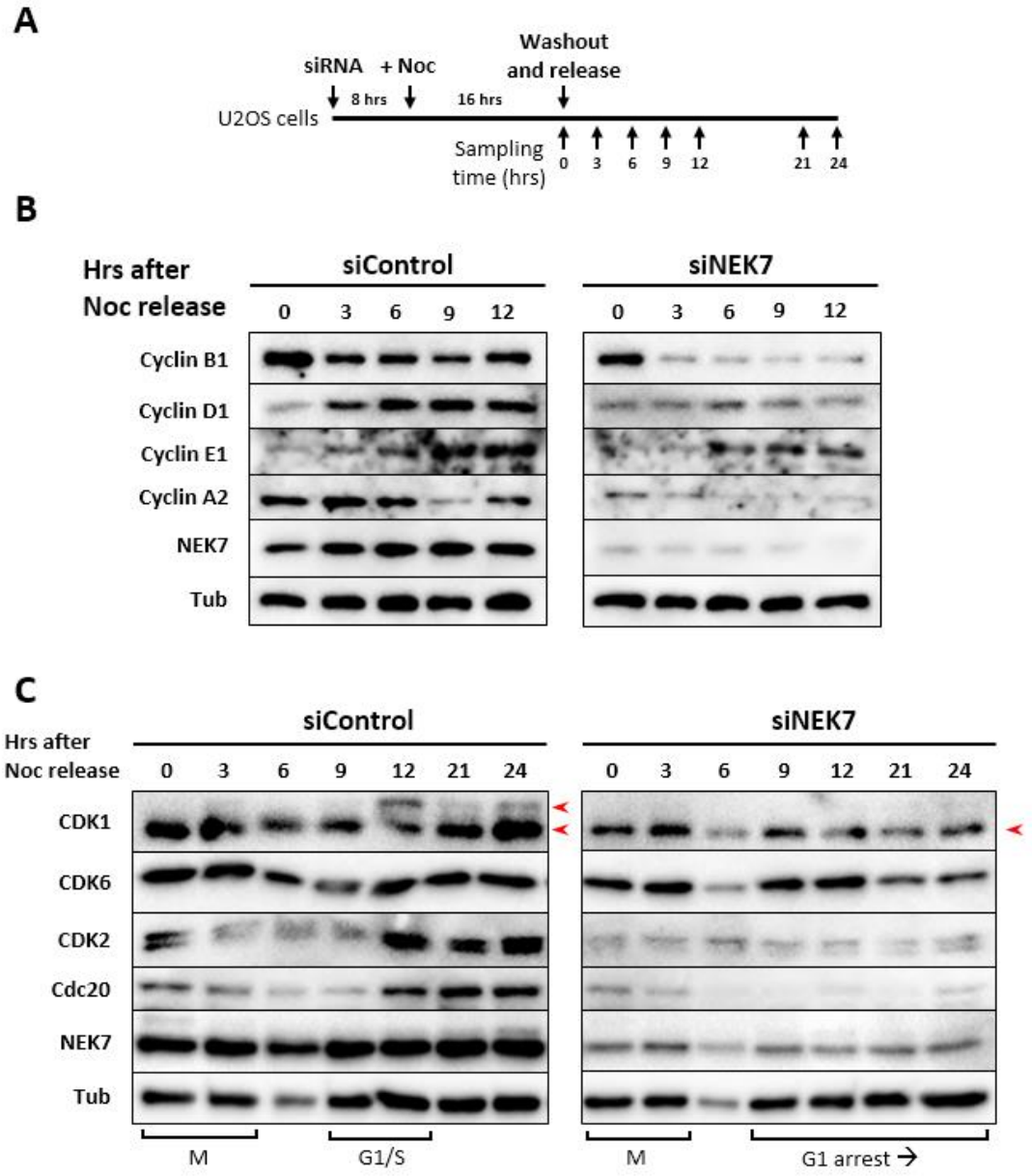

Figure 8. Reduced levels of cell cycle proteins in NEK7-depleted cells. (A) Schematic of the experimental conditions in (B-C). U2OS cells were transfected with control or NEK7 siRNAs for 8 hours, and then synchronized at early mitosis with 100 ng/ml nocodazole (Noc) for 16 hours. The cells were then released into fresh medium and collected at the indicated time points. (B, C) Total cell lysates were analyzed by immunoblotting using antibodies against the indicated proteins at least twice. All samples treated with control and NEK7 siRNAs were blotted on the same membrane; they have been separated for clarity. Red arrowheads indicate band-shifted proteins.

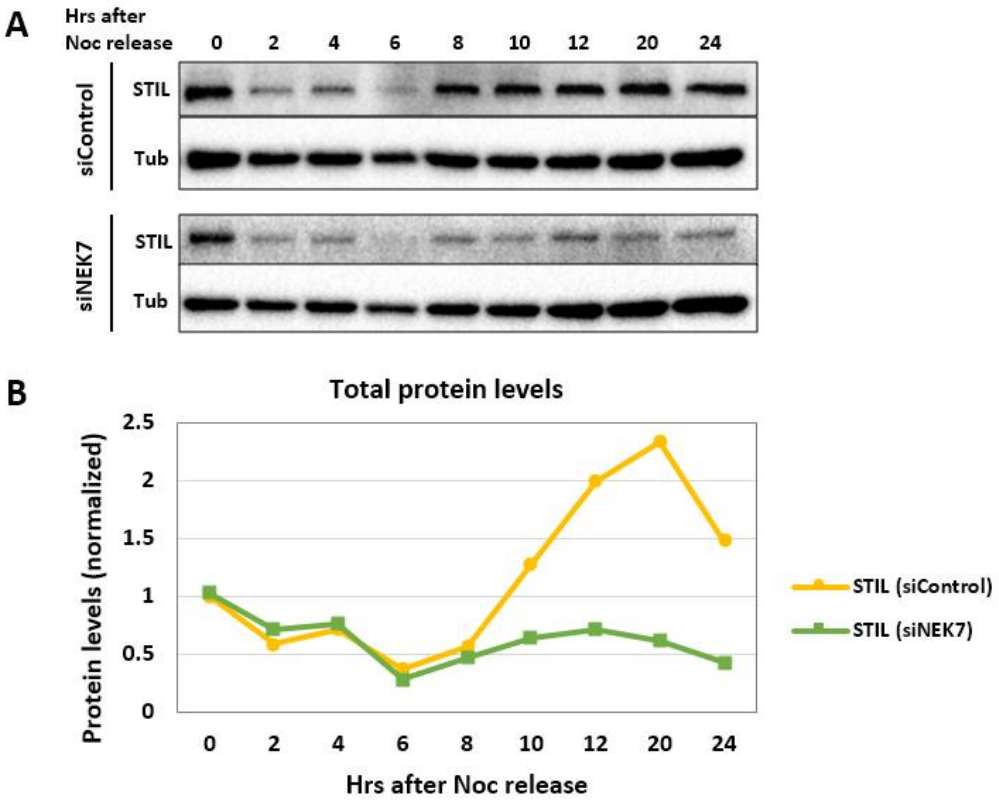

Figure 9. Reduced levels of the centriolar protein STIL in NEK7-depleted cells. U2OS cells were transfected with control or NEK7 siRNAs for 8 hours, and then synchronized at early mitosis with 100 ng/ml nocodazole (Noc) for 16 hours. The cells were then released into fresh medium and collected at the indicated time points. (A) Total cell lysates were analyzed by immunoblotting using antibodies against the indicated proteins at least twice. (B) Quantification of the protein levels shown in (A), normalized against the protein levels of tubulin.

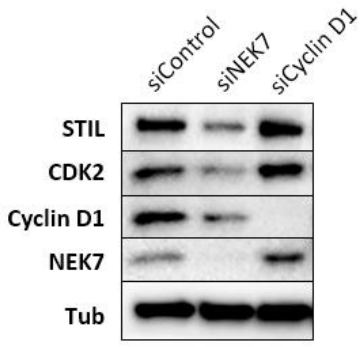

Figure 10. NEK7 depletion vs. cyclin D1 depletion. U2OS cells were transfected with control, NEK7, or cyclin D1 siRNAs for 48 hours, and total cell lysates were analyzed by immunoblotting using antibodies against the indicated proteins.

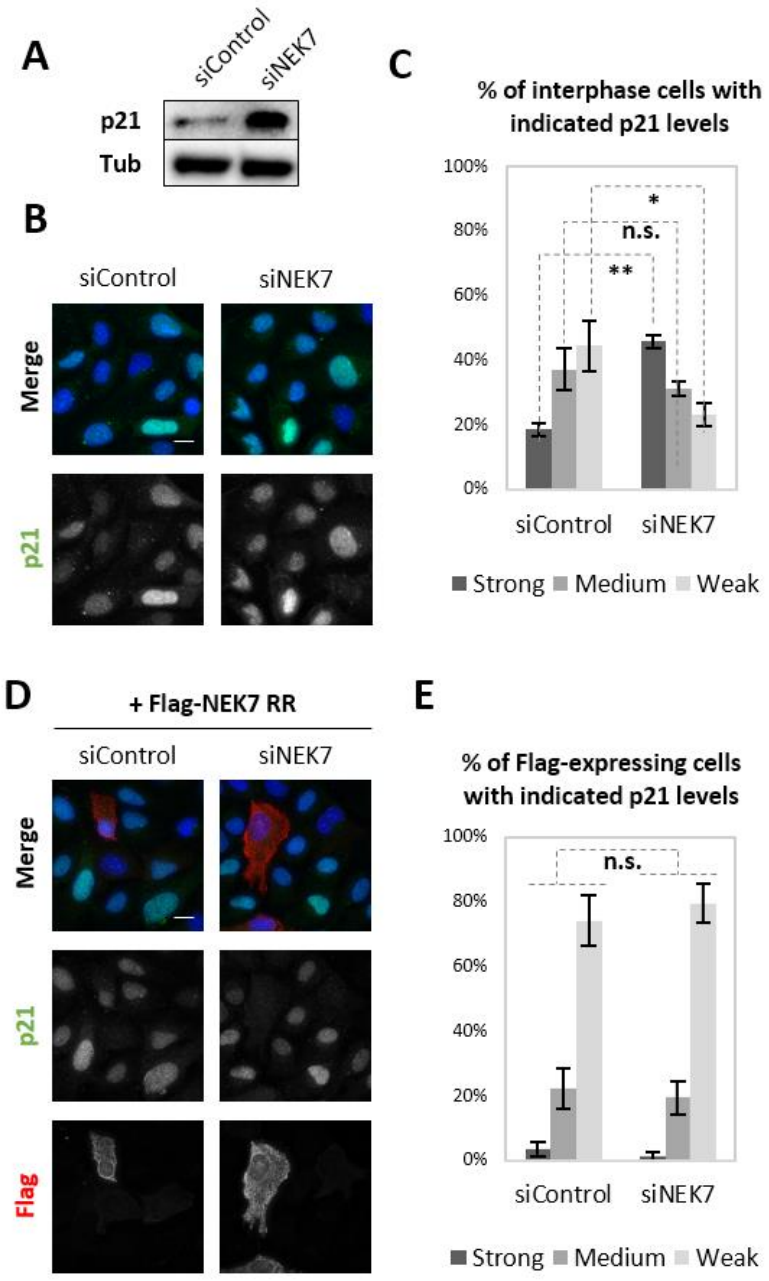

Figure 11. Differential levels of p21 in NEK7-depleted cells. (A) Asynchronous U2OS cells were transfected with control or NEK7 siRNAs for 48 hours, and total cell lysates were analyzed by immunoblotting against the indicated antibodies. (B-E) U2OS cells were transfected with control or NEK7 siRNAs for 24 hours, and then transfected with either Flag (B, C) or Flag-NEK7 RR (siRNA resistant mutant) (C, D) for another 24 hours. The cells were then fixed and immunostained with the indicated antibodies. DNA is shown in blue. Scale bar: 20 μm. (C) The histogram represents the percentage of total interphase cells with the indicated p21 levels. More than 200 cells were counted in each experimental group. (E) The histogram represents the percentage of interphase cells exhibiting high and comparable fluorescence intensities of Flag-NEK7 RR with the indicated p21 levels. More than 100 cells were counted in each experimental group. All histogram values are mean percentages ± s.d. from three independent experiments. *P<0.05; **P<0.01; n.s. not significant (one tailed *t*-test).

3.2 Differential levels of p21 in NEK7-depleted cells

To further confirm that NEK7 depletion induces a G1 arrest, I decided to look at p21 levels in U2OS cells that were treated with control and NEK7 siRNAs for 48 hours. It is known that high levels of p21 can inhibit S-phase entry through the direct inhibition of CDK2 activity as well as by binding PCNA to inhibit DNA synthesis [19]. Interestingly, I found drastically elevated levels of p21 in NEK7-depleted cells (Figure 11A), which could potentially inhibit the G1/S transition.

Additionally, I characterized the nuclear levels of p21 in control and NEK7-depleted cells by immunofluorescence analyses. Control cells showed low to medium signals of nuclear p21, however, NEK7-depleted cells showed significantly higher levels of nuclear p21 (Figure 11B, C). Furthermore, upon expression of an siRNA-resistant mutant of wild-type NEK7 (RR), I observed that cells exhibiting high cytoplasmic NEK7 RR levels contained highly reduced p21 levels (Figure 11C, D). This suggests that the expression of NEK7 may play a role in keeping the levels of p21 low, thus promoting S phase entry and cell cycle progression.

3.3 NEK7-depleted cells show cell cycle progression defects other than a G1 arrest

Considering my results that the expression levels of several important cell cycle proteins required for proper G1 progression are affected upon the depletion of NEK7 (Figures 7-11), it was certain that NEK7-depleted cells showed defects in cell cycle progression. However, it was not clear whether the low levels of these cell cycle regulatory proteins were the cause or consequence of the G1 arrest induced upon NEK7 depletion. To investigate what happens in NEK7-depleted cells in S phase, I performed the following studies.

3.3.1 NEK7-depleted cells exhibit delays in DNA replication and mitosis

I designed an experiment in I asked whether cells that are already in S phase could complete DNA replication and undergo mitosis even in the absence of NEK7. In order to overcome the G1 arrest that was induced upon a prolonged NEK7 depletion, I treated U2OS cells with either control or NEK7 siRNAs for 8 hours, and then arrested these cells at the G1/S transition or in S phase by adding thymidine to the medium for 16 hours, followed by subsequent release into fresh medium and sample collection (Figure 12A). The short duration of siRNA treatment ensured that the majority of the cells had not yet been arrested in G1 (Figure 12B, C), which allowed me to characterize the progression through the rest of the cell cycle for NEK7-depleted cells. The DNA content profiles of cells treated with siNEK7 indicated that some of these cells were able to complete DNA replication and completed mitosis as well, however, many cells exhibited delays in DNA replication and mitosis (Figure 12B, C).

3.3.2 NEK7-depleted cells have reduced levels of proteins essential for DNA replication

I further characterized the cellular environment in these cells by checking the expression levels of various cell cycle regulatory proteins such as cyclins and CDKs.

Similar to my results in Figure 8, I observed that the expression levels of cyclin D1 were strongly diminished in NEK7-depleted cells, even though they remained elevated during S phase progression in control cells (Figure 13B). Cyclin D1 has been found to play an essential role not only in passage through the restriction point during G1, but also in progression through the S and G2 phases, as an indicator of mitogenic signalling [83]. Thus, low cyclin D1 levels may impair S phase progression in NEK7-depleted cells.

Next, I looked at cyclin E1. In control cells, cyclin E1 exhibited an increase in expression followed by a reduction as cells went through S phase, indicative of cyclin E1 degradation (Figure 13B) [84,85]. In NEK7-depleted cells, cyclin E1 levels were unaffected relative to control cells, confirming that the cells were not arrested in G1 in these conditions and could progress through S phase.

On the other hand, when I looked at the expression levels of the S phase cyclin A2 and CDK2, they were still significantly low in NEK7-depleted cells compared to control cells (Figure 13B, C). Cdc20 protein levels were also drastically reduced in NEK7-depleted cells despite progression of the cell cycle (Figure 13C). Depletion of cyclin A2 has been shown to cause delays in the G2/M transition [8,86,87], and Cdc20 plays a crucial role in the spindle assembly checkpoint for chromosome segregation [88]. Hence, these low levels of cyclin A2 and Cdc20 can largely account for the significant mitotic delays as seen in these NEK7-depleted cells (Figure 13), as well as previously reported mitotic defects [68,73–75].

Lastly, I looked at the expression levels of the procentriolar protein STIL. Similar to my previous results (Figure 9), STIL exhibited very low levels in NEK7-depleted cells compared to control cells despite S phase progression (Figure 13D).

Collectively, my results suggest that the various defects in cell cycle progression observed upon depletion of NEK7 can largely be explained by the anomalous downregulation of the expression levels of several critical cell cycle proteins.

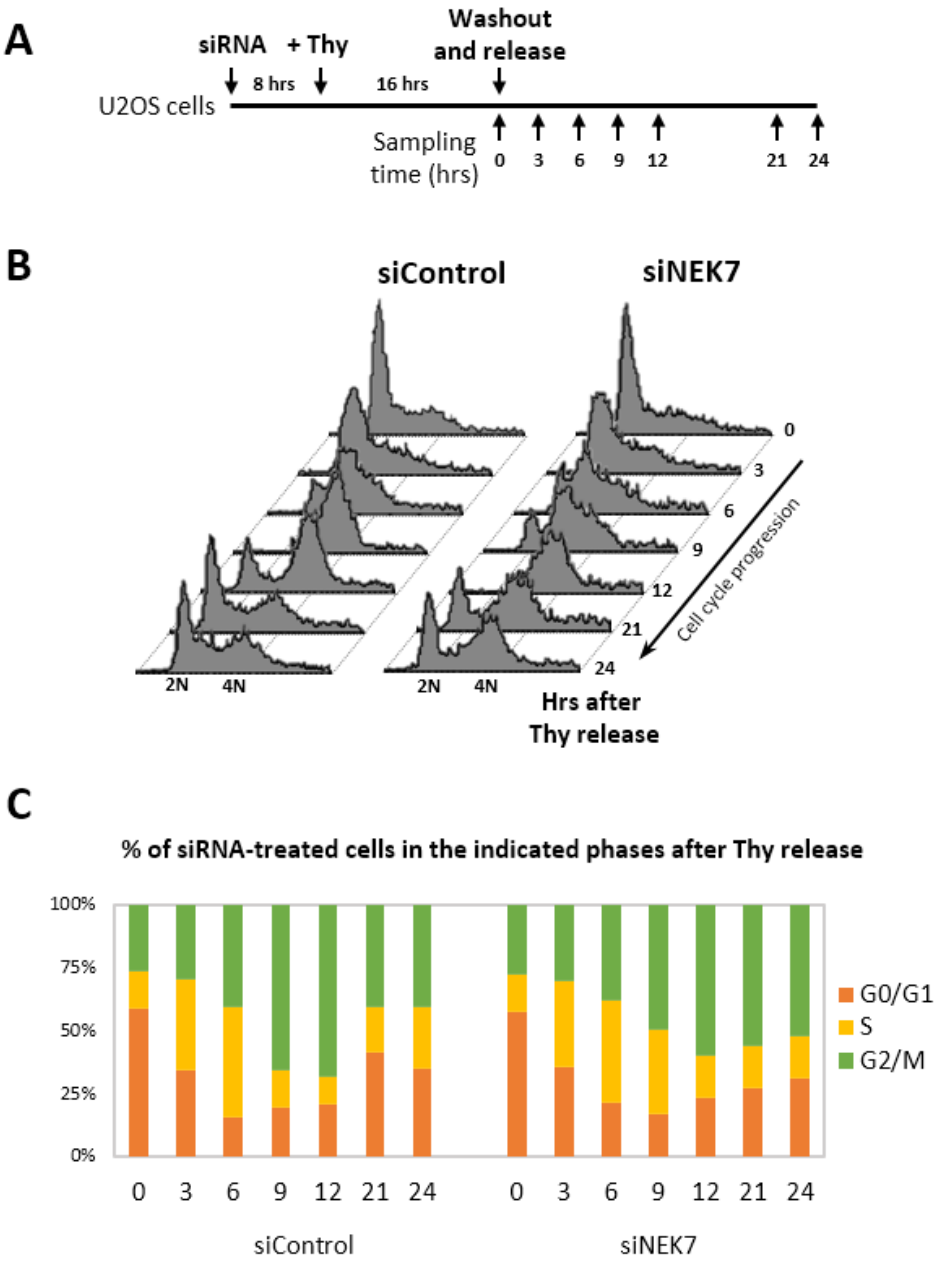

Figure 12. DNA content profiles of control and NEK7-depleted cells after a thymidine arrest. (A) Schematic of the experimental conditions in (B-C). U2OS cells were transfected with control or NEK7 siRNAs for 8 hours, and then synchronized at S phase with 2 mM thymidine (Thy) for 16 hours. The cells were then released into fresh medium and collected at the indicated time points. (B) The DNA content profiles for individual time points are indicated. (C) A histogram for the DNA content profiles in (B) is shown.

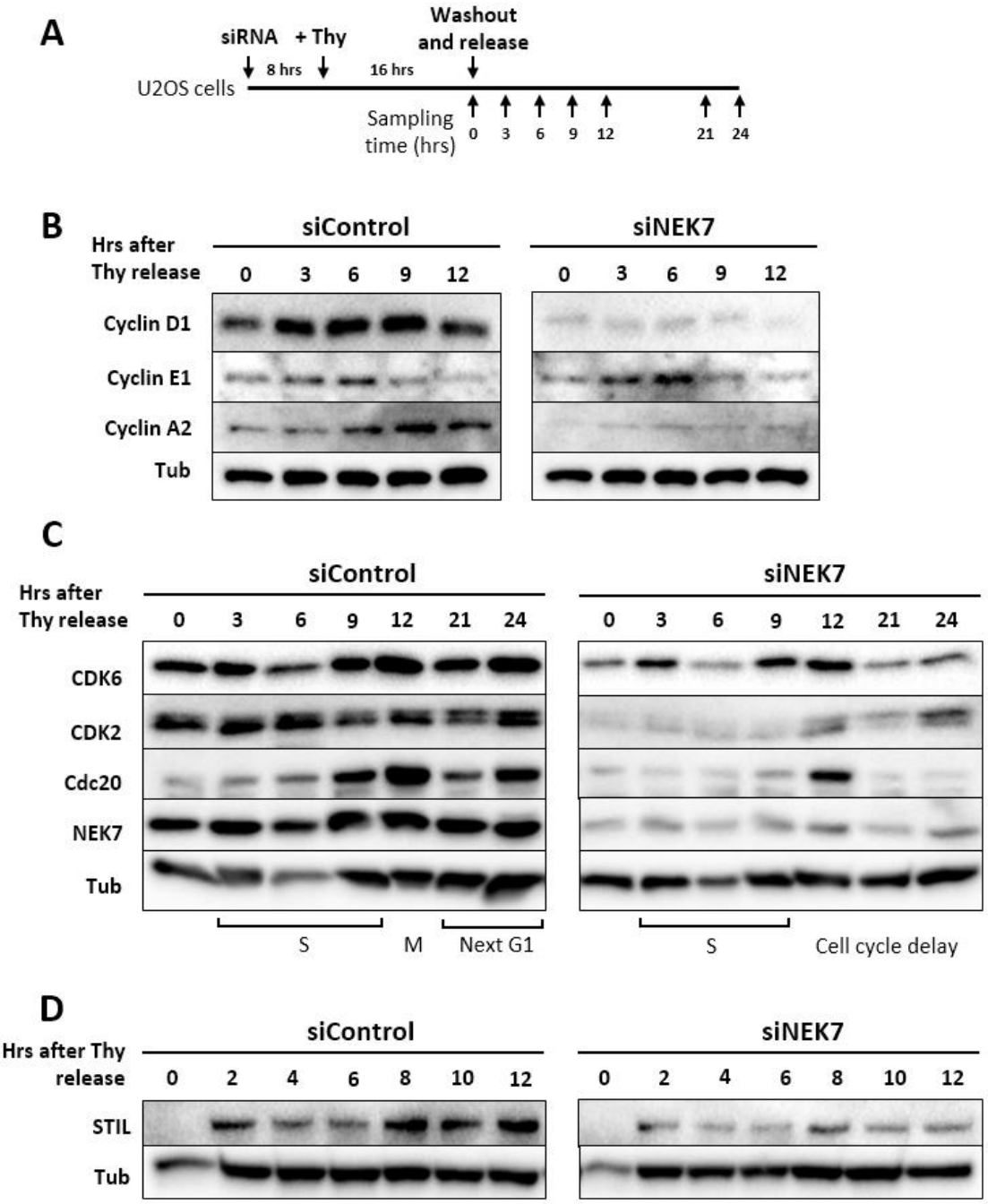

Figure 13. Reduced levels of S phase proteins in NEK7-depleted cells. (A) Schematic of the experimental conditions in (B-C). U2OS cells were transfected with control or NEK7 siRNAs for 8 hours, and then synchronized at S phase with 2 mM thymidine (Thy) for 16 hours. The cells were then released into fresh medium and collected at the indicated time points. (D) U2OS cells were treated as in (B, C) and collected at the indicated time points. (B-D) Total cell lysates were analyzed by immunoblotting using antibodies against the indicated proteins at least twice. All samples treated with control and NEK7 siRNAs were blotted on the same membrane; they have been separated for clarity.

3.4 Kinase activity of NEK7 through the cell cycle

NEK7 is known to be activated by NEK9 via phosphorylation on serine 195 (S195) [69,70], and it then undergoes dimerization and autophosphorylation upon activation [89]. Although NEK7 has been shown to play important roles throughout the cell cycle, the precise timing of NEK7 activation has not been characterized. In order to understand the duration of the cell cycle for which the NEK7 kinase is active, I performed *in vitro* kinase assays using overexpressed as well as endogenous NEK7 proteins.

First, I tested the kinase activity of immunoprecipitated Flag-NEK7 mutants by assessing autophosphorylation levels on NEK7 (Figure 14A). I used four constructs of NEK7: wild type NEK7 (WT), kinase dead NEK7 (KD, contains a single mutation of K64M), non-phosphorylatable NEK7 (S195A), and a phosphomimetic mutant at S204 (S204D). S204 on NEK7 was identified to be phosphorylated during mitosis [90], and it was also shown that the S204A mutant of NEK7 exhibited high kinase activity, whereas the S204D mutant was inactive [91], suggesting that NEK7 may be inactivated during mitosis by phosphorylation. Accordingly, I observed that the kinase dead (KD) mutant of NEK7 exhibited no kinase activity, and the S195A and S204D mutants exhibited very low activity (Figure 14A).

Additionally, I checked the kinase activity of Flag-NEK7 that had been immunoprecipitated from cells synchronized either at G1 using lovastatin (Lov), at G1/S using mimosine (Mim), or during S phase using thymidine (Thy), or at early mitosis using nocodazole (Noc) (Figure 14A). Similarly, I found that overexpressed NEK7 appeared to have high kinase activity during G1 and S, but reduced activity during mitosis. This suggests that NEK7 is active primarily during interphase.

Lastly, I analyzed the kinase activity of endogenous NEK7 which had been immunoprecipitated from U2OS cells that had been synchronized at early mitosis by a nocodazole arrest and then released into fresh medium (Figure 14B, C). I found that the autophosphorylation activity of NEK7 was relatively low during mitotic exit and early G1. However, autophoshorylation on NEK7 sharply increased towards the 10 hour time point, which corresponds to S phase entry. These results collectively suggest that NEK7 is activated around the G1/S transition and functions during interphase.

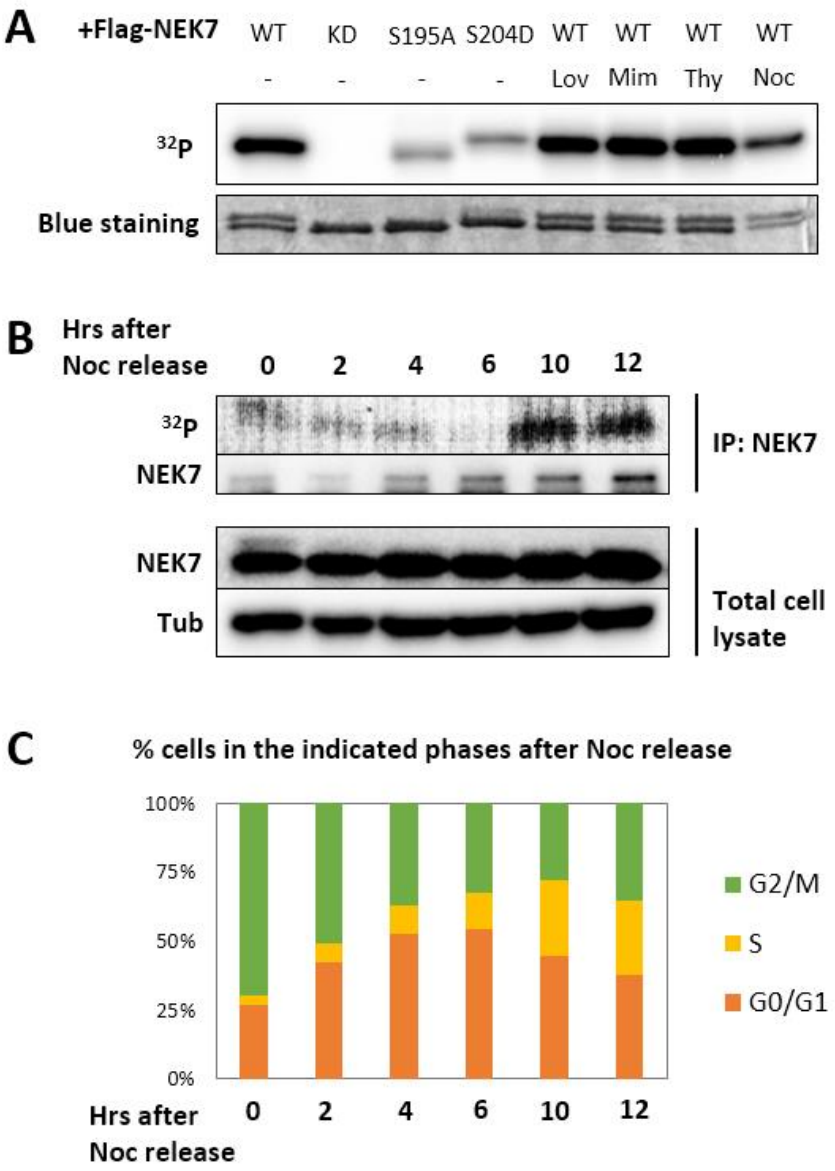

Figure 14. Kinase activity of NEK7 in the cell cycle. (A) Asynchronous U2OS cells were transfected with the indicated Flag-NEK7 plasmids for 24 hours, and synchronized at different stages for 16 hours using the indicated drugs. Flag-NEK7 proteins were then immunoprecipitated from total cell lysates, and incubated with [γ-^{32}P] ATP for *in vitro* kinase assays. The autophosphorylation of NEK7 was visualized by the incorporation of [γ-^{32}P] ATP by autoradiography, and the loaded proteins were monitored by SimplyBlue™ Safestaining. (B) U2OS cells were synchronized at mitosis with 100 ng/ml nocodazole for 16 hours. The cells were then released into fresh medium and collected at the indicated time points. Endogenous NEK7 was immunoprecipitated using the NEK7 antibody, and assessed for kinase activity by the incorporation of [γ-^{32}P]. The loaded proteins were monitored by immunoblotting. (C) DNA content profiles for the individual time points in (B) are indicated.

3.4 NEK7 is required for procentriole formation

My results so far suggested that NEK7 plays an important role in G1 phase progression, and may be required for proper progression through the rest of the cell cycle as well. Since the centrosome cycle is tightly linked to cell cycle progression, and procentriole formation is initiated at the G1/S transition, I speculated that NEK7 might perturb the earliest stages of centriole duplication as well.

The knockdown of NEK7 has been reported to inhibit centriole duplication, as well as reduce the total amount of pericentriolar material (PCM) that surrounds the centrioles and is required for the nucleation of spindles [76]. In addition, the PCM has been suggested to provide a suitable environment for centriole assembly by recruiting essential proteins [92], which was suggested to be the reason for the inhibition of centriole duplication in the absence of NEK7 [76]. However, centriole duplication is a multistage process, and both centriole duplication and PCM assembly are heavily dependent on the activities of various CDKs [60,61].

Considering my results that NEK7 is required for the G1/S transition and affects the expression of various cyclin/CDK complexes as well as the centriolar protein STIL, I speculated that some of the other components required for the early stages of procentriole formation may also be affected.

3.4.1 Loss of procentriolar components from the centrosomes upon NEK7 depletion

I examined the localization of various proteins involved in the procentriole assembly pathway by immunofluorescence, using the distal centriolar protein Centrin as a marker for the number of centrioles (Figure 15). In accordance with previous studies, most of the NEK7-depleted cells could not complete centriole duplication (Figure 15A, C), confirming that NEK7 is essential for centriole duplication.

I found that CEP192 and CEP152, which are the earliest scaffold proteins to promote procentriole assembly [36], were not affected upon NEK7 depletion (Figures 28, 30). However, the kinase PLK4 which is dependent on CEP192 and CEP152 for centriolar

recruitment was absent from the centrosomes (Figure 15A, B). Similarly, I found that STIL and SAS-6, which are essential for centriolar cartwheel formation, as well as CPAP, which is required for centriole elongation [46,50], were also absent from the centrosomes upon NEK7 depletion (Figure 15A, B).

3.4.2 Low cytoplasmic levels of procentriolar components in NEK7-depleted cells

Surprisingly, by using immunoblotting analyses, I found that the levels of STIL, SAS-6, and CPAP were low not only at the centrosomes, but also in total cell lysates upon NEK7 depletion (Figure 16A). STIL, SAS-6, and CPAP are all known to be cell cycle-regulated proteins, and their expression levels increase during late G1 [46,55,56]. Thus, it is likely that the reduction in their cytoplasmic and centrosomal levels that was observed upon NEK7 depletion is a consequence of the G1 arrest.

I also tested the stability of overexpressed centriolar proteins in NEK7-depleted cells (Figure 16B, C). Interestingly, I found that even overexpressed STIL and SAS-6 exhibited reduced protein levels in the absence of NEK7. Additionally, upon overexpression of PLK4-Flag in NEK7-depleted cells, I found similarly reduced levels. These results suggest that the levels of these proteins are regulated by a mechanism distinct from transcriptional control in NEK7-depleted cells.

3.4.3 Overexpression of centriolar proteins cannot rescue centriole duplication in NEK7-depleted cells

Overexpression of either PLK4, STIL, or SAS-6 has been shown to cause amplification of centrioles independently of cell cycle-mediated regulation of the centrosomes [53–55]. Hence, I speculated whether overexpression of these proteins might be sufficient to rescue centriole duplication in NEK7-depleted cells. While overexpression of PLK4 and STIL induced centriole overduplication in control cells as expected, in cells pretreated with NEK7 siRNA, both centriole numbers as well as the numbers of PLK4/STIL foci were reduced (Figure 17). Interestingly, in the cells depleted of NEK7 and overexpressing PLK4, PLK4 formed ring-like foci, which is reminiscent of the phenotype associated with the

depletion of STIL [39]. This result suggests that, despite high PLK4 levels, centriole amplification was inhibited by the absence of STIL and possibly other procentriolar proteins. Furthermore, given that the overexpression of STIL did not rescue the expression levels of STIL at centrioles in NEK7-depleted cells (Figure 17), NEK7 may have an additional function in the maintenance of STIL at the centrioles.

Taken together, these results suggested that the inhibition of procentriole formation upon NEK7 depletion is due to low cytoplasmic expression levels of several important procentriole proteins, possibly caused by the G1 arrest.

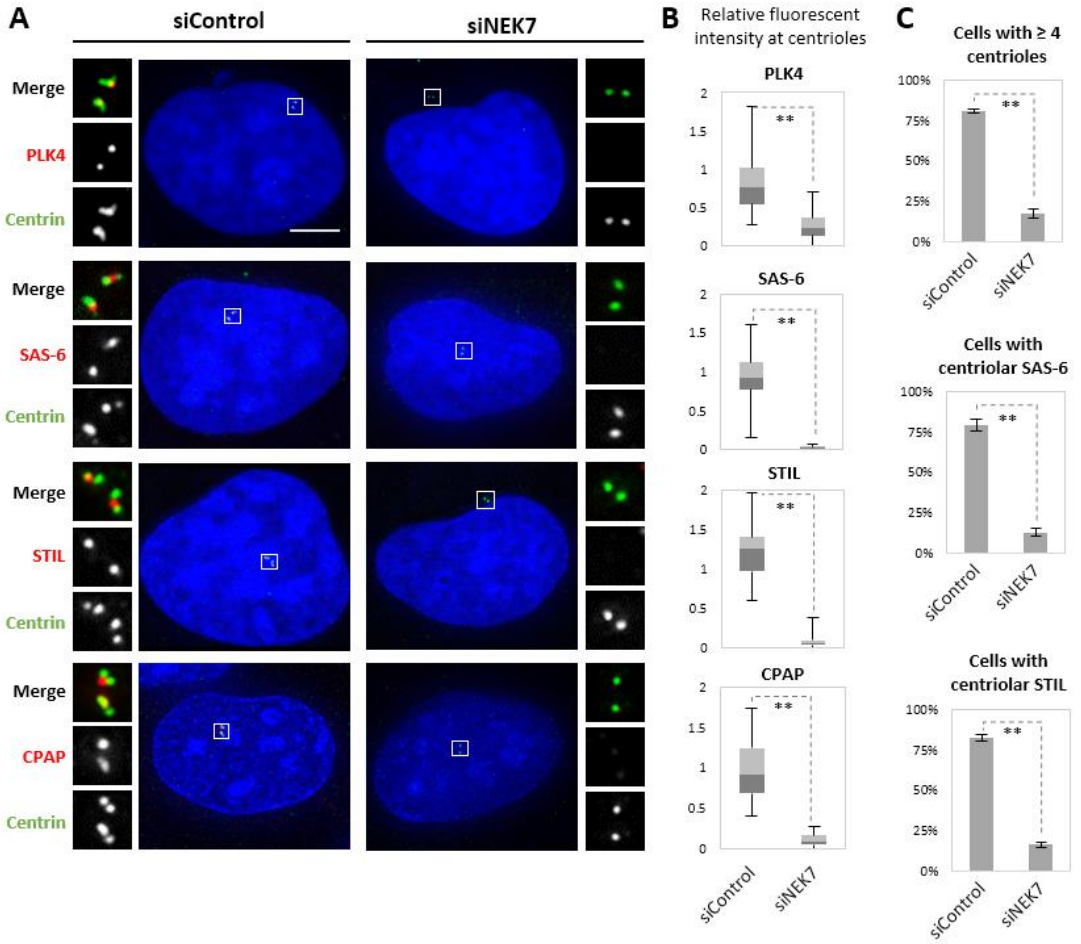

Figure 15. Loss of procentriole components from the centrosomes upon NEK7 depletion. (A) Asynchronous U2OS cells were transfected with control or NEK7 siRNAs for 48 hours, and the cells were fixed and immunostained using the indicated antibodies. DNA is shown in blue. Insets are magnified views of the centrosomes. Scale bar: 5 μm. (B) The fluorescence intensities of the indicated proteins at the centrioles were quantified on an arbitrary scale. (C) Histograms represent the percentage of interphase cells with the indicated centriolar markers. More than 50 cells were counted in each experimental group. All histogram values are mean percentages ± s.d. from three independent experiments. *P<0.05; <P<0.01; n.s. not significant (one tailed *t*-test).

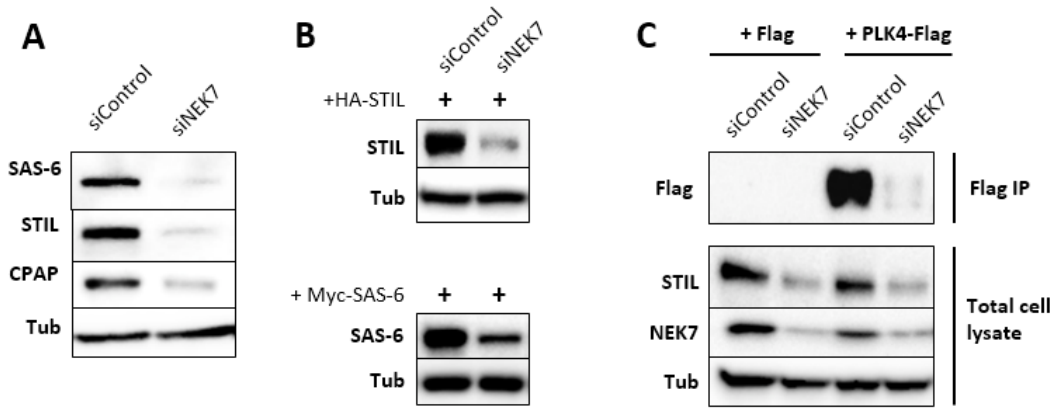

Figure 16. Low cytoplasmic levels of procentriolar proteins in NEK7-depleted cells. (A) Asynchronous U2OS cells were transfected with control or NEK7 siRNAs for 48 hours, and total cell lysates were analyzed by immunoblotting against the indicated proteins. (B, C) U2OS cells were transfected with control or NEK7 siRNAs for 24 hours, and then transfected with the indicated vectors for another 24 hours. (B) Total cell lysates were analyzed by immunoblotting against the indicated proteins. (C) PLK4-Flag proteins are difficult to detect in total cell lysates, and hence they were immunoprecipitated from total cell lysates using Flag beads. The IP fraction was analyzed by immunoblotting against the Flag epitope.

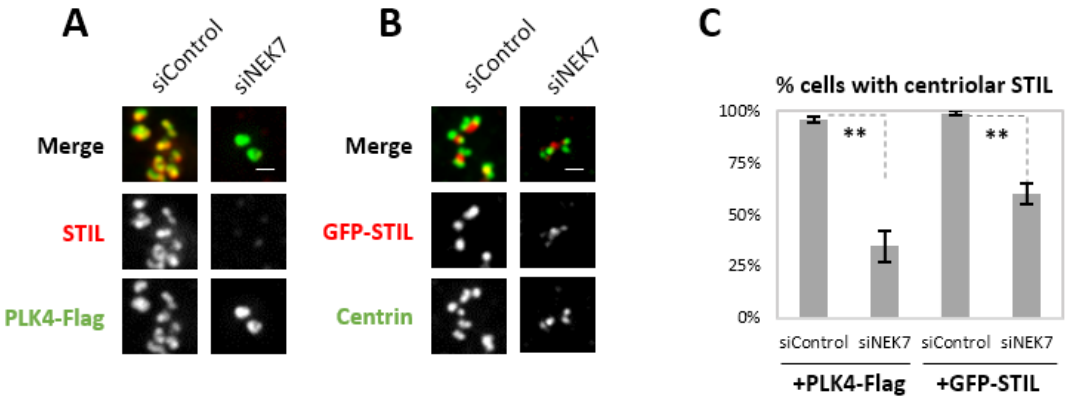

Figure 17. Overexpression of centriolar proteins cannot rescue centriole duplication in NEK7-depleted cells. (A) U2OS cells were transfected with control or NEK7 siRNAs for 24 hours, and then with PLK4-ΔPEST-Flag for another 24 hours, and finally fixed. (B) GFP-STIL U2OS cells were transfected with control or NEK7 siRNAs and simultaneously induced for overexpression of GFP-STIL, and they were fixed after 48 hours. Cells in (A) and (B) were immunostained with antibodies specific to STIL or GFP (red), and Flag or Centrin (green). Scale bar: 500 nm. (C) Histograms represent the population distributions of interphase cells containing centriolar STIL foci. More than 50 cells expressing high and comparable fluorescence intensities of PLK4-ΔPEST-Flag or GFP-STIL were counted in each experimental group. All histogram values are mean percentages ± s.d. from three independent experiments. *P<0.05; <P<0.01; n.s. not significant (one tailed *t*-test).

3.5 Depletion of NEK7 induces ciliogenesis

To assess the timing of the G1 arrest induced by the absence of NEK7, I decided to look at another centriole-associated phenotype that occurs as cells enter the G0/G1 phase. Several types of cells, such as RPE1 cells, frequently undergo ciliogenesis upon serum starvation, a method commonly used to arrest cells at the restriction point. During ciliogenesis, one of the unduplicated centrioles docks at the cell membrane for the formation of the primary cilium.

Several NEKs have previously been implicated in the regulation of ciliogenesis [65]. Additionally, my previous results suggested that the depletion of NEK7 causes a G1 arrest, which led me to speculate whether NEK7-depleted cells could also undergo ciliogenesis upon a G1 arrest. Hence, I treated RPE1 cells with NEK7 siRNA for 48 hours and tested the frequency of ciliation, compared to that of control cells following serum starvation for the same duration.

3.5.1 A G0-like state is achieved in RPE1 cells upon NEK7-depletion

To quantify ciliogenesis, I immunostained RPE1 cells with antibodies against acetylated tubulin (AcTub) and the intraflagellar transport protein IFT88, which mark both the cilium and centrioles (Figures 18 and 19). Astonishingly, I found that in NEK7-depleted cells, a high percentage of total RPE1 cells readily underwent ciliogenesis, and at approximately the same frequency as cells that had been grown in the absence of serum (Figure 18). This result suggested that the G1 arrest caused in siNEK7-treated cells may be very similar to cells that have entered G0/G1 following a prolonged serum starvation, and reinforced my hypothesis that NEK7 plays an important role in G1 progression, and particularly for overcoming the restriction point.

3.5.2 Behaviour of procentriolar proteins in ciliated cells

In RPE1 cells, centriole duplication is usually inhibited upon serum starvation, as can be seen by the presence of only two Centrin foci (Figure 18). However, in both the control

experiments with serum starvation and in NEK7-depleted cells, I found that PLK4 could localize to the basal bodies (Figure 19A). In the control experiments with serum starvation, I observed that both STIL and SAS-6 were present near the basal bodies in approximately half of all ciliated cells (Figure 19B-D), and centriolar recruitment of both STIL and SAS-6 appeared to be independent of the total expression levels of these proteins (Figure 19E). This suggested that recruitment of STIL and SAS-6 to the proximal part of mother centrioles may not entirely be contingent upon the G1/S transition unlike centriole duplication. On the other hand, in NEK7-depleted cells, I found that very few cells exhibited centrioles with STIL and SAS-6 foci, even though the total protein levels of STIL and SAS-6 in NEK7-depleted cells were not significantly different from the control serum-starved cells (Figure 19B-E). These results indicate that the G1 arrest may not be the sole reason for the defective recruitment of STIL and SAS-6 to the centrioles, but that they may be regulated by NEK7 in another manner.

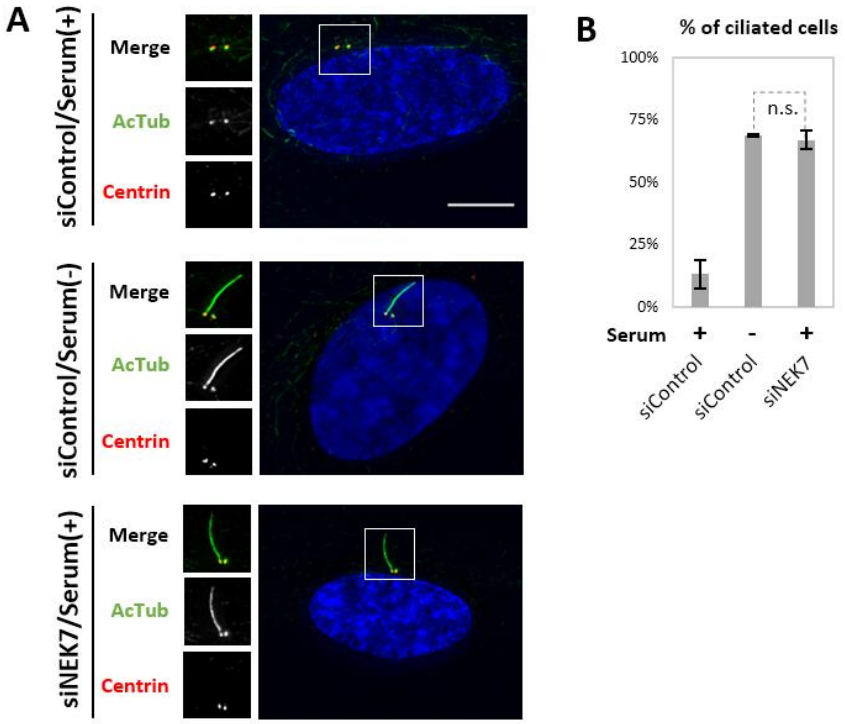

Figure 18. Depletion of NEK7 induces ciliogenesis. RPE1 cells were transfected with control and NEK7 siRNAs for a total of 48 hours, and additional samples were simultaneously treated with a control siRNA and released into serum-free medium for a total of 48 hours. (A) The cells were then fixed and stained with the indicated antibodies. DNA is shown in blue. Scale bar: 5 μm. (B) The histogram represents the percentage of interphase cells that were ciliated. More than 50 cells were counted in each experimental group.

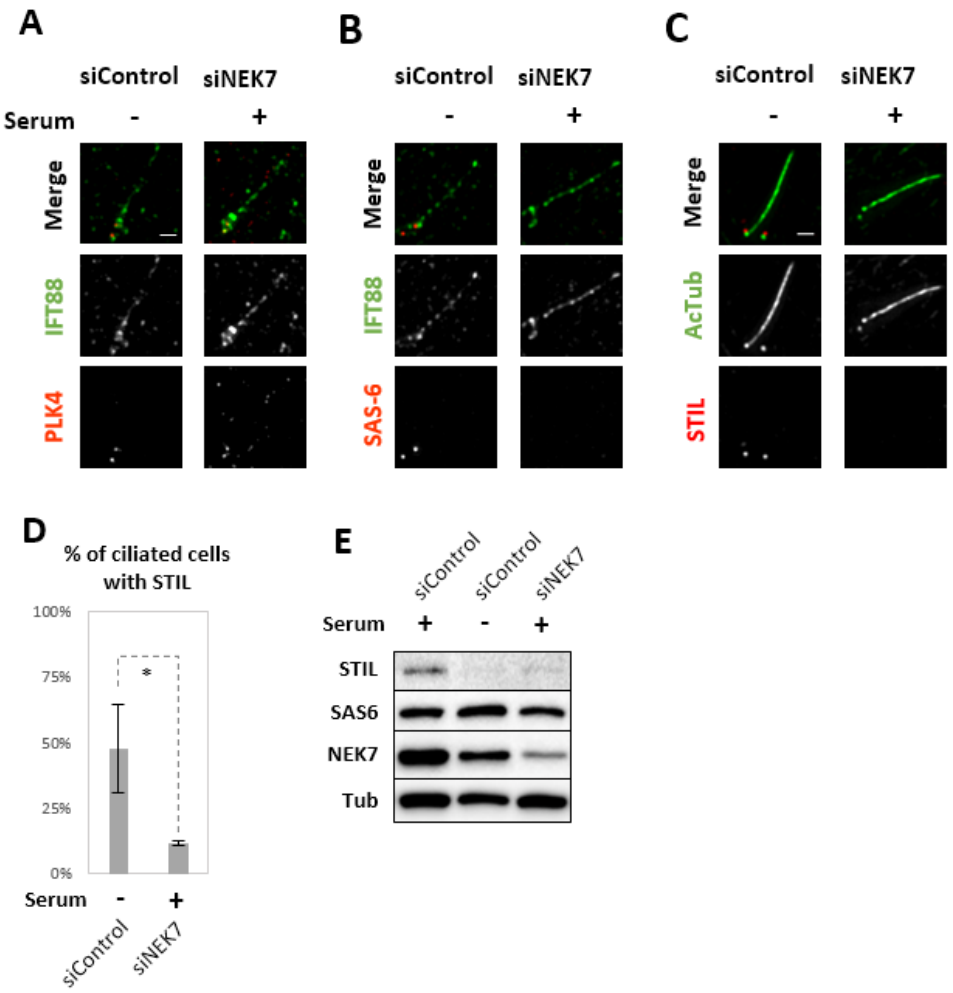

Figure 19. Behaviour of procentriolar proteins in ciliated cells. RPE1 cells were transfected with control and NEK7 siRNAs for a total of 48 hours, and additional samples were simultaneously treated with a control siRNA and released into serum-free medium for a total of 48 hours. (A-C) The cells were then fixed and stained with the indicated antibodies. The images show magnified views of centriolar proteins at the base of cilia. (D) The histogram represents the percentage of ciliated cells that exhibited STIL foci at the basal bodies. More than 50 cells were counted in each experimental group. All histogram values are mean percentages ± s.d. from three independent experiments. *P<0.05; <P<0.01; n.s. not significant (one tailed *t*-test). (E) Total cell lysates in each condition were analyzed by immunoblotting against the indicated antibodies.

3.6 Regulation of the centriolar protein STIL in NEK7-depleted cells

I found that the depletion of NEK7 induces a G1 arrest, and to a certain extent, this arrest could explain the downregulation of various procentriolar proteins, such as STIL and SAS-6, that are expressed towards the G1/S transition [3,59]. However, I also observed that in NEK7-depleted cells that could proceed through the S phase, STIL proteins were still downregulated despite cell cycle progression (Figure 13D). Similarly, when STIL proteins were ectopically expressed in NEK7-depleted cells, they continued to exhibit reduced protein levels (Figure 16B). These data suggested that the downregulation of STIL in NEK7-depleted cells may not entirely be caused by the inhibition of transcriptional activation caused by the G1 arrest. To test for mechanisms regulating the expression of STIL that were distinct from transcriptional control, I decided to examine and characterize the expression levels of STIL under different conditions.

3.6.1 STIL protein expression under various conditions

In order to understand how STIL protein expression may be impacted under different conditions with or without NEK7, I performed experiments in which I treated control or NEK7-depleted cells with various molecular inhibitors that arrest the cell cycle at different stages (Figure 20). A summary of the molecular inhibitors used and their impact on STIL expression is provided in Table 2.

Treatment of control cells with lovastatin, mimosine, or serum starvation, which cause a G1 or G1/S arrest, caused a very slight decrease in STIL levels compared to untreated cells. On the other hand, NEK7-depleted cells exhibited extremely reduced STIL levels under these conditions. Cells that were arrested in S-phase by thymidine, aphidicolin, or HU exhibited relatively elevated levels of STIL both in control and NEK7-depleted cells, presumably due to an increase in STIL transcription. Finally, treatment of these cells with nocodazole or siCdc20, both of which cause a mitotic arrest, exhibited slightly reduced levels of STIL, as well as an upshifted band that may indicate mitotic phosphorylation of STIL (Figure 20). Collectively, these data confirm that STIL is a cell cycle-regulated protein, and exhibits reduced protein levels in NEK7-depleted cells.

3.6.2 Phosphorylation on STIL fragments on NEK7 *in vitro*

Since NEK7 is a kinase, it is possible that NEK7 could directly phosphorylate different sites on STIL for its regulation. STIL is a large and mostly disordered protein (1287 aa), and it was difficult to purify full length STIL bacterially. Thus, in order to test whether NEK7 could directly phosphorylate STIL, I purified shorter fragments of STIL and performed an *in vitro* kinase assay using Flag-NEK7 purified from human cells (Figure 21A, B).

I found that the STIL fragments N2, M, and C could be phosphorylated *in vitro* by Flag-NEK7. Mass spectrometry analyses led to the identification of 11 phosphorylated serine residues within STIL M and C (Figure 21C). I mutated all of these residues individually and in different combinations to alanines in a full length HA-STIL construct to identify whether any of these mutations may alter the stability of STIL in control or NEK7-depleted cells. However, none of these mutants appeared to affect the stability of STIL (data summarized in Table 3). Indeed, several of these residues were identified to be phosphorylated by the kinase PLK4 as well *in vitro* [39], suggesting that these sites may represent promiscuous phosphorylations rather than NEK7-specific phosphorylation.

3.6.3 Mutation of the KEN-box in STIL rescues reduced STIL levels

In an effort to narrow down the region of STIL that may contribute to its downregulation upon NEK7 depletion, I generated many different mutants of STIL and tested their stability in control and NEK7-depleted cells (full list in Table 3). Among these mutants, I found that the deletion of the C-terminal region spanning residues 1001-1287 (ΔC) largely rescued the low protein levels of STIL in NEK7-depleted cells (Figure 22). I also observed that deletion of the M-region spanning residues 601-1000 (ΔM) rescued the low protein levels of STIL, and deletion of both the M- and C-regions (N) could completely rescue the low levels of STIL. I generated various mutants of STIL to identify the region in M responsible for its stability, but I was unable to narrow it down precisely.

Upon narrowing down the C-terminal region of STIL, I discovered that a triple alanine mutation of the KEN-box (KEN/AAA) in STIL was effective in rescuing the protein

expression levels of ectopically expressed STIL in NEK7-depleted cells. The KEN-box is the major recognition motif for the APC/C cofactor Cdh1 [57,58], and it is found in many proteins that are degraded by the APC/C^{Cdh1}-mediated ubiquitin-proteasomal pathway during late mitosis, including several centriolar proteins such as SAS-6 and CPAP [46,56]. Since SAS-6 also contains a KEN-box, I also tested the stability of a KEN/AAA mutant of SAS-6 in NEK7-depleted cells, but I did not observe any rescue in expression. However, SAS-6 has been reported to be targeted by another E3 ubiquitin ligase during G1 [93]; it is therefore possible that this and possibly other unidentified ubiquitin ligases may cause the low cellular levels of SAS-6 in NEK7-depleted cells.

3.6.4 Reduced STIL levels in NEK7-depleted cells are caused by APC/C^{Cdh1}-mediated proteasomal degradation

My findings that the KEN/AAA mutant of STIL could be stably expressed even in the absence of NEK7 suggested that the downregulation of STIL may in part be due to its ubiquitination by the APC/C^{Cdh1} and subsequent proteasomal degradation. To confirm whether STIL undergoes active degradation by the proteasome in NEK7-depleted cells, I treated these cells with the proteasome inhibitor, MG132 (Figure 23). As expected, both endogenous as well as ectopically expressed STIL were partially rescued upon proteasomal inhibition, whereas the protein levels of the KEN/AAA mutant of STIL were not largely affected.

3.6.5 A PACT-tagged KEN-box mutant of STIL can be stably recruited to the centrosomes

Earlier I found that despite STIL overexpression, STIL could not efficiently localize to the centrosomes in NEK7-depleted cells (Figure 17). My initial hypothesis to explain this phenotype was that recruitment of STIL to the centrosomes was affected in NEK7-depleted cells. However, in light of my findings that STIL could be degraded by the proteasome in NEK7-depleted cells, I speculated whether STIL may be undergoing localized proteasomal degradation at the centrosomes. To distinguish between these two

possibilities, I expressed a PACT-tagged construct of STIL to artificially target it to the centrosomes [94] in control and NEK7-depleted cells (Figure 24).

Similar to overexpressed STIL, I found that PACT-STIL also could not localize to the centrosomes, despite high cellular expression in NEK7-depleted cells, suggesting localized regulation of this protein. In contrast, I saw that the KEN/AAA mutant of PACT-STIL could stably localize to the centrosomes. These results strongly suggest that STIL may undergo localized degradation at the centrosomes via APC/C^{Cdh1} targeting.

In conclusion, I determined that the downregulation of STIL in NEK7-depleted cells is at least partly due to its ubiquitination by the APC/C^{Cdh1} and subsequent proteasomal degradation, and it is likely that STIL may be locally regulated at the centrosomes by the APC/C^{Cdh1}.

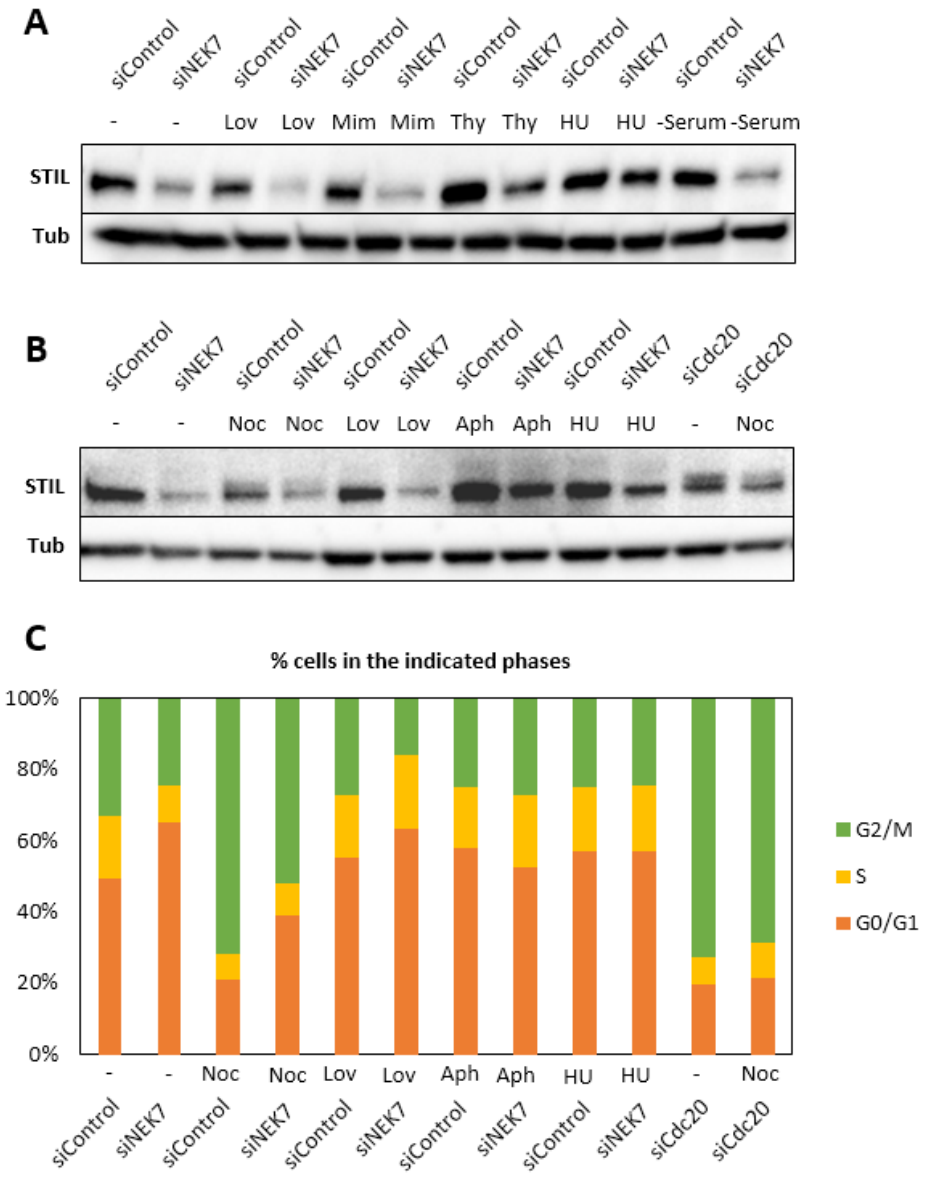

Figure 20. Expression levels of STIL under different conditions. (A, B) U2OS cells were transfected with control, NEK7, or Cdc20 siRNAs for 32 hours, and treated with the indicated conditions for an additional 16 hours. Total cell lysates were then analyzed by immunoblotting using the antibodies against STIL and Tubulin. (C) DNA content profiles of the samples shown in (B) are indicated.

Table 2. Expression levels of STIL under different conditions. This is a summary of the experiments conducted in Figure 20.

Treatment	Impact	Expression in siControl	Expression in siNEK7
No treatment	-	Normal	Low
Lovastatin (Lov)	Inhibition of cholesterol synthesis and proteasome Early G1 arrest	Slightly reduced	Very low
Mimosine (Mim)	Inhibition of thymidine, nucleotide biosynthesis Late G1 or G1/S arrest	Normal	Low
Thymidine (Thy)	Inhibition of DNA replication due to excess thymidine-induced feedback S-arrest	Elevated	Low, but slightly increased
Aphidicolin (Aph)	DNA polymerase inhibition S-arrest	Elevated	Partial expression
Hydroxyurea (HU)	Ribonucleotide reductase inhibition S-arrest	Elevated	Partial expression
Nocodazole (Noc)	Inhibition of microtubule polymerization Early M-arrest	Normal Partial band shift	Low Partial band shift
Serum starvation (-Serum)	Absence of mitogenic signalling G1 arrest	Normal	Low

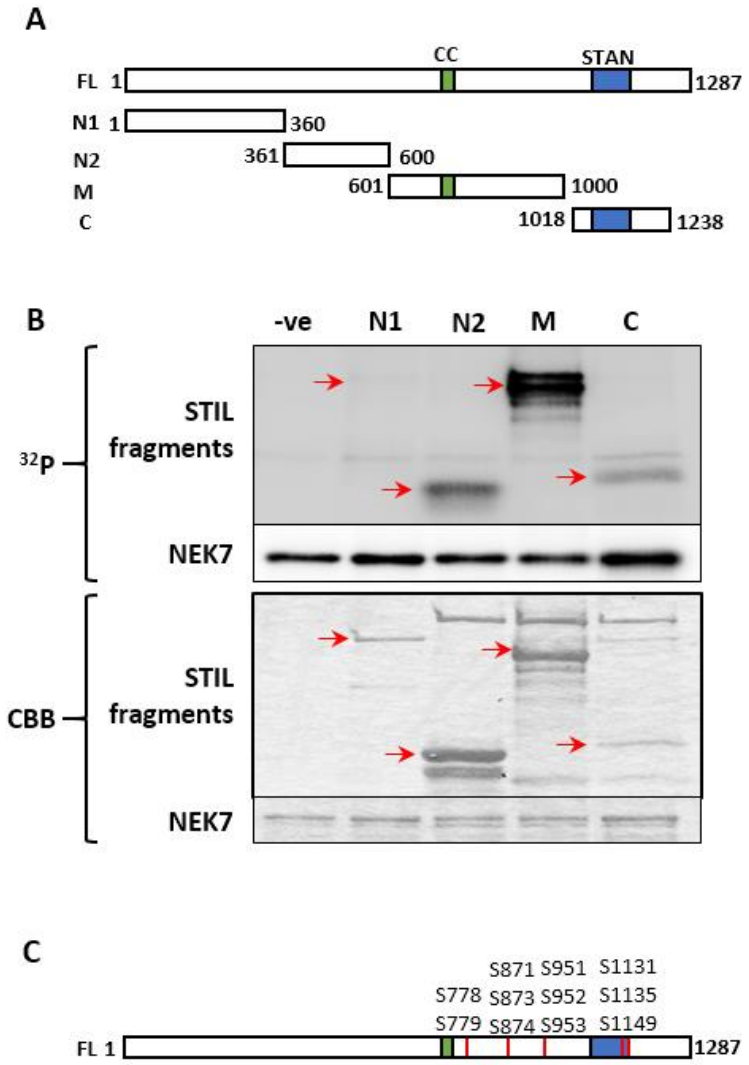

Figure 21. Phosphorylation on STIL fragments by NEK7 *in vitro*. (A) Schematic of STIL fragments that were used for the *in vitro* kinase assay. (B) STIL N2, M and C proteins were phosphorylated by NEK7 *in vitro* (top). Recombinant STIL fragments N1, N2, M, and C were bacterially expressed and purified, and were incubated with Flag-NEK7 proteins purified from HEK293T cells in the presence of [γ-^{32}P] ATP for the *in vitro* kinase assay. The incorporation of [γ-^{32}P] ATP to the substrates was visualized by autoradiography, and the loaded proteins were monitored by SimplyBlue™ Safestaining (bottom). Red arrows indicate the expected sizes of the recombinant STIL fragments. Autophosphorylation of NEK7 was used as a positive control. (C) Summary of NEK7-phosphorylated serine residues of STIL identified by mass spectrometry.

Table 3. Expression levels of STIL mutants tested in control and NEK7-depleted cells. This is a summary of the expression levels of all the different STIL constructs that were tested in control and NEK7-depleted conditions. U2OS cells were treated with control and NEK7 siRNAs for 24 hours, followed by transfection of the indicated constructs for another 24 hours in each case. Total cell lysates were analyzed by immunoblotting against STIL or HA.

HA-STIL mutant	Mutations	Expression in siNEK7 (relative to siControl)
WT	None	Low
ΔN1	Δ(1-360)	Low
ΔN2	Δ(361-600)	Low
ΔM	Δ(601-1000)	Partially expressed
ΔC	Δ(1001-1287)	Partially expressed
ΔM-N	Δ(601-720)	Low
ΔM-M	Δ(721-830)	Low
ΔM-C	Δ(831-1017)	Low
ΔCC (coiled coil)	Δ(721-750)	Low
N	1-600	Stable
M	601-1000	Low
C	1001-1287	Low
M.C	601-1287	Low
KEN/AAA	1243-1245 → AAA	Partially expressed
D-box mutant	R1135A, L1138A	Low
KEN/D-box	1243-1245 → AAA R1135A, L1138A	Low
ΔSTAN	Δ(1061-1083)	Low
ΔSTAN-N	Δ(1061-1083)	Low
ΔSTAN-M	Δ(1084-1105)	Low
ΔSTAN-C	Δ(1106-1147)	Low
ΔC1	Δ(1001-1100)	Low

ΔC2	Δ(1101-1200)	Low
ΔC3	Δ(1201-1287)	Partially expressed
ΔC4	Δ(1241-1287)	Low
ANAA	S871A, S873A, S874A	Low
AAAK	S951A, S952A, S953A	Low
7A	S871A, S873A, S874A, S951A, S952A, S953A, T998A	Low
AADNA	S1131A, S1132A, S1135A	Low
QAAP	S778A, S779A	Low
S1131A	S1131A	Low
S1135A	S1135A	Low
S1149A	S1149A	Low
E728R	E728R	Low
EXXR/RXXE	E969R, R972E	Low

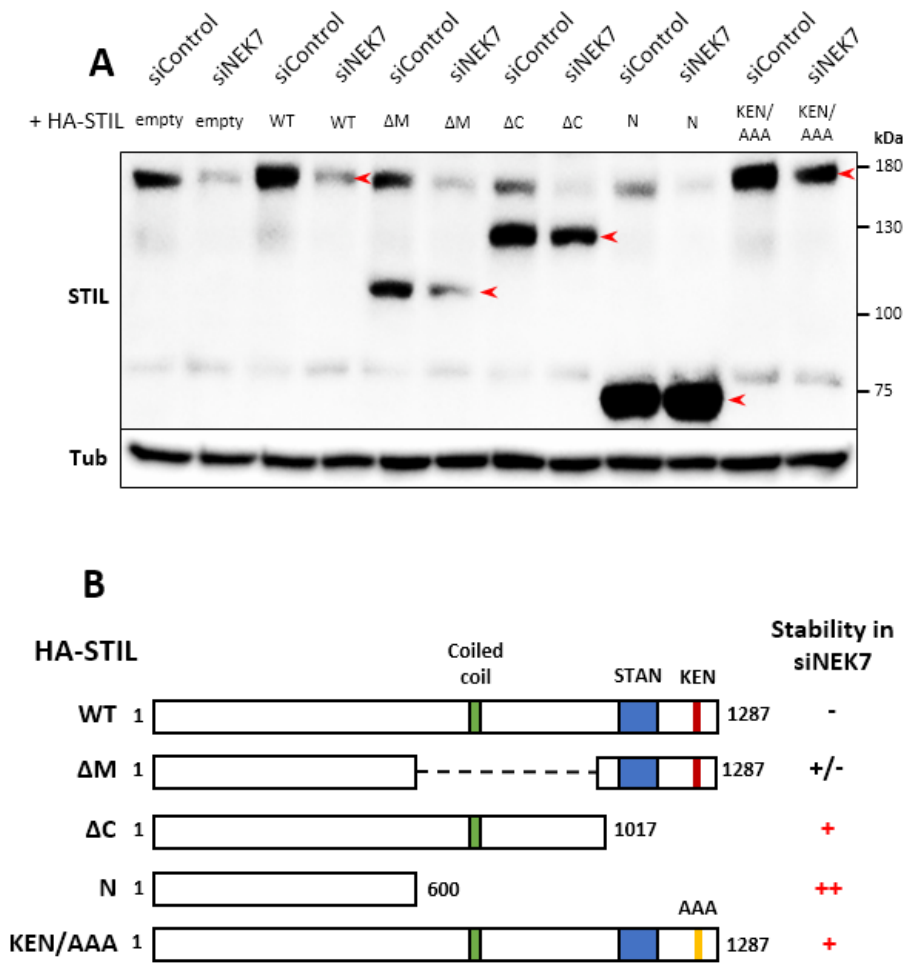

Figure 22. Expression levels of HA-STIL constructs in NEK7-depleted cells. (A) U2OS cells were transfected with control or NEK7 siRNAs for 24 hours and then transfected with the indicated HA-STIL vectors for another 24 hours. Total cell lysates were analyzed by immunoblotting using antibodies against HA or tubulin. The values on the right indicate approximate protein sized in kDa. Red arrowheads indicate expected bands for different constructs. (B) Schematic of the HA-STIL constructs that were used in (A).

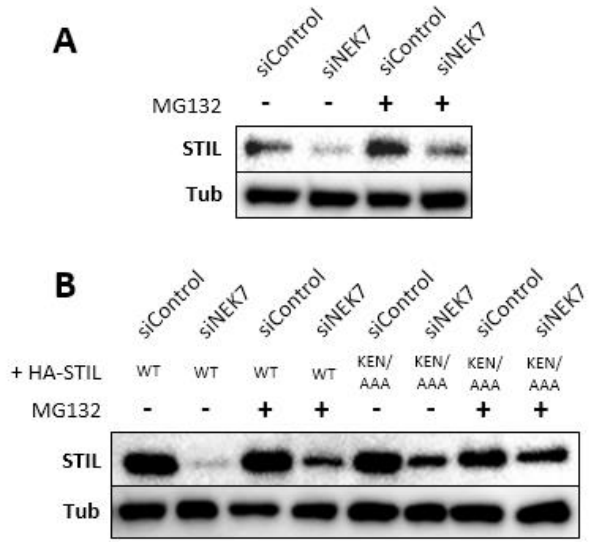

Figure 23. Proteasomal degradation of STIL in NEK7-depleted cells. (A) U2OS cells were transfected with control or NEK7 siRNAs for 48 hours, and 10 μM MG132 was added for the last 6 hours of the siRNA treatment. (B) U2OS cells were transfected with control or NEK7 siRNAs for 24 hours, and then with the indicated vectors for another 24 hours. 10 μM MG132 was added for the last 6 hours of the experiment, and total cell lysates were analyzed by immunoblotting.

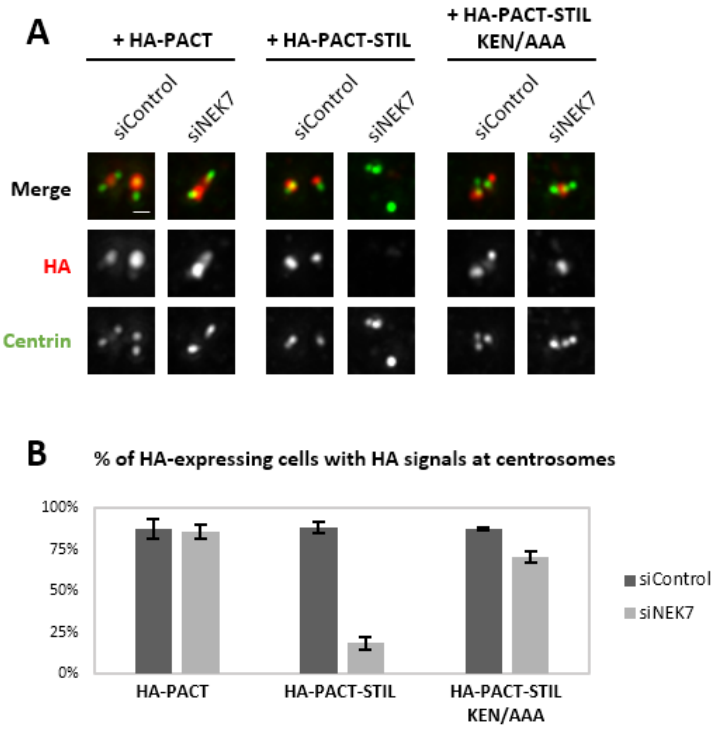

Figure 24. Expression of HA-PACT-STIL constructs in NEK7-depleted cells. (A) U2OS cells were transfected with control or NEK7 siRNAs for 24 hours, and then transfected with the indicated HA-PACT constructs for another 24 hours. The cells were then fixed and stained with the indicated antibodies. Scale bar: 500 nm. (B) Histograms represent the percentage of interphase cells that exhibited centrosomal HA signals. More than 50 cells expressing high and comparable levels of cytoplasmic HA fluorescence were counted in each experimental group.

3.7 Regulation of the APC/C cofactor Cdh1 in NEK7-depleted cells

The APC/C^{Cdh1} is typically active from late mitosis to late G1, and plays a role in preventing premature DNA replication by regulating the levels of G1 cyclins as well as the CDK inhibitor p21 [22,23]. Several feedback loops involving CDK-mediated phosphorylation of Cdh1 are necessary for the inactivation of APC/C^{Cdh1} at late G1, without which entry into the S phase is blocked.

Based on my previous results, I suspected that APC/C^{Cdh1} may exist in an activated state in the G1-arrested cells lacking NEK7. However, it is technically difficult to address the activation state of APC/C^{Cdh1} *in vivo*. Instead, I attempted to characterize the expression patterns of Cdh1 in control and NEK7-depleted cells.

3.7.1 Characterization of the localization patterns of Cdh1

Firstly, I found overall Cdh1 expression levels were not affected upon a prolonged treatment of NEK7 siRNA (not shown). Next, I looked at the localization patterns of Cdh1 within the cell. It has been shown that Cdh1 exists both in the cytoplasm and the nucleus, and possibly shuttles between these two locations depending on its phosphorylation status [95,96]. In *Drosophila* embryos, Cdh1/FZR1 has also been reported to localize to the centrosomes throughout the cell cycle [97], and a recent study indicated that its centrosomal localization in *Drosophila* at least is cell-cycle dependent [98]. Interestingly, when I looked at Cdh1 localization in control human U2OS cells, I also found that Cdh1 localized to the centrosomes throughout the cell cycle, and its localization followed a very specific pattern associated with cell cycle progression (Figure 25).

In early G1, there appeared to be low levels of Cdh1 present at the centrosomes, but as the cells continued into S and G2, Cdh1 gradually accumulated at the centrosomes. Cdh1 levels at the centrosomes peaked around prophase or metaphase, where it localized in small quantities at daughter centrioles, and formed ring-like structures around mother centrioles. Immediately at the metaphase-anaphase transition, most of the Cdh1 disappeared from the centrosomes. I speculated that at this point, Cdh1 may relocalize to replace Cdc20 in the APC/C^{Cdc20} complex elsewhere in the cell, as APC/C^{Cdh1} activation

and Cdc20 degradation are known to occur during this timeframe [22,23]. Thus, I determined that Cdh1 follows very specific localization patterns during the cell cycle in human cells, and I hypothesized that Cdh1's function and activity may be tied to its localization.

3.7.2 Cdh1 exhibits abnormally high centrosomal levels in NEK7-depleted cells

Following characterization of Cdh1 localization patterns in control cells, I looked at Cdh1 in NEK7-depleted U2OS cells. I found astoundingly high amounts of Cdh1 present at the centrosomes in these cells (Figures 25B and 26A, B). This centrosomal accumulation of Cdh1 in NEK7-depleted cells appeared to be quite different from the mitosis-specific accumulation in control cells. Hence, I furthered examined the finer details of Cdh1 localization using three-dimensional structured illumination microscopy (3D-SIM). I found that while Cdh1 in control G1 cells did not show a specific localization pattern within the centrosomes, in control metaphase cells as well as NEK7-depleted cells, Cdh1 seemed to localize alongside the walls of the mother centrioles (Figure 26B).

I also checked whether Cdh1 could accumulate at the centrosomes in RPE1 cells that had been treated with NEK7 siRNA and exhibited cilia, but I did not observe any such accumulation (Figure 26C). This may be a cell type-specific phenotype, as the environment around the basal bodies in ciliated RPE1 cells is quite different from that of centrosomes in U2OS cells.

3.7.3 PCM-dependent accumulation of Cdh1 in control mitotic cells

At least in control cells, I wondered if the mitotic accumulation of Cdh1 at the centrosomes may be dependent on the expansion of the pericentriolar material (PCM) surrounding the centrioles. Organization of the PCM in interphase and metaphase is inherently different; from early mitosis to metaphase, the PCM grows substantially in size for the formation of the mitotic spindle, and then rapidly disassembles as the cells advance to anaphase. The core centrosomal protein CEP192 plays a major role in this process; not only is it required for centriole duplication in interphase, but it also is a crucial component for PCM

assembly during mitosis. Accordingly, depletion of CEP192 frequently results in the formation of disorganized spindles [99].

When I co-immunostained mitotic cells with Cdh1 and several centriolar markers, I found that the outer diameter of the Cdh1 ring was larger than that of CEP152, which is an inner PCM component, yet the diameter was significantly smaller than that of CEP192 (Figure 27, 28A, 29A). Based on these data and past studies [100,101], I conclude that Cdh1 tends to accumulate in the inner to intermediate regions of the PCM, which is consistent with a recent study on *Drosophila* Cdh1/FZR1 [98].

Next, I sought to identify the factors involved in Cdh1 accumulation at the centrosomes during mitosis. I found that although CEP152 seemingly localizes closer to the centrosomes compared to Cdh1, depletion of CEP152 had no noticeable impact on Cdh1 localization (Figure 28). Similarly, depletion of NEK7 had no noticeable impact on CEP152 localization, suggesting that CEP152 is not involved in Cdh1 accumulation.

To examine the PCM-dependency of Cdh1 centrosomal localization, I depleted CEP192 in U2OS cells in order to inhibit PCM assembly, and quantified the amount of Cdh1 that is present at the centrosomes in interphase cells, as well as in mitotic cells containing monopolar spindles that were caused by siCEP192 (Figure 29). Interestingly, I found that although the centrosomal levels of Cdh1 in interphase cells were unaffected upon CEP192 depletion, most of the mitotic accumulation of centrosomal Cdh1 was lost. This led me to hypothesize about the existence of two independent populations of Cdh1 at the centrosomes; small quantities of Cdh1 are present at the centrosomes throughout the cell cycle and are independent of PCM assembly, whereas the mitotic accumulation of Cdh1 at the centrosomes appears to be largely PCM-dependent.

3.7.4 Centrosomal accumulation of Cdh1 in NEK7-depleted cells is PCM-independent

I next sought to investigate whether Cdh1 accumulation at the centrosomes in the absence of NEK7 is PCM-dependent as well. To do so, I compared the amounts of CEP192 and Cdh1 at the centrosomes during interphase in control and NEK7 siRNA-treated cells

(Figure 30). Similar to a previous study that reported a slight loss in the PCM content in NEK7-depleted cells [76], I found no significant increase in the amounts of CEP192 present at the centrosomes, even though Cdh1 levels were elevated. This result suggests that Cdh1 accumulation at interphase centrosomes in the absence of NEK7 is PCM-independent, and is possibly recruited by other pathways.

3.7.5 Role of centriolar satellites in Cdh1 localization

Finally, in an attempt to understand the centrosomal accumulation of Cdh1 in NEK7-depleted cells, I tried to characterize the Cdh1 localization patterns in control interphase cells. During interphase, I observed that Cdh1 localized not only at the centrosomes, but also in small discrete foci near the centrosomes (Figure 25A), which were reminiscent of centriolar satellite staining. Centriolar satellites are small cytoplasmic granules surrounding the centrosomes, and they are believed to be required for protein trafficking to and from centrosomes [102]. To determine whether Cdh1 is associated with centriolar satellites, I co-immunostained Cdh1 with the satellite marker PCM1 (Figure 31A). Interestingly, I found that many cytoplasmic Cdh1 foci appeared to overlap with PCM1 foci in control interphase cells. Additionally, upon knockdown of PCM1, many of the cytoplasmic Cdh1 foci disappeared and Cdh1 appeared to substantially accumulate at the centrosomes (Figure 31B, C), in a pattern very similar to NEK7 depletion. These results suggest that Cdh1 accumulation in NEK7-depleted cells may be caused due to defective satellite function, which may be required to transport Cdh1 away from the centrosomes during G1.

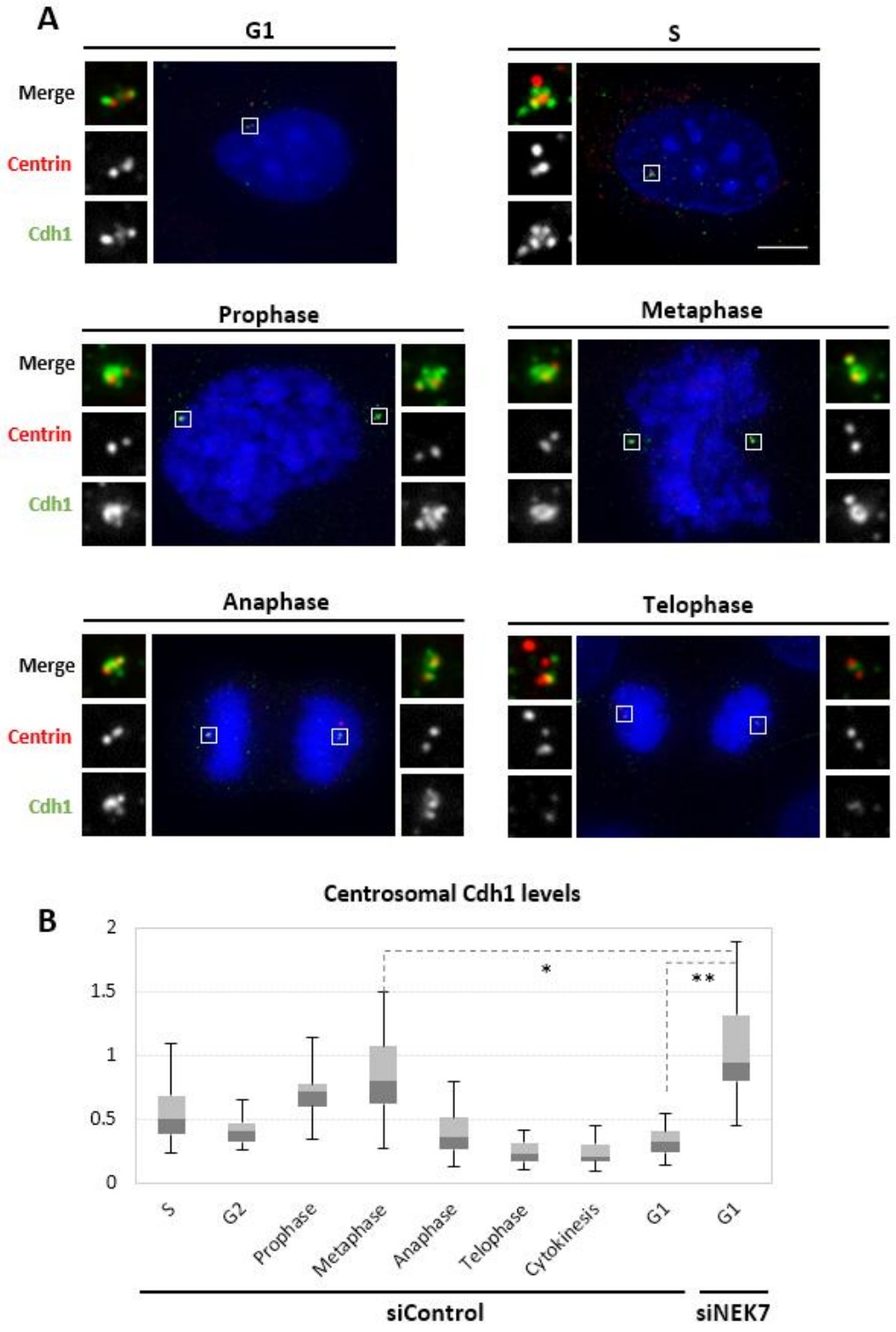

Figure 25. Localization patterns of the APC/C cofactor Cdh1 in control cells. (A) U2OS cells were transfected with control siRNA for 48 hours, and the cells were fixed and immunostained with antibodies specific to Cdh1 (green) and Centrin (red). DNA is shown in blue. Insets are magnified views of the centrosomes. Scale bar: 5 μm. The fluorescence intensities of Cdh1 at the centrosomes were quantified on an arbitrary scale at different cell cycle phases, and are indicated as box plots in (B). *P<0.05; <P<0.01; n.s. not significant (one tailed *t*-test).

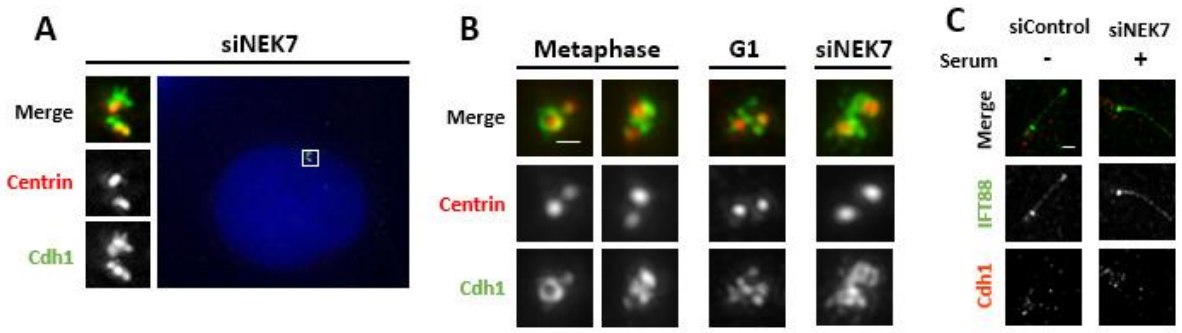

Figure 26. Localization patterns of the APC/C cofactor Cdh1 in NEK7-depleted cells. (A) U2OS cells were transfected with NEK7 siRNA for 48 hours, and the cells were fixed and immunostained with antibodies specific to Cdh1 (green) and Centrin (red). DNA is shown in blue. Insets are magnified views of the centrosomes. Scale bar: 5 μm. (B) RPE1 cells were transfected with control and NEK7 siRNAs for a total of 48 hours, and the control sample was simultaneously released into serum-free medium. The cells were then fixed and stained with the indicated antibodies. Scale bar: 1 μm. (C) U2OS cells were treated with control or NEK7 siRNAs as in (A), and imaged by 3D-SIM to address the localization of Cdh1 around the centrosomes. The fluorescence intensities of centrosomal Cdh1 are not comparable between images in (C). Scale bar: 500 nm.

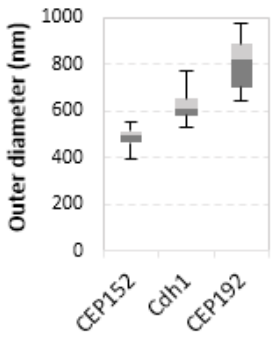

Protein	Outer ring diameter during mitosis
CEP152	485 ± 46 nm
Cdh1	628 ± 64 nm
CEP192	804 ± 105 nm

Figure 27. Characterization of Cdh1 centrosomal localization to the PCM in mitosis. U2OS cells were and immunostained with antibodies specific to Cdh1, CEP152, or CEP192, and the approximate outer diameters of these proteins at mitotic centrosomes was quantified.

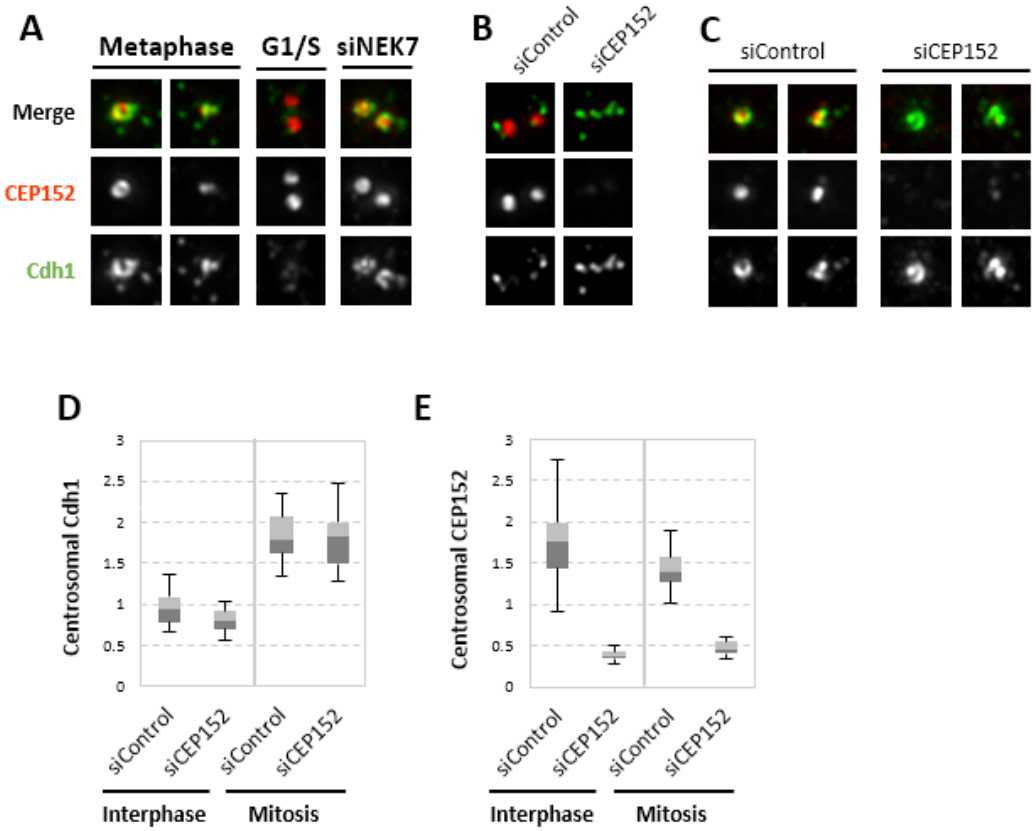

Figure 28. Centrosomal localization of Cdh1 is not affected by CEP152 depletion. (A-E) U2OS cells were transfected with control, NEK7, or CEP152 siRNAs for 48 hours, and the cells were fixed and immunostained with the indicated antibodies. The fluorescence intensities of Cdh1 and CEP152 at the centrosomes in interphase (B) and mitotic (C) cells were quantified on arbitrary scales, and are indicated as box plots in (D, E).

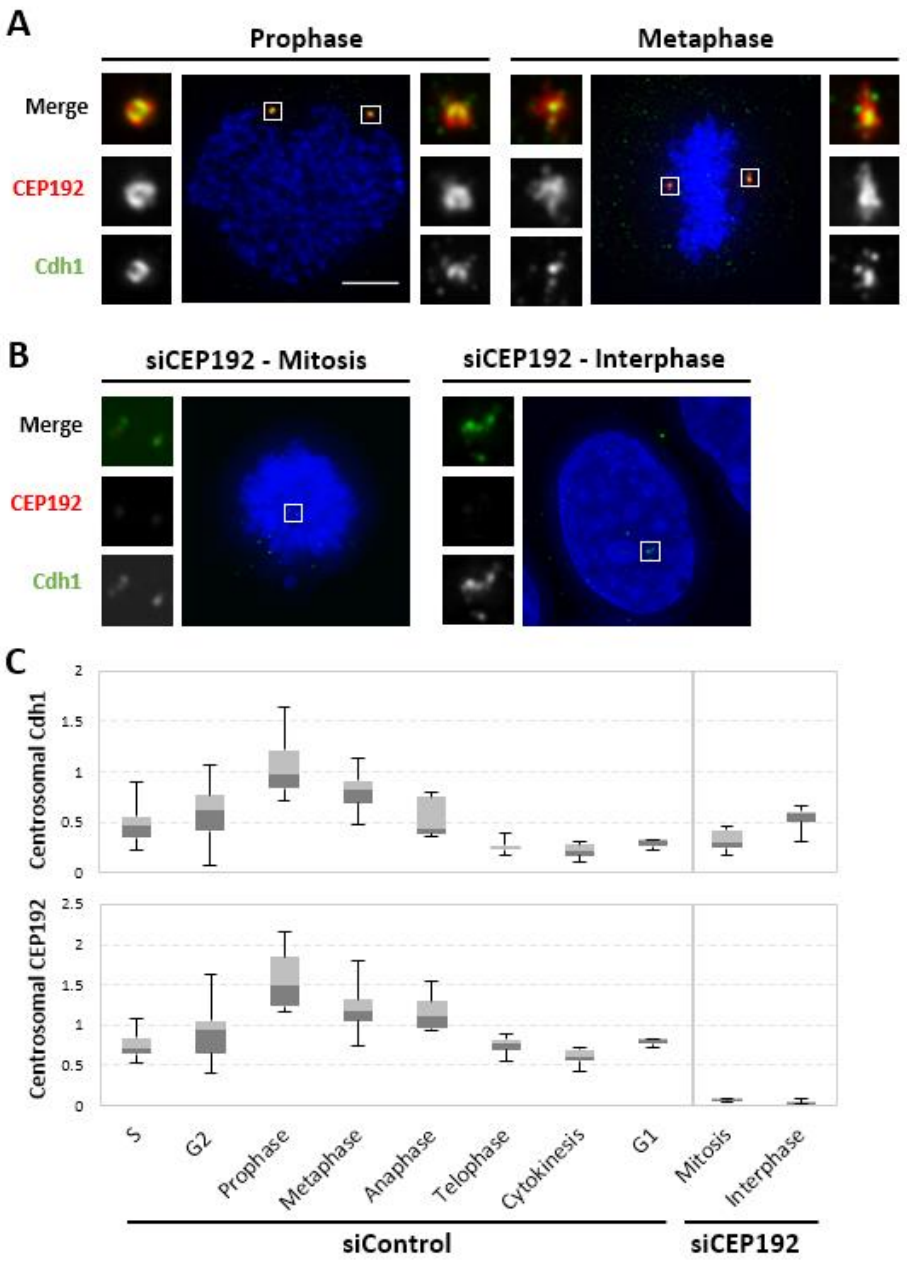

Figure 29. Mitotic accumulation of Cdh1 at the centrosomes in control cells is PCM-dependent. U2OS cells were transfected with control (A) or CEP192 (B) siRNAs for 48 hours, and the cells were fixed and immunostained with the indicated antibodies. DNA is shown in blue. Insets are magnified views of the centrosomes. Scale bar: 5 μm. (C) The fluorescence intensities of Cdh1 and CEP192 at the centrosomes were quantified on an arbitrary scale at different cell cycle phases, and are indicated as box plots.

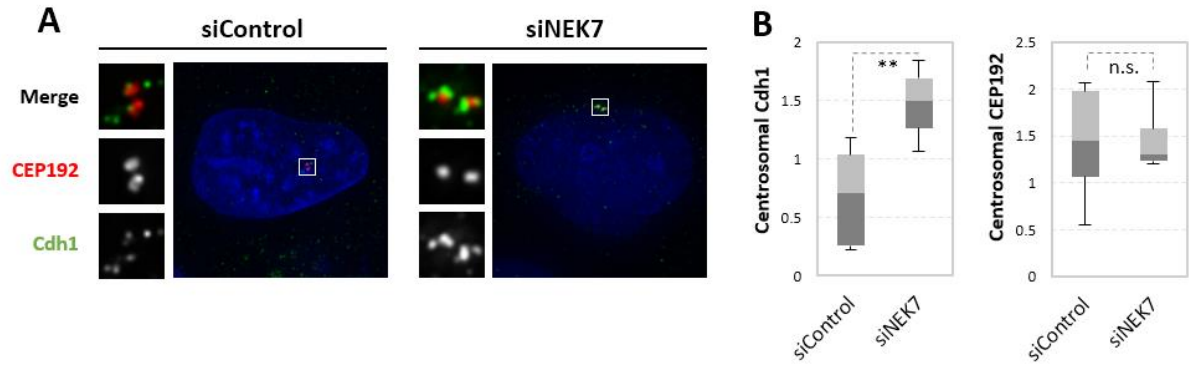

Figure 30. Centrosomal accumulation of Cdh1 in NEK7-depleted cells is PCM-independent. (A) U2OS cells were transfected with control or NEK7 siRNAs for 48 hours, and the cells were fixed and immunostained with the indicated antibodies. DNA is shown in blue. Insets are magnified views of the centrosomes. (B) The fluorescence intensities of Cdh1 and CEP192 at the centrosomes were quantified on an arbitrary scale in interphase cells, and are indicated as box plots. *P<0.05; <P<0.01; n.s. not significant (one tailed *t*-test).

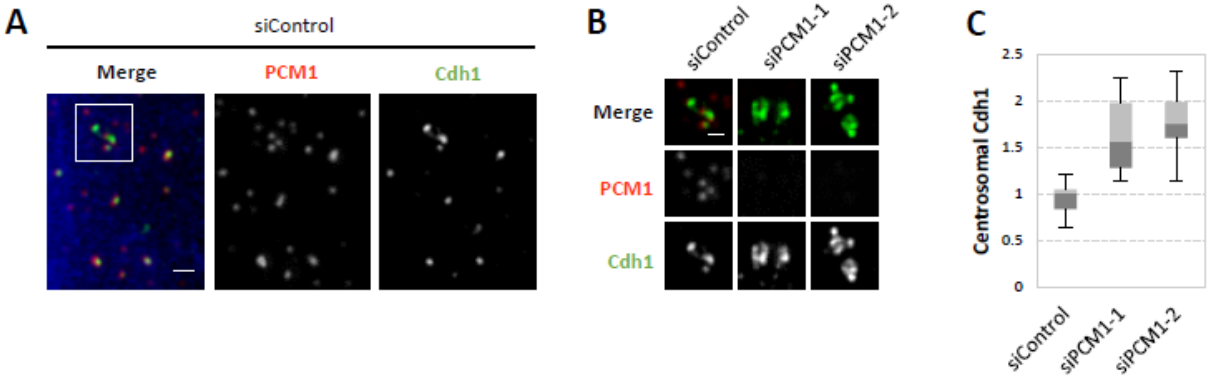

Figure 31. Cdh1 localizes to centriolar satellites in interphase, and is redistributed upon PCM1 inhibition. (A-C) U2OS cells were transfected with control or PCM1 siRNAs for 48 hours, and the cells were fixed and immunostained with the indicated antibodies. DNA is shown in blue. (A) The boxed area indicates the centrosomes as seen in (B). The fluorescence intensities of Cdh1 at interphase centrosomes were quantified on an arbitrary scale, and are indicated as box plots in (C).

4. Discussion

4.1 NEK7 and the cell cycle

NEK7 has been reported to be required for many different cellular processes, suggesting that it acts upon and regulates many different substrates, and may itself lie under complex cell cycle control. A recent study identified many different interactors of NEK7 using a proteomics-based approach, and these proteins were found to be involved in several other processes not previously reported for NEK7, such as mitochondrial regulation, intracellular protein transport, and DNA repair [103]. It was also shown that NEK7 could phosphorylate several of its binding partners, suggesting that it acts as a multifunctional kinase. However, the specific roles of NEK7 and NEK7-mediated phosphorylation events in the cell cycle have not yet been identified, making it difficult to clarify the significance of NEK7 in specific biological processes.

Here, I characterized the impact of NEK7 upon cell cycle progression by analyzing the effects of NEK7 depletion in cycling cells. Through my research, I propose that NEK7 plays crucial roles in the expression and stability of various G1 proteins, as well as in the regulation of APC/C^{Cdh1} activity and localization, both of which contribute to a timely transition from the G1 to S phase. My results demonstrate that NEK7 may play an integral and indispensable role in progression through the G1 phase and subsequent commitment to the rest of the cell cycle.

4.2 The role of NEK7 in G1 progression

During G1 progression in cycling cells, the expression levels of various cyclins and activity levels of cyclin/CDK complexes determine whether the cells will proliferate or become quiescent (Figure 32). Another factor that affects this decision is the activity of the E3 ubiquitin ligase APC/C^{Cdh1}, which regulates the expression levels of cyclins and other regulatory proteins through intricately linked feedback loops.

In my study, I showed that NEK7 is required for the timely expression of various cyclins, CDKs, and other cell cycle-regulated proteins. In the absence of these cyclin/CDK complexes, cells lacking NEK7 are inevitably arrested in the G1 phase, presumably before they can pass the restriction point (Figure 32). APC/C^{Cdh1} also appears to remain active in NEK7-depleted cells, and the inhibition of APC/C^{Cdh1} inactivation may further contribute to the G1 arrest [22,23].

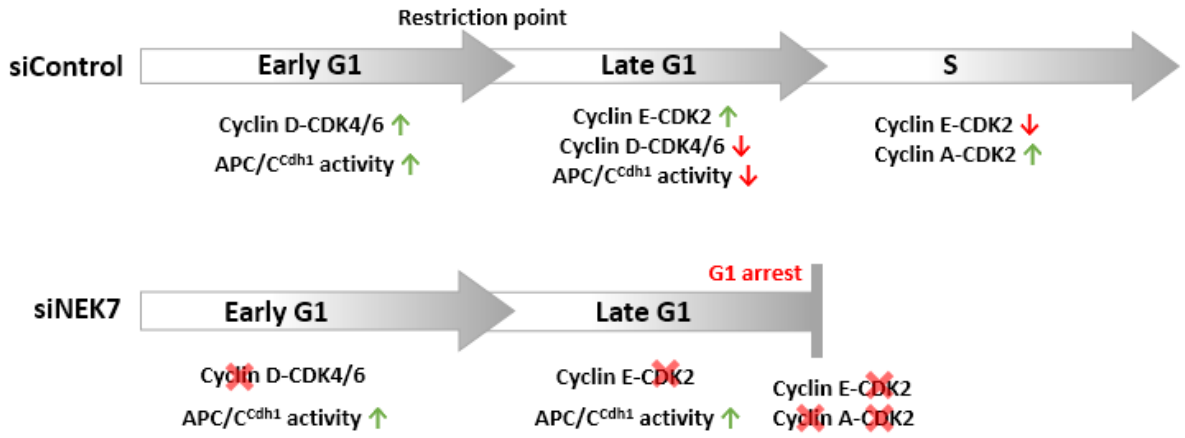

Figure 32. Depletion of NEK7 inhibits G1 progression. (Top) Schematic of how progression through G1 and the G1/S transition are regulated in control cells. During early G1, increases in cyclin D/CDK4 and cyclin D/CDK6 activity are necessary to pass the restriction point, and these complexes are subsequently inactivated in later G1. The G1/S transition largely depends on cyclin E/CDK2 activity, and inactivation of APC/C^{Cdh1} is essential for S phase entry. Towards S phase, cyclin A replaces cyclin E in the complex with CDK2 to complete DNA replication. (Bottom) In the absence of NEK7, the expression of various cyclins is inhibited; in particular, expression of the early G1 cyclin D is blocked. Low levels of cyclin D could lead to an arrest at the restriction point. In the absence of cyclin D/CDK4 or cyclin D/CDK6 activity, expression of late G1 cyclins and CDKs is also reduced. Additionally, the inactivation of APC/C^{Cdh1} is inhibited, which also contributes to the G1 arrest in NEK7-depleted cells.

4.2.1 What are the targets of NEK7 in G1?

Not many substrates of NEK7 have yet been identified, although it has been suggested that NEK7 can phosphorylate several of its interactors. Despite their similar sizes and high sequence similarity (87%) in the kinase domains, NEK6 and NEK7 do not share any common interactors with the exception of NEK9, which also functions as an upstream

activator of both NEK6 and NEK7 [103,104]. However, it has been proposed that these two enzymes have opposing kinase activities in the cell cycle [91].

NEK6 and NEK7 are known to have common substrates. Both kinases were found to be able to phosphorylate microtubules *in vitro* [68], although the functional significance of these modifications was not determined. NEK6 and NEK7 could also phosphorylate p70S6K at T412 [105], which is a ribosomal kinase that functions in the mTOR signalling pathway, and promotes protein synthesis and cell proliferation upon activation. NEK6 at least was shown to be required for the activation of p70S6K, which suggests that NEK7 could act in a similar manner.

It is likely that NEK7 can phosphorylate many more substrates for the regulation of several processes in G1 progression and the G1/S transition. It would be very informative to perform a comprehensive screening of proteins that can be phosphorylated by NEK7, in order to further elucidate its functions.

4.2.2 What pathways is NEK7 involved in?

NEK7 is likely to be a mitotic-inactive kinase [90,91], and my studies indicate that NEK7 is activated sometime during G1 or the G1/S transition. Based on these and past data, it is likely that NEK7 is involved in at least one or more pathways essential for G1 progression and the G1/S transition.

The most upstream protein to be affected in the absence of NEK7 is cyclin D, which exhibited reduced expression levels even in early G1 in NEK7-depleted cells. Mitogen-activated protein kinase (MAPK)-mediated signalling is perhaps the best-studied activator of cyclin D gene expression during early G1 [106], suggesting NEK7 may play a role in at least one or more of the growth factor signalling pathways regulating the transcriptional activation of cyclin D. Further evidence for NEK7 being involved in growth factor-mediated signalling is the formation of primary cilia in NEK7-depleted RPE1 cells, a phenotype that is characteristic of cells arrested in G0/G1 upon serum starvation. Another signalling network that may be affected by NEK7 is the mTOR pathway, which plays a complex role in G1 progression by regulating cyclin E/CDK2 activity levels [3].

Additionally, although not much is currently known about the transcriptional regulation of the CDK2 gene, my results suggest that NEK7 may function upstream of CDK2 gene transcription, or alternatively, it may directly or indirectly regulate CDK2 protein stability.

4.2 NEK7 and the centrosome cycle

The initiation of centriole duplication is tightly linked to the decision of the cell to enter the cell cycle, which occurs at the G1/S transition. Considering that NEK7 is required for progression through G1 and the G1/S transition, it is not surprising that the depletion of NEK7 can inhibit procentriole formation at the earliest stages, and also induce ciliogenesis under certain conditions (Figure 33). Accordingly, I found that various procentriolar proteins exhibited very low expression in NEK7-depleted cells, which are caused in part due to the G1 arrest, and in part due to APC/C^{Cdh1}-mediated proteasomal degradation. However, although NEK7 can localize to the centrosomes in small quantities, there is no evidence so far about whether it regulates the centrosomes directly.

4.3 Cdh1 and the centrosomes

Some particularly interesting phenotypes that I observed were the localization patterns of Cdh1 at the centrosomes during the cell cycle, especially the high accumulation of Cdh1 at the centrosomes in NEK7-depleted cells. These results raise important questions about the significance and functions of centrosomal Cdh1.

4.3.1 How is Cdh1 recruited to the centrosomes?

Upon characterization of the centrosome-associated populations of Cdh1, I found that small populations of Cdh1 remain associated with the centrosomes at all times, and Cdh1 gradually accumulates at the centrosomes as the cell cycle progresses, reaching peak levels around prometaphase or metaphase. This mitosis-specific accumulation of Cdh1 is largely due to expansion of the PCM around the centrosomes, as depletion of the PCM protein CEP192 was sufficient to remove most centrosomal Cdh1 in mitotic cells. In

Drosophila, it has been shown that Cdh1/FZR1 localizes at mitotic centrosomes through direct interaction with Spd2, which is a CEP192 orthologue [98]. However, the domain in Spd2 that is necessary for interaction with *Drosophila* Cdh1/FZR1 is absent in human CEP192, and likewise, I could not detect an interaction between human CEP192 and Cdh1 proteins (data not shown). This suggests that another PCM component may interact with Cdh1 for its centrosomal accumulation during mitosis.

During interphase, centrosomal levels of Cdh1 were found to be lower than in mitosis, however, many Cdh1 foci that were associated with centriolar satellites were observed. Indeed, depletion of the satellite protein PCM1 caused the disappearance of the satellite-associated Cdh1 foci and an increase in the amount of Cdh1 at the centrosomes, a pattern which was reminiscent of NEK7-depleted cells. This suggests that in cycling cells, centriolar satellites may be required for trafficking Cdh1 away from the centrosomes. Indeed, previous studies have shown that PCM1 depletion caused relocalization of several satellite proteins to the centrosomes [107]. Thus, it is possible that the increased centrosomal levels of Cdh1 in NEK7-depleted cells may be due to defective centriolar satellite-mediated protein trafficking. However, the molecules responsible for anchoring Cdh1 at the centrosomes remain to be identified.

4.3.2 What is the significance of centrosomal Cdh1?

One obvious question is whether Cdh1 exists in a complex with APC/C at the centrosomes, and if so, whether centrosomal APC/C^{Cdh1} is active or inactive. The protein Emi1, which can bind to and inhibit both APC/C activators Cdc20 and Cdh1 [26,108], has been shown to localize to the spindle pole in a complex with APC/C during early mitosis [109], where it inhibits centrosomal APC/C to prevent degradation of spindle pole-associated cyclins and premature mitotic exit. Hence, I hypothesize that the PCM-associated Cdh1 seen during mitosis might be kept inactive in a complex with APC/C and Emi1. Following chromosome segregation and activation of APC/C^{Cdh1}, it is possible that it disperses throughout the cytoplasm to target various substrates, which may explain the disappearance of Cdh1 from the centrosomes. In the next cell cycle, APC/C^{Cdh1} remains active until the G1/S transition, wherein Emi1 stably binds and irreversibly inactivates APC/C^{Cdh1} to commit cells to enter the cell cycle [9,27,28].

One of the more important implications of my study is that the abnormally high levels of centrosomal Cdh1 in NEK7-depleted cells represent an active APC/C^{Cdh1} at the centrosomes. This raises several important possibilities. The centrosomes have long been recognized as hubs for localized proteasomal degradation of ubiquitinated proteins [110]. Thus, it is possible that centrosomal APC/C^{Cdh1} in G1-arrested cells serves to rapidly mark various substrates for destruction to prevent proliferation. Another possible function of centrosomal APC/C^{Cdh1} may be to inhibit centriole duplication, as it could potentially occupy and block the assembly sites of new procentrioles. Thus, APC/C^{Cdh1} could perform several important functions at the centrosomes both in cycling cells as well as G1-arrested cells lacking NEK7.

In conclusion, my study strongly suggests that NEK7 is an important kinase involved in the regulation of G1 phase progression and the G1/S transition. In the future, it would be worthwhile to identify and characterize the direct downstream targets of NEK7, as well as the pathways in which it plays important roles. Since NEK7 has already been reported to be upregulated in various cancers, the strong G1 arrest that is induced upon NEK7 depletion makes it a promising candidate for the development of various anticancer drugs.

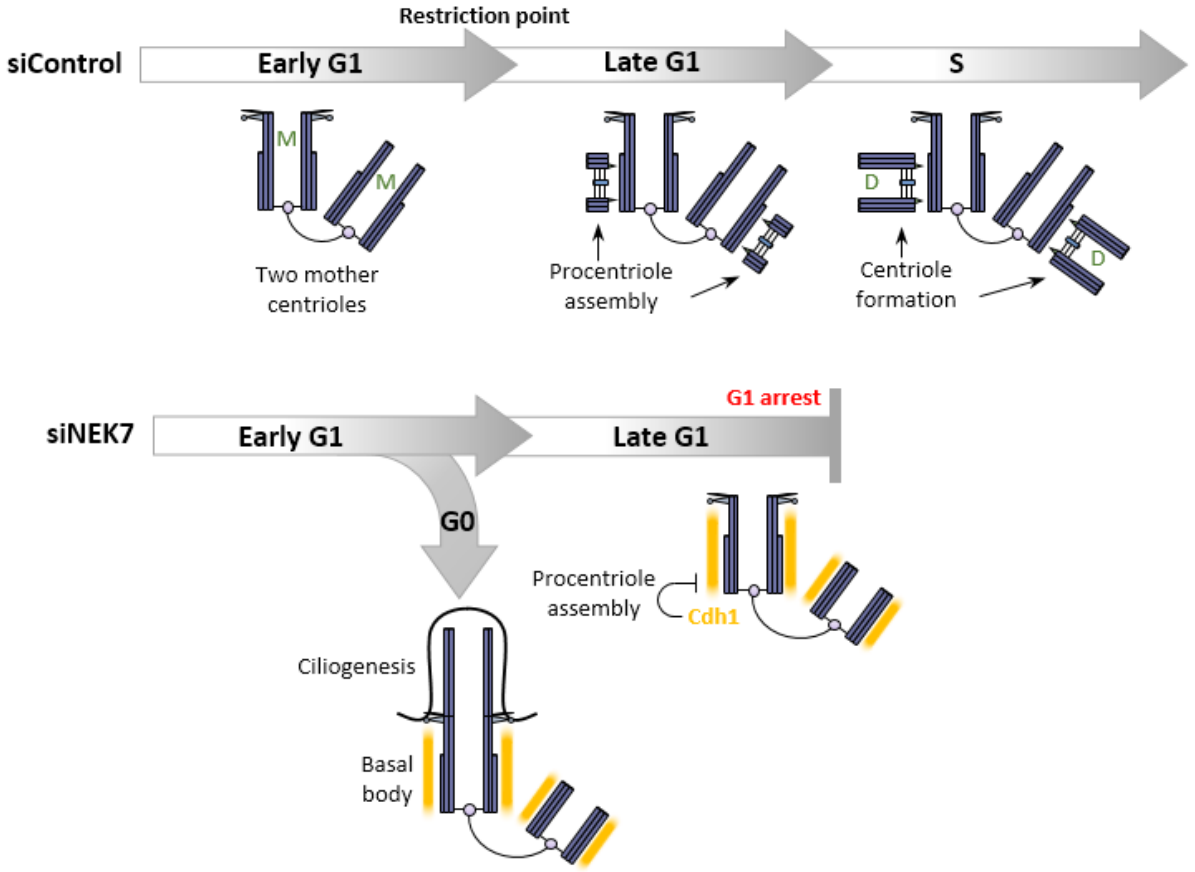

Figure 33. Depletion of NEK7 inhibits procentriole assembly. (Top) Centriole duplication involves the expression and recruitment of several procentriolar proteins at the base of the mother centriole (M) towards late G1. As the cells progress through the G1/S transition and complete S phase, the procentrioles elongate and mature to form daughter centrioles (D). (Bottom) In the absence of NEK7, low levels of G1 cyclins could lead to an arrest at the restriction point, which induces ciliogenesis. Cdh1 can accumulate near the walls of the centrioles in these conditions, which may lead to the degradation of procentriolar proteins, thus inhibiting procentriole formation.

5. Current and Future Studies

In this section, I will briefly introduce what is currently known about the core proteins that are required for centriole assembly, and how they might contribute to formation of centriolar microtubules. I will also detail some of the novel interactors of the centriolar protein CEP120 that I identified during my research, and the possible significance of these interactions.

My primary research interests involve the assembly of the triplet microtubule structures that are unique to centrioles, however, most of the molecular mechanisms that are involved in their assembly remain elusive due to various experimental limitations. Thus, I would like to close my thesis with a discussion on our current understanding of the factors that may play roles in the formation of centriolar triplet microtubules, and what questions still remain to be answered.

5.1 Core centriolar proteins required for human centriole formation

The hierarchical recruitment of the "core" proteins required for centriole duplication in humans has been well-characterized (Figure 34), however, we are far from understanding how centriole duplication occurs at a molecular and structural level. For instance, many of the proteins involved in centriole duplication are larger in size than the average cytoplasmic protein (on the order of 60-400 kDa), and may contain large coiled coil as well as disordered regions [111]. Many centrosomal proteins are often insoluble or unstable when expressed on their own, and this renders it near-impossible to characterize them structurally. As a consequence, while some of the interactions between the core centrosomal proteins have been mapped out, we are still unable to locate most of these proteins on the 3D maps of centrioles that have been reconstructed using cryoelectron microscopy [112]. Thus, further characterization of the molecular features and interactions of centriolar proteins is necessary.

Of all the centriolar proteins, the structural significance of SAS-6 in centriole assembly is the least ambiguous. SAS-6 is capable of forming dimers via a long coiled coil region, and the SAS-6 dimers can assemble together in a 9-fold radially symmetric manner [40,41]. These SAS-6 oligomers primarily constitute the cartwheel structure that is often observed at the proximal regions of daughter centrioles. On the other hand, even though the protein STIL (which interacts with SAS-6) is known to be an essential protein for procentriole assembly, its structural roles remain unknown.

The functional significance of the microtubule-binding protein CEP135 has until now been somewhat controversial, as various studies claim different roles for CEP135 in centriole duplication [43,113,114], however, these differences may boil down to organism-specific requirements. Interestingly, a recent study has indicated that Bld10, which is the CEP135 homologue in *Chlamydomonas reinhardtii*, plays a role in the stabilization of SAS-6 cartwheels [44], suggesting that human CEP135 may also have similar functions.

Lastly, CPAP and CEP120, which are both microtubule-binding proteins, play a joint role in controlling the formation and elongation of centriolar microtubule structures [46,49]. Centriolar microtubules are some of the slowest-growing microtubule structures found in human cells, and a recent study on CPAP suggested that its association with microtubules limited their growth rates [115]. CEP120 appears to function in similar ways as CPAP, as overexpression of either CPAP or CEP120 results in overly long centrioles [48]. In *C. reinhardtii*, the UNI2 gene has been identified to be a putative orthologue of human CEP120 (Figure 35), and mutation of this gene causes an incomplete transition of triplet to doublet microtubules near the transition zone, resulting in defective flagella containing triplet microtubules instead of the usual doublets [116]. This suggests that CEP120/UNI2 may play a more conserved role in the assembly of centriolar microtubules; on the other hand, no orthologue for CPAP has been identified in *C. reinhardtii*.

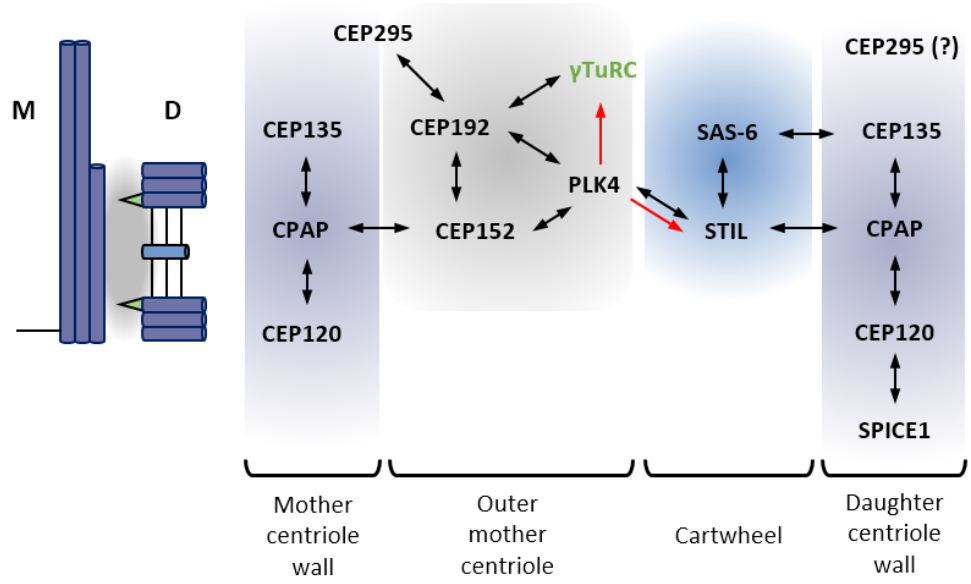

Figure 34. Essential proteins required for procentriole formation in humans. The microtubule-interacting proteins CPAP, CEP120, and CEP135 localize along the walls of both the mother and daughter centrioles, and are presumably required for the recruitment of outer centriolar components CEP192 and CEP152 (and possibly CEP295) to the centrioles. CEP192 and CEP152 localize in a ring along the outer walls of the mother centriole (M), and are required to recruit the kinase PLK4, which can phosphorylate multiple substrates to trigger formation of the daughter centriole (D). STIL can be phosphorylated by PLK4 and interact with SAS-6, and these two molecules localize at the cartwheel. Following cartwheel assembly, several other centriolar proteins are recruited to the centrioles which facilitate centriole elongation and maturation. Black lines between proteins indicate previously characterized interactions. Red lines indicate phosphorylation.

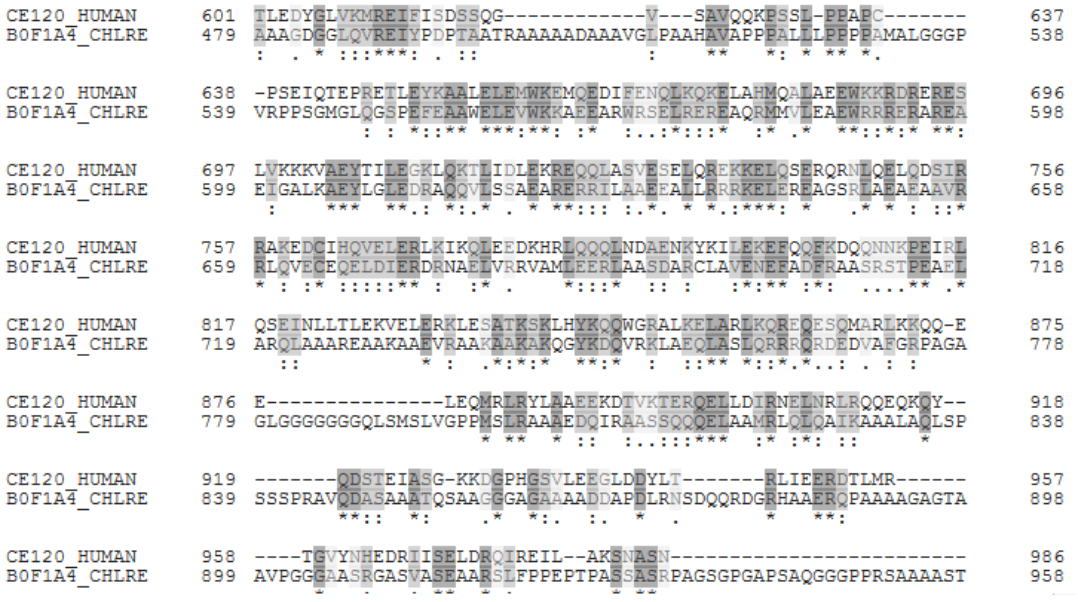

Figure 35. Alignment between human CEP120 and *C. reinhardtii* UNI2. The proteins CEP120 and UNI2 share a conserved domain which has been identified to be a coiled coil region, suggesting that they may share functional similarities.

5.2 Novel interactions of CEP120 with centriolar proteins

In an effort to better understand how centriolar proteins might be spatially arranged in the cartwheel and the surrounding microtubules, I built a comprehensive map of all the interactions that have been reported for the proteins required for the centriole duplication pathway (part of this map is shown in Figure 36).

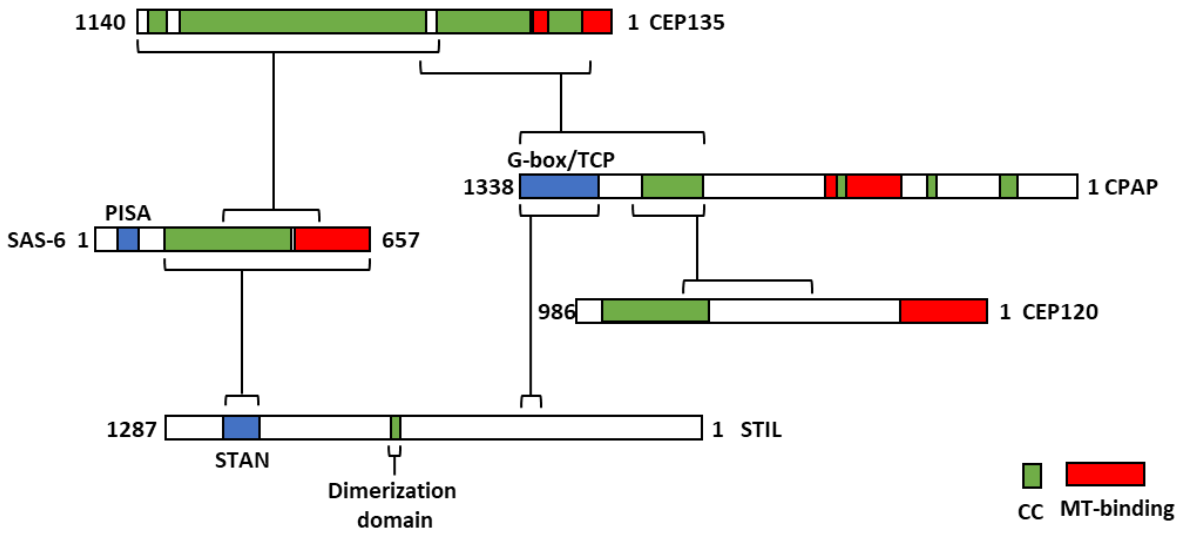

Figure 36. Mapping the interaction domains of centriolar proteins. A summary of the interacting domains that have been identified for SAS-6, STIL, CEP135, CPAP, and CEP120 [39,43,48,49,117]. The sizes of the proteins and their relative orientation to each other are indicated by the numbers on either side, "1" representing the N-terminal for each protein. The sizes of all the proteins are to scale. Blue boxes indicate conserved domains, green boxes indicate coiled coil regions, and red boxes indicate microtubule-binding domains. Interactions between pairs of proteins are depicted as curved connectors.

In particular, I was trying to identify a function for the N-terminal region of STIL spanning residues 26-360, which is highly conserved in vertebrates. CEP120 appeared to be a likely candidate that could interact with STIL, as it could potentially localize near the N-terminal region of STIL based on my protein interaction mapping (Figure 36). Thus, I decided to check whether CEP120 could form a complex with STIL.

Accordingly, I amplified the CEP120 gene product from total human mRNA and inserted it into a Flag vector for co-immunoprecipitation (Co-IP) with HA-STIL constructs in

HEK293T cells. Co-IP analyses showed that full length HA-STIL could indeed interact with Flag-CEP120 (Figure 37). Furthermore, deletion mutants of HA-STIL indicated that the interacting regions of STIL with CEP120 were likely to be either in N-terminal region or middle regions of STIL, as deletions of these regions showed reduced binding with Flag-CEP120.

Additionally, I found that CEP120 could interact not only with STIL, but also with the centriolar proteins SAS-6 and CEP135, which has not been previously reported. This suggests that CEP120 may have a much larger part to play in the assembly of centrioles, although further studies need to be performed to elucidate its exact functions.

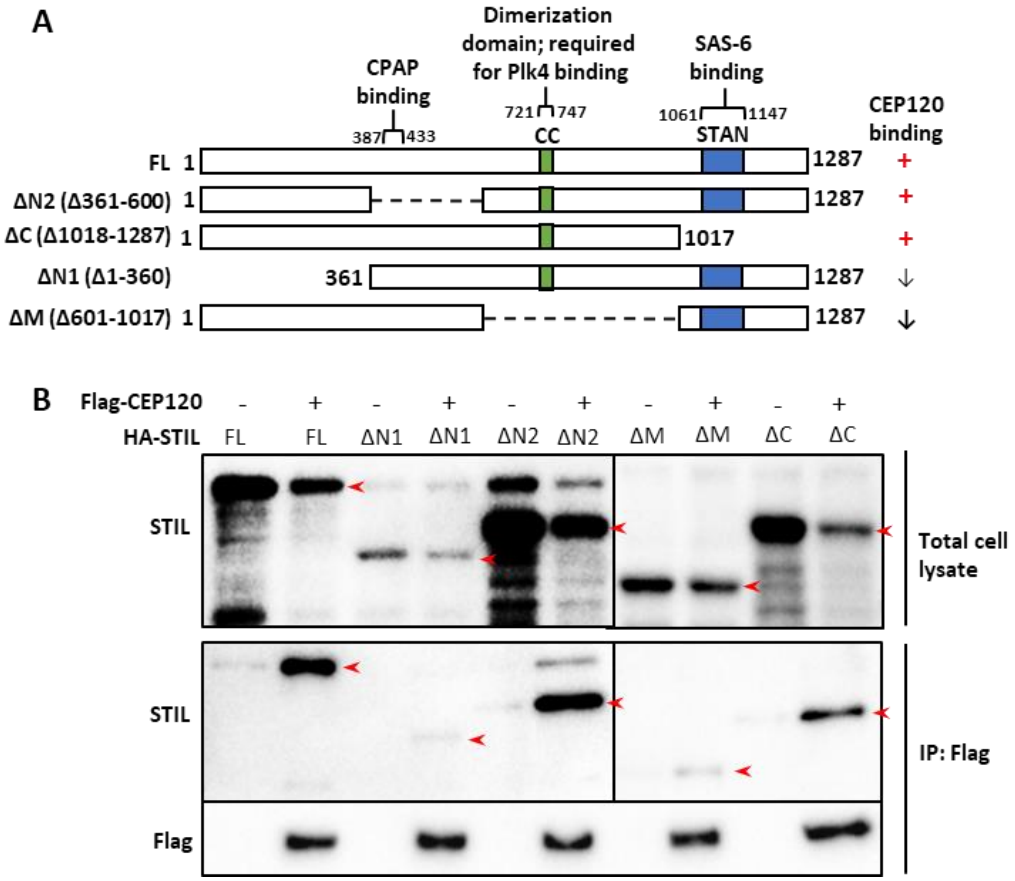

Figure 37. A novel interaction between CEP120 and STIL. (A) Schematic of the STIL deletion constructs that were used for co-immunoprecipitation (Co-IP) assays with Flag-CEP120 in HEK293T cells. The right column shows a summary of the interactions. (B) HEK293T cells were co-transfected with an empty Flag vector (-) or Flag-CEP120 and the indicated STIL constructs. Flag-CEP120 was immunoprecipitated using Flag antibodies. Total cell lysates and the immunoprecipitated fractions were analyzed by immunoblotting using the indicated antibodies.

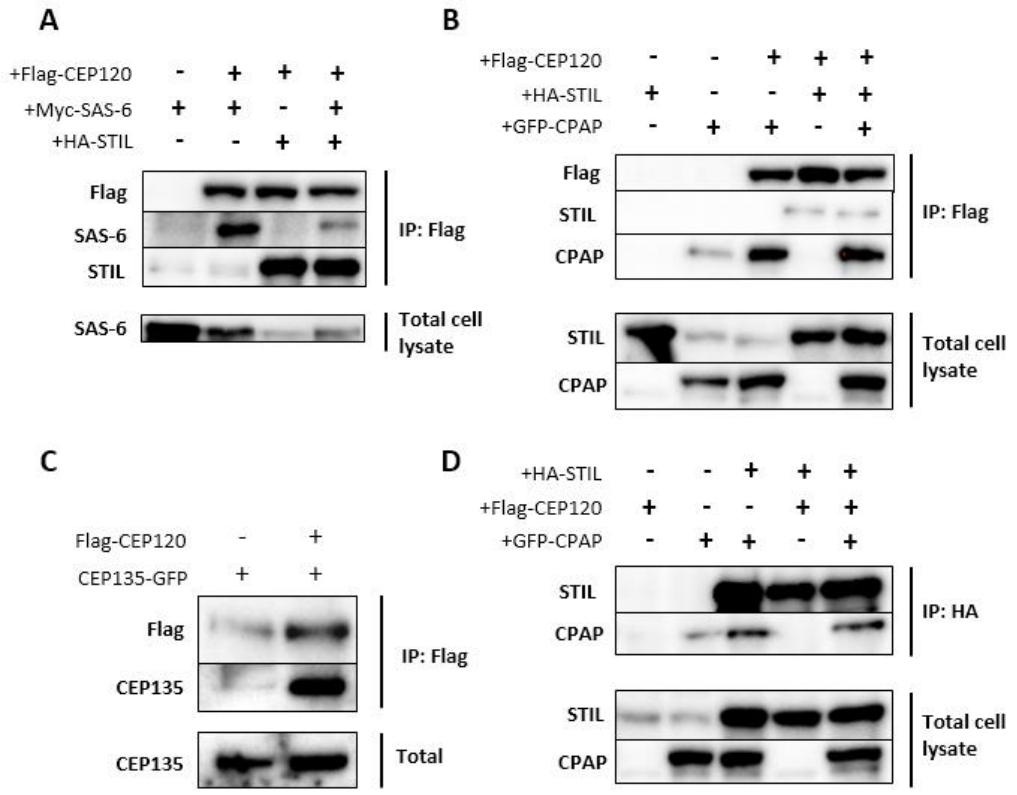

Figure 38. CEP120 interacts with several procentriolar proteins. (A-D) HEK293T cells were co-transfected with the indicated vectors. Flag-CEP120 (A-C) or HA-STIL (D) were immunoprecipitated using antibodies against the Flag or HA epitopes. Total cell lysates and the immunoprecipitated fractions were analyzed by immunoblotting using the indicated antibodies.

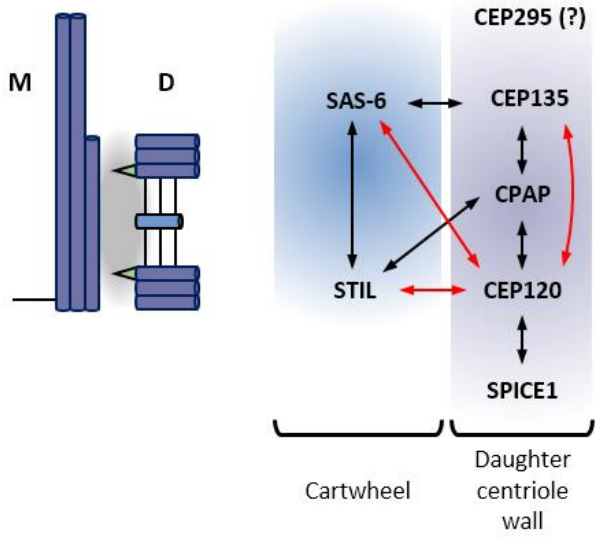

Figure 39. CEP120 interacts with several centriolar proteins. A summary of the centriolar interactions determined previously (black arrows) and identified in this study (red arrows).

5.3 Centriolar triplet microtubules: How are they assembled?

Centrioles are highly conserved organelles that are best-defined by the uniquely symmetric array of nine sets of triplet microtubules, and they are found in most eukaryotes, with the notable exception of most land plants. Centriolar triplet microtubules are not like conventional microtubules found in the cell; high resolution 3D reconstructions of centrioles from various organisms have revealed that the individual protofilaments of the A-tubule have highly variable curvatures which result in some "flattening" of the A-tubule [112,118], and the B- and C-tubules are composed of less than 13 protofilaments and do not close completely. The structural basis for the formation of triplet microtubules is not very well understood, largely due to the technical limitations of purifying and visualizing centriolar microtubules.

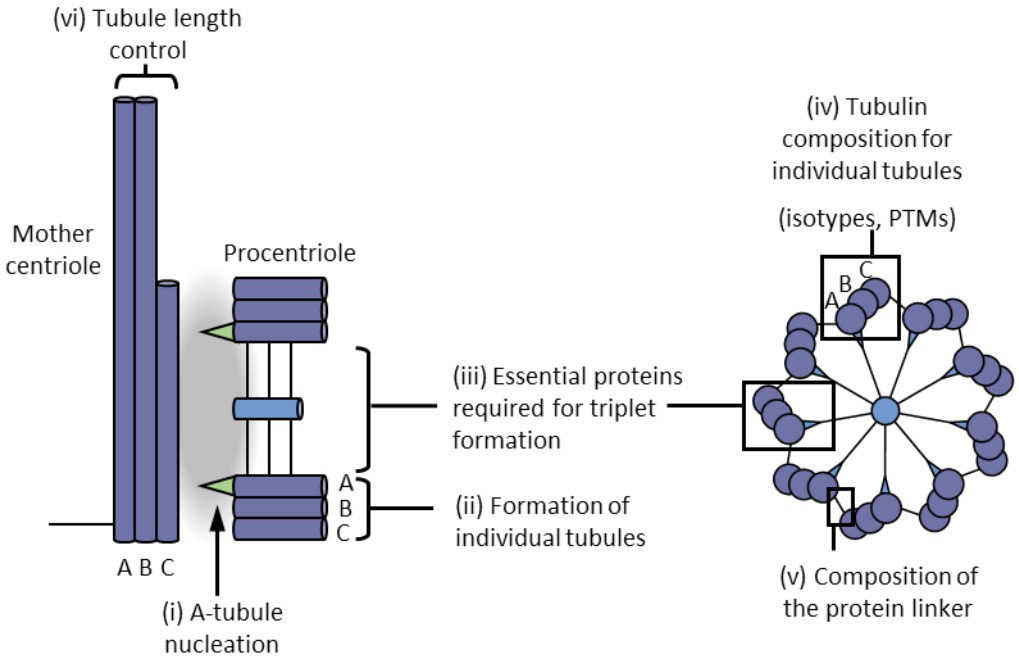

Figure 40. The formation and regulation of centriolar triplet microtubules is largely unknown. Many questions remain to be answered regarding how centriolar triplet microtubules are assembled, such as: (i) How are the A-tubules nucleated? (ii) How are the individual A-, B-, and C-tubules formed? (iii) What are the essential proteins required for triplet microtubule formation? (iv) What is the tubulin isotypes and modifications required for formation of the individual tubules? (v) What is the composition of the protein linker connecting the C-tubule and the next A-tubule? (vi) How are the lengths of individual tubules regulated?

Some of the larger questions about triplet microtubule assembly that remain unanswered are summarized in Figure 40. Various clues exist in past literature that may aid us in understanding the molecular mechanisms at play during centriolar microtubule growth, however, many more studies need to be performed in order to support these hypotheses. For example, the α- and β-tubulins in humans are composed of various isotypes which are highly divergent in their C-terminal tails [119], and it has been suggested that the post-translational modifications of these tails may play a part in the assembly of centriolar and ciliary microtubules [120]. Indeed, the triplet microtubules of centrioles have been found to be rich in acetylated and glutamylated tubulins, which have been suggested to somehow contribute to the high stability of these microtubules. Although whether these post-translational modifications exist on all the tubulin proteins of a single centriole, or on individual tubules, or even on individual protofilaments of specific tubules is not yet known.

There are also open questions about whether additional tubulin families play a part in centriolar microtubule assembly. α- and β-tubulin form irreversibly linked heterodimers that serve as the building blocks of all microtubules, and γ-tubulin forms complexes with several other molecules to facilitate the nucleation of microtubules; these three tubulin families are found ubiquitously in all eukaryotes [121]. However, additional tubulin families such as δ- and ε-tubulins have been identified in recent decades, and it is slowly becoming evident that they may indeed be involved in the formation of centriole-specific doublet or triplet microtubules [122–126]. More and more tubulin families are being identified in different organisms with time, but their roles remain largely unknown [127].

For my future research, I would like to pursue a more detailed investigation about the formation of centriolar triplet microtubules in various organisms. In particular, I would like to focus upon the nucleation and the formation of the individual A-, B-, and C-tubules, and the possible roles of tubulin modifications, or of δ- and ε-tubulin in their assembly. I hope that many new and exciting discoveries are made in this niche field in the upcoming years.

6. Materials and Methods

6.1 Cell culture and transfection

Human U2OS cells were obtained from the ECACC (European Collection of Authenticated Cell Cultures), and have been authenticated by STR profiling in ECACC. Telomerase-immortalized human RPE1 (hTERT-RPE1) cells were obtained from Clontech. U2OS and RPE1 cells were cultured in Dulbecco's Modified Eagle Medium (DMEM) and Dulbecco's modified Eagle Medium: Nutrient Mixture F-12 (DMEM/F-12) respectively, supplemented with 10% fetal bovine serum (FBS), and penicillin/streptomycin at 37°C in a 5% CO_2 incubator. The lines were mycoplasma free, as confirmed by Hoechst 33258 staining. Transfection of siRNA or DNA constructs into U2OS and RPE1 cells was performed using Lipofectamine RNAiMAX (Life Technologies) or Lipofectamine 2000 (Life Technologies) according to the manufacturer's instruction. Unless otherwise noted, transfected cells were analysed 48 hours after transfection with siRNA and 24 hours after transfection with DNA constructs.

6.2 RNA interference and plasmids

The following siRNAs were used: Silencer® Select siRNA (Life Technologies) against the CDS of NEK7 (s44316), CEP192 (s226819), and PCM1 (s10128 and s10129). Custom siRNAs were used against the 3' UTR of NEK7 (5'-GCA UUU GUA AAC UUA AAA ATT-3') and the CDS of CEP152 (5'-GCG GAU CCA ACU GGA AAU CUA TT-3').

The following plasmids were used: pFlag-NEK7 RR (subcloned from the pFlag-CMV2-NEK7 vector gifted by Andrew M. Fry), pEBTet-GFP-STIL, pcDNA3-PLK4-ΔPEST-Flag (a gift from Hiroyuki Mano), pCMV5-HA-STIL WT, pCMV5-Myc-SAS-6. pCMV5-HA-STIL constructs were subcloned from the pCMV5-HA-STIL WT vector using PrimeSTAR mutagenesis basal kit (TaKaRa).

6.3 Cell cycle synchronization and flow cytometric analysis

For cell synchronization at prometaphase, cells were treated with 100 ng/ml nocodazole for 16 hours, and released in fresh medium. For cell synchronization at S phase, cells were treated with 2 mM thymidine for 16 hours, and released in fresh medium. For flow cytometric analyses, cells cultured on dishes were trypsinized, washed twice with PBS, and fixed in 70% cold ethanol at -20° for >3 hours. The fixed cells were then washed with PBS and incubated with Muse™ Cell Cycle Reagent at room temperature (RT) for 30 minutes. The DNA contents of the cells were then measured using Muse™ Cell Analyzer (Merck Millipore).

6.4 Antibodies

The following primary antibodies were used in this study: Rabbit polyclonal antibodies against STIL (Abcam, ab89314, immunofluorescence (IF) 1:500, immunoblotting (IB) 1:1000), GFP (MBL, #598, IF 1:500), NEK7 (Bethyl Laboratories, A302-684A, IB 1:1000), Centrin-1 (Abcam, ab11257, IF: 1:500), CPAP/CENP-J (Proteintech, 11517-1-AP, IF 1:500, IB 1:1000), Cdc20 (Bethyl Laboratories, A301-180A, IB 1:500), IFT88 (Proteintech, 13967-1-AP, IF 1:100), CEP192 (Bethyl Laboratories, A302-324A, IF 1:500), CEP152 (Bethyl Laboratories, A302-324A, IF 1:500), HA-tag (Abcam, ab9110, IF 1:500), PCM1 (Sigma, HPA023370, IF 1:500); mouse monoclonal antibodies against p21 Waf1/Cip1 (Cell Signalling Technology, DCS60, IF 1:500, IB 1:1000, a gift from Masato Kanemaki), Centrin-2 (Millipore, 20H5, IF 1:1000), SAS-6 (Santa Cruz Biotechnology, Inc., sc-81431, WB 1:1000), PLK4 (Merck Millipore, clone 6H5, MABC544, IF 1:300), Flag-tag (Sigma, F1804, IF 1:1000, WB 1:1000), Cdh1/FZR1 (Abcam, ab89535, IF 1:100, WB 1:500), acetylated- α-tubulin at K40 (Sigma, 611B1, IF 1:500) and α-tubulin (Sigma, DM1A, WB 1:2000). The CDK and cyclin antibodies were used from the CDK and Cyclin Antibody Sampler Kits (Cell Signalling Technology, #9868 and #9869 respectively) as per recommended dilutions. The following secondary antibodies were used: Alexa Fluor 488 goat anti-mouse IgG (H+L) (Molecular probe, 1:500), Alexa Fluor 568 goat anti-rabbit IgG (H+L) (Molecular probe, 1:500) for IF; Goat polyclonal antibodies-HRP against mouse IgG (Promega, W402B, 1:10000), rabbit IgG (Promega, W401B, 1:10000) for WB. Centrin-1

(rabbit) and Centrin-2 (mouse) antibodies were used as centriolar markers. Acetylated-α-tubulin at K40 (mouse) and IFT88 (rabbit) antibodies were used as ciliary markers.

6.5 Immunofluorescence

For indirect immunofluorescence microscopy, cells cultured on coverslips were fixed using ice-cold methanol for 10 minutes at -20°C. The cells were then washed with PBS three times, and incubated for blocking with 1% BSA in PBS/0.5% TritonX-100 (PBSX) for 30 minutes at room temperature (RT). The cells were then incubated with primary antibodies for 3 hours at RT, washed with PBSX once and PBS three times, and incubated with secondary antibodies for 1 hour at RT. The cells were thereafter washed with PBSX twice, stained with 0.2 µg/ml Hoechst 33258 in PBS for 5 minutes at RT, washed again with PBS and mounted onto glass slides.

Counting of immunofluorescence signals was performed using an Axioplan2 fluorescence microscope (Carl Zeiss) with a 100x/1.4 NA plan-APOCHROMAT objective. Data acquisition for the images was performed using a DeltaVision Personal DV-SoftWoRx system (Applied Precision) equipped with a CoolSNAP CH350 CCD camera. The images were acquired as serial sections along the Z-axis and stacked using the 'quick projection' algorithm in SoftWoRx. The signal intensities for centrosomal proteins were quantified using the Data Inspector tool in SoftWoRx. The captured images were processed using ImageJ. Unless otherwise noted, all immunofluorescence analyses were repeated at least three times.

3D-SIM images were taken by the Nikon N-SIM imaging system with Piezo stage, Apo TIRF 100x oil objective lens (NA 1.49), excitation wavelengths 488 and 561 nm, and iXon DU-897 EMCCD camera (Andor Technology Ltd.). The images were collected at 100 nm Z-steps.

6.6 Immunoblotting

For preparation of cell lysates for immunoblotting, the cells were collected and lysed by vortexing at 4°C in lysis buffer (20 mM Tris/HCl pH 7.5, 100mM NaCl, 0.5% NP40, 1 mM EDTA, 1 mM DTT and 1/1000 protease 26 inhibitor cocktail (Nacalai Tesque, Inc.)). Lysates were cleared by centrifugation for 10 minutes at 13000 rpm at 4°C and the supernatants were collected for immunoblotting. SDS-PAGE was performed using 6-12% polyacrylamide gels, followed by transfer on Immobilon-P membrane (Millipore Corporation). The membranes were probed with the primary antibodies, followed by incubation with their respective HRP-conjugated secondary antibodies (Promega). Washes were performed in PBS containing 0.02% Tween (PBST). The signals were detected by a Chemi Doc XRS+ (BioRad) and band intensities were calculated using the inbuilt Image Lab software (BioRad). Unless otherwise specified, all immunoblotting analyses were repeated at least three times. The antibody against α-tubulin was used as a loading control.

6.7 Immunoprecipitation

For preparation of cell lysates for immunoprecipitation (IP), the cells were collected and lysed in ice-cold lysis buffer by vortexing at 4°C, and the lysates were cleared by centrifugation for 10 minutes at 13,000 rpm. For immunoprecipitation, whole cell lysates were incubated with Flag or HA antibodies conjugated to agarose for 2 hours at 4°C; the bead were then washed three times with lysis buffer before loading onto an SDS-acrylamide gel.

6.8 *In vitro* kinase assay and mass spectrometry

For the *in vitro* kinase assay, U2OS or HEK293T cells were transfected with pCMV-Flag-NEK7 constructs using Lipofectamine 2000. The cells were harvested after the indicated amount of time, and lysed by vortexing in lysis buffer. The cleared supernatant was immunoprecipitated with beads conjugated to Flag antibodies. The beads were washed three times with lysis buffer, and then incubated with or without the indicated bacterially-

purified proteins in 20 µl kinase buffer containing 10 mM $MgCl_2$, 30 µM ATP and 5 µCi [γ-^{32}P] ATP for 30 minutes at 30°C. The proteins were separated by SDS-PAGE, stained with SimplyBlue™ SafeStain (Invitrogen), and phosphorylation was visualized by autoradiography (Typhoon FLA 9000, GE Healthcare).

For mass spectrometry analysis, the STIL fragments phosphorylated by Flag-NEK7 *in vitro* were digested into shorter peptides in solution by trypsin. The peptides were subsequently desalted and analysed by a nanoLC-ESI-Q-TOF mass spectrometer.

References

[1] A. Gupta, Y. Tsuchiya, M. Ohta, G. Shiratsuchi, D. Kitagawa, NEK7 is required for G1 progression and procentriole formation, Mol Biol Cell 28. (2017) 2123-2134. doi:10.1091/mbc.E16-09-0643.

[2] M.L.M. Jongsma, I. Berlin, J. Neefjes, On the move: Organelle dynamics during mitosis, Trends Cell Biol. 25 (2015) 112–124. doi:10.1016/j.tcb.2014.10.005.

[3] D.A. Foster, P. Yellen, L. Xu, M. Saqcena, Regulation of G1 Cell Cycle Progression: Distinguishing the Restriction Point from a Nutrient-Sensing Cell Growth Checkpoint(s), Genes Cancer. 1 (2010) 1124–1131. doi:10.1177/1947601910392989.

[4] A.B. Pardee, A Restriction Point for Control of Normal Animal Cell Proliferation, Proc Natl Acad Sci. 71 (1974) 1286–1290. doi:10.1073/pnas.71.4.1286.

[5] A. Zetterberg, O. Larsson, Kinetic analysis of regulatory events in G1 leading to proliferation or quiescence of Swiss 3T3 cells., Proc Natl Acad Sci. 82 (1985) 5365–5369. doi:10.1073/pnas.82.16.5365.

[6] S. Kim, L. Tsiokas, Cilia and cell cycle re-entry: More than a coincidence, Cell Cycle. 10 (2011) 2683–2690. doi:10.4161/cc.10.16.17009.

[7] A. Zetterberg, O. Larsson, K.G. Wiman, What is the restriction point?, Curr Opin Cell Biol. 7 (1995) 835–842. doi:10.1016/0955-0674(95)80067-0.

[8] A.R. Barr, F.S. Heldt, T. Zhang, C. Bakal, B. Nov??k, A Dynamical Framework for the All-or-None G1/S Transition, Cell Syst. 2 (2016) 27–37. doi:10.1016/j.cels.2016.01.001.

[9] S. Cappell, M. Chung, A. Jaimovich, S. Spencer, T. Meyer, Irreversible APCCdh1 Inactivation Underlies the Point of No Return for Cell-Cycle Entry, Cell. 166 (2016) 167–180. doi:10.1016/j.cell.2016.05.077.

[10] C. Bertoli, J.M. Skotheim, R.A.M. de Bruin, Control of cell cycle transcription during G1 and S phases, Nat Rev Mol Cell Biol. 14 (2013) 518–528. doi:10.1038/nrm3629.

[11] N. Bendris, B. Lemmers, J.M. Blanchard, Cell cycle, cytoskeleton dynamics and beyond: the many functions of cyclins and CDK inhibitors, Cell Cycle. 14 (2015) 1786–1798. doi:10.1080/15384101.2014.998085.

[12] D. Frescas, M. Pagano, Deregulated proteolysis by the F-box proteins SKP2 and β-TrCP: tipping the scales of cancer, Nat Rev Cancer. 8 (2008) 438–449. doi:10.1038/nrc2396.

[13] S. Meloche, J. Pouysségur, The ERK1/2 mitogen-activated protein kinase pathway as a master regulator of the G1- to S-phase transition, Oncogene. 26 (2007) 3227–3239. doi:10.1038/sj.onc.1210414.

[14] R.J. Duronio, Y. Xiong, Signaling pathways that control cell proliferation., Cold Spring Harb Perspect Biol. 5 (2013) a008904. doi:10.1101/cshperspect.a008904.

[15] A.M. Narasimha, M. Kaulich, G.S. Shapiro, Y.J. Choi, P. Sicinski, S.F. Dowdy, Cyclin D activates the Rb tumor suppressor by mono-phosphorylation, Elife. 3 (2014). doi:10.7554/eLife.02872.

[16] C. Giacinti, A. Giordano, RB and cell cycle progression, Oncogene. 25 (2006) 5220–5227. doi:10.1038/sj.onc.1209615.

[17] A. Karimian, Y. Ahmadi, B. Yousefi, Multiple functions of p21 in cell cycle, apoptosis and transcriptional regulation after DNA damage, DNA Repair (Amst). 42 (2016) 63–71. doi:10.1016/j.dnarep.2016.04.008.

[18] J. Labaer, M.D. Garrett, L.F. Stevenson, J.M. Slingerland, C. Sandhu, H.S. Chou, A. Fattaey, E. Harlow, New functional activities for the p21 family of CDK inhibitors, Genes Dev. 11 (1997) 847–862. doi:10.1101/gad.11.7.847.

[19] T. Abbas, A. Dutta, p21 in cancer: intricate networks and multiple activities, Nat Rev Cancer. 9 (2009) 400–414. doi:10.1038/nrc2657.

[20] L. Delavaine, N.B. La Thangue, Control of E2F activity by p21Waf1/Cip1., Oncogene. 18 (1999) 5381–5392. doi:10.1038/sj.onc.1202923.

[21] C. Prives, V. Gottifredi, The p21 and PCNA partnership: A new twist for an old plot, Cell Cycle. 7 (2008) 3840–3846. doi:10.4161/cc.7.24.7243.

[22] J. Pines, Cubism and the cell cycle: the many faces of the APC/C, Nat Rev Mol Cell Biol. 12 (2011) 427–438. doi:10.1038/nrm3132.

[23] X. Qiao, L. Zhang, A.M. Gamper, T. Fujita, Y. Wan, APC/C-Cdh1: From cell cycle to cellular differentiation and genomic integrity, Cell Cycle. 9 (2010) 3904–3912. doi:10.4161/cc.9.19.13585.

[24] M. Veas-Pérez de Tudela, C. Maestre, M. Delgado-Esteban, J.P. Bolaños, A. Almeida, Cdk5-mediated inhibition of APC/C-Cdh1 switches on the cyclin D1-Cdk4-pRb pathway causing aberrant S-phase entry of postmitotic neurons., Sci Rep. 5 (2015) 18180. doi:10.1038/srep18180.

[25] D. Gao, H. Inuzuka, M. Korenjak, A. Tseng, T. Wu, L. Wan, M. Kirschner, N. Dyson, W. Wei, Cdh1 Regulates Cell Cycle through Modulating the Claspin/Chk1 and the Rb/E2F1 Pathways, Mol Biol Cell. 20 (2009) 3305–3316. doi:10.1091/mbc.E09-01-0092.

[26] J.J. Miller, M.K. Summers, D. V. Hansen, M. V. Nachury, N.L. Lehman, A. Loktev, P.K. Jackson, Emi1 stably binds and inhibits the anaphase-promoting complex/cyclosome as a pseudosubstrate inhibitor, Genes Dev. 20 (2006) 2410–2420. doi:10.1101/gad.1454006.

[27] Y.J. Machida, A. Dutta, The APC/C inhibitor, Emi1, is essential for prevention of rereplication, Genes Dev. 21 (2007) 184–194. doi:10.1101/gad.1495007.

[28] J.Y. Hsu, J.D.R. Reimann, C.S. Sørensen, J. Lukas, P.K. Jackson, E2F-dependent accumulation of hEmi1 regulates S phase entry by inhibiting APC/Cdh1, Nat Cell Biol. 4 (2002) 358–366. doi:10.1038/ncb785.

[29] M. Bettencourt-Dias, F. Hildebrandt, D. Pellman, G. Woods, S. a Godinho, Centrosomes and cilia in human disease, Trends Genet. 27 (2011) 307–315. doi:10.1016/j.tig.2011.05.004.

[30] D. Hansemann, Ueber pathologische Mitosen, Virch. Arch. Path. Anat. 123 (1891) 356–370. doi:10.1007/BF01884400.

[31] J. Azimzadeh, W.F. Marshall, Building the centriole, Curr Biol. 20 (2010) R816-25. doi:10.1016/j.cub.2010.08.010.

[32] D. Izquierdo, W.J. Wang, K. Uryu, M.F.B. Tsou, Stabilization of cartwheel-less centrioles for duplication requires CEP295-mediated centriole-to-centrosome conversion, Cell Rep. 8 (2014) 957–965. doi:10.1016/j.celrep.2014.07.022.

[33] Y. Tsuchiya, S. Yoshiba, A. Gupta, K. Watanabe, D. Kitagawa, Cep295 is a conserved scaffold protein required for generation of a bona fide mother centriole, Nat Commun. 7 (2016) 12567. doi:10.1038/ncomms12567.

[34] C.-W. Chang, W.-B. Hsu, J.-J. Tsai, C.-J.C. Tang, T.K. Tang, CEP295 interacts with microtubules and is required for centriole elongation, J Cell Sci. 129 (2016) 2501–2513. doi:10.1242/jcs.186338.

[35] J. Fu, Z. Lipinszki, H. Rangone, M. Min, C. Mykura, J. Chao-Chu, S. Schneider, N.S. Dzhindzhev, M. Gottardo, M.G. Riparbelli, G. Callaini, D.M. Glover, Conserved molecular interactions in centriole-to-centrosome conversion, Nat Cell Biol. 18 (2015) 87–99. doi:10.1038/ncb3274.

[36] K.F. Sonnen, A.-M. Gabryjonczyk, E. Anselm, Y.-D. Stierhof, E.A. Nigg, Human Cep192 and Cep152 cooperate in Plk4 recruitment and centriole duplication, J Cell Sci. 126 (2013) 3223–3233. doi:10.1242/jcs.129502.

[37] T.-S. Kim, J.-E. Park, A. Shukla, S. Choi, R.N. Murugan, J.H. Lee, M. Ahn, K. Rhee, J.K. Bang, B.Y. Kim, J. Loncarek, R.L. Erikson, K.S. Lee, Hierarchical recruitment of Plk4 and regulation of centriole biogenesis by two centrosomal scaffolds, Cep192 and Cep152, Proc Natl Acad Sci. 110 (2013) E4849–E4857. doi:10.1073/pnas.1319656110.

[38] N.S. Dzhindzhev, G. Tzolovsky, Z. Lipinszki, S. Schneider, R. Lattao, J. Fu, J. Debski, M. Dadlez, D.M. Glover, Plk4 phosphorylates Ana2 to trigger SAS-6 recruitment and procentriole formation, Curr Biol. 24 (2014) 2526–2532. doi:10.1016/j.cub.2014.08.061.

[39] M. Ohta, T. Ashikawa, Y. Nozaki, H. Kozuka-Hata, H. Goto, M. Inagaki, M. Oyama, D. Kitagawa, Direct interaction of Plk4 with STIL ensures formation of a single procentriole per parental centriole, Nat Commun. 5 (2014) 5267. doi:10.1038/ncomms6267.

[40] M. van Breugel, M. Hirono, A. Andreeva, H. Yanagisawa, S. Yamaguchi, Y. Nakazawa, N. Morgner, M. Petrovich, I.-O. Ebong, C. V Robinson, C.M. Johnson, D. Veprintsev, B. Zuber, Structures of SAS-6 Suggest Its Organization in Centrioles, Science. 331 (2011) 1196–1199. doi:10.1126/science.1199325.

[41] D. Kitagawa, I. Vakonakis, N. Olieric, M. Hilbert, D. Keller, V. Olieric, M. Bortfeld, M.C. Erat, I. Flückiger, P. Gönczy, M.O. Steinmetz, Structural basis of the 9-fold symmetry of centrioles, Cell. 144 (2011) 364–375. doi:10.1016/j.cell.2011.01.008.

[42] Z. Carvalho-Santos, P. Machado, I. Alvarez-Martins, S.M. Gouveia, S.C. Jana, P. Duarte, T. Amado, P. Branco, M.C. Freitas, S.T.N. Silva, C. Antony, T.M. Bandeiras, M. Bettencourt-Dias, BLD10/CEP135 Is a Microtubule-Associated Protein that Controls the Formation of the

Flagellum Central Microtubule Pair, Dev Cell. 23 (2012) 412–424. doi:10.1016/j.devcel.2012.06.001.

[43] Y.-C. Lin, C.-W. Chang, W.-B. Hsu, C.-J.C. Tang, Y.-N. Lin, E. Chou, C.-T. Wu, T.K. Tang, Human microcephaly protein CEP135 binds to hSAS-6 and CPAP, and is required for centriole assembly, EMBO J. 32 (2013) 1141–1154. doi:10.1038/emboj.2013.56.

[44] P. Guichard, V. Hamel, M. Le Guennec, N. Banterle, I. Iacovache, V. Nemčíková, I. Flückiger, K.N. Goldie, H. Stahlberg, D. Lévy, B. Zuber, P. Gönczy, Cell-free reconstitution reveals centriole cartwheel assembly mechanisms, Nat Commun. 8 (2017) 14813. doi:10.1038/ncomms14813.

[45] J. Chang, O. Cizmecioglu, I. Hoffmann, K. Rhee, PLK2 phosphorylation is critical for CPAP function in procentriole formation during the centrosome cycle, EMBO J. 29 (2010) 2395–2406. doi:10.1038/emboj.2010.118.

[46] C.-J.C. Tang, R.-H. Fu, K.-S. Wu, W.-B. Hsu, T.K. Tang, CPAP is a cell-cycle regulated protein that controls centriole length, Nat Cell Biol. 11 (2009) 825–831. doi:10.1038/ncb1889.

[47] R. Bahtz, J. Seidler, M. Arnold, U. Haselmann-weiss, C. Antony, W.D. Lehmann, I. Hoffmann, GCP6 is a substrate of Plk4 and required for centriole duplication, J Cell Sci. 2 (2012) 486–496. doi:10.1242/jcs.093930.

[48] Y.-C.Y.-N. Lin, C.-T. Wu, Y.-C.Y.-N. Lin, W.-B. Hsu, C.-J.C. Tang, C.-W. Chang, T.K. Tang, CEP120 interacts with CPAP and positively regulates centriole elongation., J Cell Biol. 202 (2013) 211–9. doi:10.1083/jcb.201212060.

[49] D. Comartin, G.D. Gupta, E. Fussner, É. Coyaud, M. Hasegan, M. Archinti, S.W.T. Cheung, D. Pinchev, S. Lawo, B. Raught, D.P. Bazett-Jones, J. Lüders, L. Pelletier, CEP120 and SPICE1 cooperate with CPAP in centriole elongation, Curr Biol. 23 (2013) 1360–1366. doi:10.1016/j.cub.2013.06.002.

[50] T.I. Schmidt, J. Kleylein-Sohn, J. Westendorf, M. Le Clech, S.B. Lavoie, Y.D. Stierhof, E.A. Nigg, Control of Centriole Length by CPAP and CP110, Curr Biol. 19 (2009) 1005–1011. doi:10.1016/j.cub.2009.05.016.

[51] Z. Carvalho-Santos, P. Machado, P. Branco, F. Tavares-Cadete, A. Rodrigues-Martins, J.B. Pereira-Leal, M. Bettencourt-Dias, Stepwise evolution of the centriole-assembly pathway, J Cell Sci. 123 (2010) 1414–26. doi:10.1242/jcs.064931.

[52] M.E. Hodges, N. Scheumann, B. Wickstead, J.A. Langdale, K. Gull, Reconstructing the evolutionary history of the centriole from protein components, J Cell Sci. 123 (2010) 1407–1413. doi:10.1242/jcs.064873.

[53] R. Habedanck, Y.-D. Stierhof, C.J. Wilkinson, E.A. Nigg, The Polo kinase Plk4 functions in centriole duplication, Nat Cell Biol. 7 (2005) 1140–1146. doi:10.1038/ncb1320.

[54] S. Leidel, M. Delattre, L. Cerutti, K. Baumer, P. Gönczy, SAS-6 defines a protein family required for centrosome duplication in C. elegans and in human cells, Nat Cell Biol. 7 (2005) 115–125. doi:10.1038/ncb1220.

[55] C. Arquint, K.F. Sonnen, Y. Stierhof, E.A. Nigg, Cell-cycle-regulated expression of STIL controls centriole number in human cells, J Cell Sci. 125 (2012) 1342–1352. doi:10.1242/jcs.099887.

[56] P. Strnad, S. Leidel, T. Vinogradova, U. Euteneuer, A. Khodjakov, P. Gönczy, Regulated HsSAS-6 Levels Ensure Formation of a Single Procentriole per Centriole during the Centrosome Duplication Cycle, Dev Cell. 13 (2007) 203–213. doi:10.1016/j.devcel.2007.07.004.

[57] C. Arquint, E.A. Nigg, STIL microcephaly mutations interfere with APC/C-mediated degradation and cause centriole amplification, Curr Biol. 24 (2014) 351–360. doi:10.1016/j.cub.2013.12.016.

[58] D. Barford, Structural insights into anaphase-promoting complex function and mechanism, Philos Trans R Soc L Biol Sci. 1584 (2011) 3605–24. doi:10.1098/rstb.2011.0069.

[59] A. Erez, M. Chaussepied, A. Castiel, T. Colaizzo-Anas, P.D. Aplan, D. Ginsberg, S. Izraeli, The mitotic checkpoint gene, SIL is regulated by E2F1, Int J Cancer. 123 (2008) 1721–1725. doi:10.1002/ijc.23665.

[60] M.K. Harrison, A.M. Adon, H.I. Saavedra, The G1 phase Cdks regulate the centrosome cycle and mediate oncogene-dependent centrosome amplification, Cell Div. 6 (2011) 2. doi:10.1186/1747-1028-6-2.

[61] G. Wang, Q. Jiang, C. Zhang, The role of mitotic kinases in coupling the centrosome cycle with the assembly of the mitotic spindle., J Cell Sci. 127 (2014) 4111–22. doi:10.1242/jcs.151753.

[62] H. Ishikawa, W.F. Marshall, Ciliogenesis: building the cell's antenna, Nat Rev Mol Cell Biol. 12 (2011) 222–234. doi:10.1038/nrm3085.

[63] M.W. Leigh, J.E. Pittman, J.L. Carson, T.W. Ferkol, S.D. Dell, S.D. Davis, M.R. Knowles, M.A. Zariwala, Clinical and genetic aspects of primary ciliary dyskinesia/Kartagener syndrome, Genet Med. 11 (2009) 473–487. doi:10.1097/GIM.0b013e3181a53562.

[64] A.H. Osmani, S.L. McGuire, S.A. Osmani, Parallel activation of the NIMA and p34cdc2 cell cycle-regulated protein kinases is required to initiate mitosis in A. nidulans, Cell. 67 (1991) 283–291. doi:10.1016/0092-8674(91)90180-7.

[65] A.M. Fry, L. O'Regan, S.R. Sabir, R. Bayliss, Cell cycle regulation by the NEK family of protein kinases, J Cell Sci. 125 (2012) 4423–4433. doi:10.1242/jcs.111195.

[66] L.M. Quarmby, Caught Nek-ing: cilia and centrioles, J Cell Sci. 118 (2005) 5161–5169. doi:10.1242/jcs.02681.

[67] Y. Fang, X. Zhang, Targeting NEK2 as a promising therapeutic approach for cancer treatment, Cell Cycle. 15 (2016) 895–907. doi:10.1080/15384101.2016.1152430.

[68] L. O'Regan, A.M. Fry, The Nek6 and Nek7 Protein Kinases Are Required for Robust Mitotic Spindle Formation and Cytokinesis, Mol Cell Biol. 29 (2009) 3975–3990. doi:10.1128/MCB.01867-08.

[69] C. Belham, J. Roig, J. a Caldwell, Y. Aoyama, B.E. Kemp, M. Comb, J. Avruch, A mitotic cascade of NIMA family kinases: Nercc1/Nek9 activates the Nek6 and Nek7 kinases, J Biol Chem. 278 (2003) 34897–34909. doi:10.1074/jbc.M303663200.

[70] M.W. Richards, L. O'Regan, C. Mas-Droux, J.M.Y. Blot, J. Cheung, S. Hoelder, A.M. Fry, R. Bayliss, An Autoinhibitory Tyrosine Motif in the Cell-Cycle-Regulated Nek7 Kinase Is Released through

Binding of Nek9, Mol Cell. 36 (2009) 560–570. doi:10.1016/j.molcel.2009.09.038.

[71] S. Sdelci, M. Schütz, R. Pinyol, M.T. Bertran, L. Regué, C. Caelles, I. Vernos, J. Roig, Nek9 phosphorylation of NEDD1/GCP-WD contributes to Plk1 control of γ-tubulin recruitment to the mitotic centrosome, Curr Biol. 22 (2012) 1516–1523. doi:10.1016/j.cub.2012.06.027.

[72] M.T. Bertran, S. Sdelci, L. Regué, J. Avruch, C. Caelles, J. Roig, Nek9 is a Plk1-activated kinase that controls early centrosome separation through Nek6/7 and Eg5, EMBO J. 30 (2011) 2634–2647. doi:10.1038/emboj.2011.179.

[73] N. Yissachar, H. Salem, T. Tennenbaum, B. Motro, Nek7 kinase is enriched at the centrosome, and is required for proper spindle assembly and mitotic progression, FEBS Lett. 580 (2006) 6489–6495. doi:10.1016/j.febslet.2006.10.069.

[74] S. Kim, K. Lee, K. Rhee, NEK7 is a centrosomal kinase critical for microtubule nucleation, Biochem Biophys Res Commun. 360 (2007) 56–62. doi:10.1016/j.bbrc.2007.05.206.

[75] H. Salem, I. Rachmin, N. Yissachar, S. Cohen, A. Amiel, R. Haffner, L. Lavi, B. Motro, Nek7 kinase targeting leads to early mortality, cytokinesis disturbance and polyploidy, Oncogene. 29 (2010) 4046–4057. doi:10.1038/onc.2010.162.

[76] S. Kim, S. Kim, K. Rhee, NEK7 is essential for centriole duplication and centrosomal accumulation of pericentriolar material proteins in interphase cells, J Cell Sci. 124 (2011) 4126–4126. doi:10.1242/jcs.104133.

[77] R. Wang, Y. Song, X. Xu, Q. Wu, C. Liu, The expression of Nek7, FoxM1, and Plk1 in gallbladder cancer and their relationships to clinicopathologic features and survival, Clin Transl Oncol. 15 (2013) 626–632. doi:10.1007/s12094-012-0978-9.

[78] V. Saloura, H.-S. Cho, K. Kiyotani, H. Alachkar, Z. Zuo, M. Nakakido, T. Tsunoda, T. Seiwert, M. Lingen, J. Licht, Y. Nakamura, R. Hamamoto, WHSC1 Promotes Oncogenesis through Regulation of NIMA-Related Kinase-7 in Squamous Cell Carcinoma of the Head and Neck, Mol Cancer Res. 13 (2015) 293–304. doi:10.1158/1541-7786.MCR-14-0292-T.

[79] L. Zhou, Z. Wang, X. Xu, Y. Wan, K. Qu, H. Fan, Q. Chen, X. Sun, C. Liu, Nek7 is overexpressed in hepatocellular carcinoma and promotes hepatocellular carcinoma cell proliferation in vitro and in vivo, Oncotarget. 7 (2016) 18620–30. doi:10.18632/oncotarget.7620.

[80] I.E. Kooi, B.M. Mol, M.P.G. Massink, M.C. De Jong, P. De Graaf, P. Der Van Valk, H. Meijers-Heijboer, G.J.L. Kaspers, A.C. Moll, H. Te Riele, J. Cloos, J.C. Dorsman, A meta-analysis of retinoblastoma copy numbers refines the list of possible driver genes involved in tumor progression, PLoS One. 11 (2016) e0153323. doi:10.1371/journal.pone.0153323.

[81] J.O. Ayeni, S.D. Campbell, "Ready, set, go": checkpoint regulation by Cdk1 inhibitory phosphorylation, Fly (Austin). 8 (2014) 140–147. doi:10.4161/19336934.2014.969147.

[82] C.P. Masamha, D.M. Benbrook, Cyclin D1 degradation is sufficient to induce G1 cell cycle arrest despite constitutive expression of cyclin E2 in ovarian cancer cells, Cancer Res. 69 (2009) 6565–6572. doi:10.1158/0008-5472.CAN-09-0913.

[83] Y. Guo, J. Harwalkar, D.W. Stacey, M. Hitomi, Destabilization of cyclin D1 message plays a critical

role in cell cycle exit upon mitogen withdrawal, Oncogene. 24 (2005) 1032–1042. doi:10.1038/sj.onc.1208299.

[84] K.T. Siu, M.R. Rosner, A.C. Minella, An integrated view of cyclin E function and regulation, Cell Cycle. 11 (2012) 57–64. doi:10.4161/cc.11.1.18775.

[85] J.E. Grim, M.P. Gustafson, R.K. Hirata, A.C. Hagar, J. Swanger, M. Welcker, H.C. Hwang, J. Ericsson, D.W. Russell, B.E. Clurman, Isoform- and cell cycle-dependent substrate degradation by the Fbw7 ubiquitin ligase, J Cell Biol. 181 (2008) 913–920. doi:10.1083/jcb.200802076.

[86] L. De Boer, V. Oakes, H. Beamish, N. Giles, F. Stevens, M. Somodevilla-Torres, C. DeSouza, B. Gabrielli, Cyclin A/cdk2 coordinates centrosomal and nuclear mitotic events, Oncogene. 27 (2008) 4261–4268. doi:10.1038/onc.2008.74.

[87] D. Gong, J.E. Ferrell, The Roles of Cyclin A2, B1, and B2 in Early and Late Mitotic Events, Mol Biol Cell. 21 (2010) 3149–3161. doi:10.1091/mbc.E10-05-0393.

[88] A. Musacchio, E.D. Salmon, The spindle-assembly checkpoint in space and time, Nat Rev Mol Cell Biol. 8 (2007) 379–393. doi:10.1038/nrm2163.

[89] T. Haq, M.W. Richards, S.G. Burgess, P. Gallego, S. Yeoh, L. O'Regan, D. Reverter, J. Roig, A.M. Fry, R. Bayliss, Mechanistic basis of Nek7 activation through Nek9 binding and induced dimerization, Nat Commun. 6 (2015) 8771. doi:10.1038/ncomms9771.

[90] N. Dephoure, C. Zhou, J. Villen, S.A. Beausoleil, C.E. Bakalarski, S.J. Elledge, S.P. Gygi, A quantitative atlas of mitotic phosphorylation, Proc Natl Acad Sci. 105 (2008) 10762–10767. doi:10.1073/pnas.0805139105.

[91] S. Minoguchi, M. Minoguchi, A. Yoshimura, Differential control of the NIMA-related kinases, Nek6 and Nek7, by serum stimulation, Biochem Biophys Res Commun. 301 (2003) 899–906. doi:10.1016/S0006-291X(03)00049-4.

[92] P. Strnad, P. Gönczy, Mechanisms of procentriole formation, Trends Cell Biol. 18 (2008) 389–396. doi:10.1016/j.tcb.2008.06.004.

[93] A. Puklowski, Y. Homsi, D. Keller, M. May, S. Chauhan, U. Kossatz, V. Grünwald, S. Kubicka, A. Pich, M.P. Manns, I. Hoffmann, P. Gönczy, N.P. Malek, The SCF-FBXW5 E3-ubiquitin ligase is regulated by PLK4 and targets HsSAS-6 to control centrosome duplication., Nat Cell Biol. 13 (2011) 1004–9. doi:10.1038/ncb2282.

[94] A.K. Gillingham, S. Munro, The PACT domain, a conserved centrosomal targeting motif in the coiled-coil proteins AKAP450 and pericentrin., EMBO Rep. 1 (2000) 524–529. doi:10.1093/embo-reports/kvd105.

[95] Y. Zhou, Y.P. Ching, A.C.S. Chun, D.Y. Jin, Nuclear localization of the cell cycle regulator CDH1 and its regulation by phosphorylation, J Biol Chem. 278 (2003) 12530–12536. doi:10.1074/jbc.M212853200.

[96] Y. Zhou, Y.-P. Ching, R.W.M. Ng, D.-Y. Jin, Differential expression, localization and activity of two alternatively spliced isoforms of human APC regulator CDH1, Biochem J. 374 (2003) 349–358. doi:10.1042/bj20030600.

[97] J.W. Raff, K. Jeffers, J.Y. Huang, The roles of Fzy/Cdc20 and Fzr/Cdh1 in regulating the destruction of cyclin B in space and time, J Cell Biol. 157 (2002) 1139–1149. doi:10.1083/jcb.200203035.

[98] F. Meghini, T. Martins, X. Tait, K. Fujimitsu, H. Yamano, D.M. Glover, Y. Kimata, Targeting of Fzr/Cdh1 for timely activation of the APC/C at the centrosome during mitotic exit, Nat Commun. 7 (2016) 12607. doi:10.1038/ncomms12607.

[99] M.A. Gomez-Ferreria, U. Rath, D.W. Buster, S.K. Chanda, J.S. Caldwell, D.R. Rines, D.J. Sharp, Human Cep192 Is Required for Mitotic Centrosome and Spindle Assembly, Curr Biol. 17 (2007) 1960–1966. doi:10.1016/j.cub.2007.10.019.

[100] S. Lawo, M. Hasegan, G.D. Gupta, L. Pelletier, Subdiffraction imaging of centrosomes reveals higher-order organizational features of pericentriolar material, Nat Cell Biol. 14 (2012) 1148–1158. doi:10.1038/ncb2591.

[101] K.F. Sonnen, L. Schermelleh, H. Leonhardt, E.A. Nigg, 3D-structured illumination microscopy provides novel insight into architecture of human centrosomes, Biol Open. 1 (2012) 965–976. doi:10.1242/bio.20122337.

[102] A. Hori, T. Toda, Regulation of centriolar satellite integrity and its physiology, Cell Mol Life Sci. 74 (2016) 213–229. doi:10.1007/s00018-016-2315-x.

[103] E.E. De Souza, G.V. Meirelles, B.B. Godoy, A.M. Perez, J.H.C. Smetana, S.J. Doxsey, M.E. McComb, C.E. Costello, S. a Whelan, J. Kobarg, Characterization of the human NEK7 interactome suggests catalytic and regulatory properties distinct from those of NEK6, J Proteome Res. 13 (2014) 4074–4090. doi:10.1021/pr500437x.

[104] G. Vaz Meirelles, D.C. Ferreira Lanza, J.C. Da Silva, J. Santana Bernachi, A.F. Paes Leme, J. Kobarg, Characterization of hNek6 interactome reveals an important role for its short N-terminal domain and colocalization with proteins at the centrosome, J Proteome Res. 9 (2010) 6298–6316. doi:10.1021/pr100562w.

[105] C. Belham, M.J. Comb, J. Avruch, Identification of the NIMA family kinases NEK6 / 7 as regulators of the p70 ribosomal S6 kinase, Curr Biol. 11 (2001) 1155–1167.

[106] R.K. Klein, E.A., ja Assoian, Transcriptional regulation of the cyclin D1 gene at a glance, J Cell Sci. 1 (2008) 3853–3857. doi:10.14440/jbm.2015.54.A.

[107] L. Wang, K. Lee, R. Malonis, I. Sanchez, B.D. Dynlacht, Tethering of an E3 ligase by PCM1 regulates the abundance of centrosomal KIAA0586/Talpid3 and promotes ciliogenesis, Elife. 5 (2016). doi:10.7554/eLife.12950.

[108] J.D.R. Reimann, B.E. Gardner, F. Margottin-Goguet, P.K. Jackson, Emi1 regulates the anaphase-promoting complex by a different mechanism than Mad2 proteins, Genes Dev. 15 (2001) 3278–3285. doi:10.1101/gad.945701.

[109] K.H. Ban, J.Z. Torres, J.J. Miller, A. Mikhailov, M. V. Nachury, J.J. Tung, C.L. Rieder, P.K. Jackson, The END Network Couples Spindle Pole Assembly to Inhibition of the Anaphase-Promoting Complex/Cyclosome in Early Mitosis, Dev Cell. 13 (2007) 29–42.

doi:10.1016/j.devcel.2007.04.017.

[110] H.A. Fisk, Many pathways to destruction: The role of the centrosome in, and its control by regulated proteolysis, in: Centrosome Cell Mol Mech Funct Dysfunctions Dis, Humana Press, Totowa, NJ, 2012: pp. 133–155. doi:10.1007/978-1-62703-035-9_8.

[111] H.G. Dos Santos, D. Abia, R. Janowski, G. Mortuza, M.G. Bertero, M. Boutin, N. Guarín, R. Méndez-Giraldez, A. Nuñez, J.G. Pedrero, P. Redondo, M. Sanz, S. Speroni, F. Teichert, M. Bruix, J.M. Carazo, C. Gonzalez, J. Reina, J.M. Valpuesta, I. Vernos, J.C. Zabala, G. Montoya, M. Coll, U. Bastolla, L. Serrano, Structure and Non-Structure of Centrosomal Proteins, PLoS One. 8 (2013) e62633. doi:10.1371/journal.pone.0062633.

[112] P. Guichard, V. Hachet, N. Majubu, A. Neves, D. Demurtas, N. Olieric, I. Fluckiger, A. Yamada, K. Kihara, Y. Nishida, S. Moriya, M.O. Steinmetz, Y. Hongoh, P. Gönczy, Native architecture of the centriole proximal region reveals features underlying its 9-fold radial symmetry, Curr Biol. 23 (2013) 1620–1628. doi:10.1016/j.cub.2013.06.061.

[113] H. Roque, A. Wainman, J. Richens, K. Kozyrska, A. Franz, J.W.W. Raff, Drosophila Cep135/Bld10 maintains proper centriole structure but is dispensable for cartwheel formation, J Cell Sci. 125 (2012) 5881–5886. doi:10.1242/jcs.113506.

[114] K.D. Dahl, D.G. Sankaran, B.A. Bayless, M.E. Pinter, D.F. Galati, L.R. Heasley, T.H. Giddings, C.G. Pearson, A short CEP135 splice isoform controls centriole duplication, Curr Biol. 25 (2015) 2591–2596. doi:10.1016/j.cub.2015.08.039.

[115] A. Sharma, A. Aher, N.J. Dynes, D. Frey, E.A. Katrukha, R. Jaussi, I. Grigoriev, M. Croisier, R.A. Kammerer, A. Akhmanova, P. Gönczy, M.O. Steinmetz, Centriolar CPAP/SAS-4 Imparts Slow Processive Microtubule Growth, Dev Cell. 37 (2016) 362–376. doi:10.1016/j.devcel.2016.04.024.

[116] B.P. Piasecki, C.D. Silflow, The UNI1 and UNI2 Genes Function in the Transition of Triplet to Doublet Microtubules between the Centriole and Cilium in Chlamydomonas, Mol Biol Cell. 20 (2009) 368–378. doi:10.1091/mbc.E08.

[117] C.-J.C. Tang, S.-Y. Lin, W.-B. Hsu, Y.-N. Lin, C.-T. Wu, Y.-C. Lin, C.-W. Chang, K. Wu, T.K. Tang, The human microcephaly protein STIL interacts with CPAP and is required for procentriole formation, EMBO J. 30 (2011) 4790–4804. doi:10.1038/emboj.2011.378.

[118] M. Ichikawa, D. Liu, P.L. Kastritis, K. Basu, T.C. Hsu, S. Yang, K.H. Bui, Subnanometre-resolution structure of the doublet microtubule reveals new classes of microtubule-associated proteins, Nat Commun. 8 (2017) 15035. doi:10.1038/ncomms15035.

[119] C. Janke, The tubulin code: Molecular components, readout mechanisms, functions, J Cell Biol. 206 (2014) 461–472. doi:10.1083/jcb.201406055.

[120] C. Janke, J. Chloë Bulinski, Post-translational regulation of the microtubule cytoskeleton: mechanisms and functions, Nat Rev Mol Cell Biol. 12 (2011) 773–786. doi:10.1038/nrm3227.

[121] P. Findeisen, S. Mühlhausen, S. Dempewolf, J. Hertzog, A. Zietlow, T. Carlomagno, M. Kollmar, Six subgroups and extensive recent duplications characterize the evolution of the eukaryotic

tubulin protein family, Genome Biol Evol. 6 (2014) 2274–2288. doi:10.1093/gbe/evu187.

[122] P. Dupuis-Williams, A. Fleury-Aubusson, N.G. De Loubresse, H. Geoffroy, L. Vayssié, A. Galvani, A. Espigat, J. Rossier, Functional role of ε-tubulin in the assembly of the centriolar microtubule scaffold, J Cell Biol. 158 (2002) 1183–1193. doi:10.1083/jcb.200205028.

[123] P. Chang, T. Stearns, Tubulin and ε -tubulin : two new human centrosomal tubulins reveal new aspects of centrosome structure and function, Nat Cell Biol. 2 (2000) 30–5. http://www.ncbi.nlm.nih.gov/pubmed/10620804.

[124] S. Li, J.J. Fernandez, W.F. Marshall, D.A. Agard, Three-dimensional structure of basal body triplet revealed by electron cryo-tomography, EMBO J. (2012). doi:10.1038/emboj.2011.460.

[125] I. Ross, C. Clarissa, T.H. Giddings, M. Winey, ε-tubulin is essential in Tetrahymena thermophila for the assembly and stability of basal bodies, J Cell Sci. 126 (2013) 3441–51. doi:10.1242/jcs.128694.

[126] Y.F. Inclán, E. Nogales, Structural models for the self-assembly and microtubule interactions of gamma-, delta- and epsilon-tubulin., J Cell Sci. 114 (2001) 413–422.

[127] L. Libusová, P. Dráber, Multiple tubulin forms in ciliated protozoan Tetrahymena and Paramecium species, Protoplasma. 227 (2006) 65–76. doi:10.1007/s00709-005-0152-0.